FEDERAL UNIVERSITY OF CEARÁ
DEPARTMENT OF TELEINFORMATICS ENGINEERING
POSTGRADUATE PROGRAM IN TELEINFORMATICS ENGINEERING

Utility-Based Scheduling Algorithms to Enhance User Satisfaction in OFDMA Systems

Master of Science Thesis

Author
Francisco Hugo Costa Neto

Advisor
Prof. Dr. Tarcisio Ferreira Maciel

Co-Advisor
Prof. Dr. Emanuel Bezerra Rodrigues

FORTALEZA – CEARÁ
FEBRUARY 2016

UNIVERSIDADE FEDERAL DO CEARÁ
DEPARTAMENTO DE ENGENHARIA DE TELEINFORMÁTICA
PROGRAMA DE PÓS-GRADUAÇÃO EM ENGENHARIA DE TELEINFORMÁTICA

Utility-Based Scheduling Algorithms to Enhance User Satisfaction in OFDMA Systems

Autor
Francisco Hugo Costa Neto

Orientador
Prof. Dr. Tarcisio Ferreira Maciel

Co-orientador
Prof. Dr. Emanuel Bezerra Rodrigues

Dissertação apresentada à Coordenação do Programa de Pós-graduação em Engenharia de Teleinformática da Universidade Federal do Ceará como parte dos requisitos para obtenção do grau de ***Mestre em Engenharia de Teleinformática****. Área de concentração: Sinais e sistemas.*

FORTALEZA – CEARÁ
FEVEREIRO 2016

This page was intentionally left blank

Dados Internacionais de Catalogação na Publicação
Universidade Federal do Ceará
Biblioteca de Pós-Graduação em Engenharia - BPGE

C874u Costa Neto, Francisco Hugo.
Utility-based scheduling algorithms to enhance user satisfaction in OFDMA systems / Francisco Hugo Costa Neto. – 2016.
84 f. : il. color. , enc. ; 30 cm.

Dissertação (mestrado) – Universidade Federal do Ceará, Centro de Tecnologia, Departamento de Engenharia de Teleinformática, Programa de Pós-Graduação em Engenharia de Teleinformática, Fortaleza, 2016.
Área de concentração: Sinais e Sistemas.
Orientação: Prof. Dr. Tarcisio Ferreira Maciel.
Coorientação: Prof. Dr. Emanuel Bezerra Rodrigues.

1. Teleinformática. 2. Usuários - Satisfação. 3. Sistemas de comunicação sem fio. 4. Qualidade de serviços. I. Título.

CDD 621.38

UNIVERSIDADE FEDERAL DO CEARÁ
CENTRO DE TECNOLOGIA
PROGRAMA DE PÓS-GRADUAÇÃO EM ENGENHARIA DE TELEINFORMÁTICA

CAMPUS DO PICI, CAIXA POSTAL 6007 CEP 60.738-640
FORTALEZA – CEARÁ - BRASIL

FRANCISCO HUGO COSTA NETO

UTILITY-BASED SCHEDULING ALGORITHMS TO ENHANCE USER SATISFACTION IN OFDMA SYSTEMS

Dissertação submetida à Coordenação do Programa de Pós-Graduação em Engenharia de Teleinformática, da Universidade Federal do Ceará, como requisito parcial para a obtenção do grau de Mestre em Engenharia de Teleinformática.
Área de concentração: Sinais e Sistemas

Aprovada em: 25/02/2016.

BANCA EXAMINADORA

Tarcisio Ferreira Maciel
Prof. Dr. TARCISIO FERREIRA MACIEL (Orientador)
Universidade Federal do Ceará

Emanuel Bezerra Rodrigues
Prof. Dr. EMANUEL BEZERRA RODRIGUES (Co-orientador)
Universidade Federal do Ceará

Yuri Carvalho Barbosa Silva
Prof. Dr. YURI CARVALHO BARBOSA SILVA
Universidade Federal do Ceará

Prof. Dr. LEONARDO SAMPAIO CARDOSO
INSA-Lyon

Contents

Acknowledgements

First of all, I would like to thank God who has guide me through the good and bad times of my life.

I would like to thank my parents, Ana and Valmir, for their unconditional support. Without your encouragement and assistance I would not have come so far. To my brother, Lui Magno, with whom I could always talk to and laugh. I also thank my beloved Thalita, who always gives to me understanding and encouragement - this work is also your.

I am very grateful to my advisor Prof. Dr. Tarcisio F. Maciel and to my co-advisor Prof. Dr. Emanuel Bezerra Rodrigues, for the support, guidance, and valuable suggestions during the supervision of my studies. I would like to thank Prof. Dr. Fco. Rodrigo P. Cavalcanti for giving me the opportunity to work on the Wireless Telecommunications Research Group (GTEL). It is an honor to be part of this great team.

To my friends from GTEL, Mairton Barros, Yuri Victor, Marciel Barros, Diego Sousa, Victor Farias, Laszlon Costa, Darlan Cavalcante, Khaled Ardah, Rafael Vasconcelos, Daniel Araujo, Samuel Valduga, Igor Guerreiro, Carlos Silva, Juan Salustiano, Marcio Caldas and Yosbel Rodriguez.

Thanks to the Innovation Center, Ericsson Telecomunicações S.A., Brazil, under EDB/UFC.40 Technical Cooperation Contract. I would like also to acknowledge CAPES for the scholarship support.

Fortaleza, February 2016.

Francisco Hugo Costa Neto.

Abstract

The increasing market demand for wireless services and the scarcity of radio resources calls more than ever for the enhancement of the performance of wireless communication systems. Nowadays, it is mandatory to ensure the provision of better radio services and to improve coverage and capacity, thereby increasing the number of satisfied subscribers.

This thesis deals with scheduling algorithms aiming at the maximization and adaptive control of the satisfaction index in the downlink of an Orthogonal Frequency Division Multiple Access (OFDMA) network, considering different types of traffic models of Non-Real Time (NRT) and Real Time (RT) services; and more realistic channel conditions, e.g., imperfect Channel State Information (CSI). In order to solve the problem of maximizing the satisfaction with affordable complexity, a cross layer optimization approach uses the utility theory to formulate the problem as a weighted sum rate maximization.

This study is focused on the development of an utility-based framework employing the shifted log-logistic function, which due to its characteristics allows novel scheduling strategies of Quality of Service (QoS)-based prioritization and channel opportunism, for an equal power allocationn among frequency resources.

Aiming at the maximization of the satisfaction of users of NRT and RT services, two scheduling algorithms are proposed: Modified Throughput-based Satisfaction Maximization (MTSM) and Modified Delay-based Satisfaction Maximization (MDSM), respectively. The modification of parameters of the shifted log-logistic utility function enables different strategies of distribution of resources. Seeking to track satisfaction levels of users of NRT services, two adaptive scheduling algorithms are proposed: Adaptive Throughput-based Efficiency-Satisfaction Trade-Off (ATES) and Adaptive Satisfaction Control (ASC). The ATES algorithm performs an average satisfaction control by adaptively changing the scale parameter, using a feedback control loop that tracks the overall satisfaction of the users and keep it around the desired target value, enabling a stable strategy to deal with the trade-off between satisfaction and capacity. The ASC algorithm is able to ensure a dynamic variation of the shape parameter, guaranteeing a strict control of the user satisfaction levels.

System level simulations indicate the accomplishment of the objective of development of efficient and low complexity scheduling algorithms able to maximize and control the satisfaction indexes. These strategies can be useful to the network operator who is able to design and operate the network according to a planned user satisfaction profile.

Keywords: Utility Theory, QoS Provision, Satisfaction Maximization

Resumo

A crescente demanda de mercado por serviços sem fio e a escassez de recursos de rádio apela mais do que nunca para a melhoria do desempenho dos sistema de comunicação sem fio. Desse modo, é obrigatório garantir o provimento de melhores serviços de rádio e aperfeiçoar a cobertura e a capacidade, com isso aumentando o número de consumidores satisfeitos.

Esta dissertação lida com algoritmos de escalonamento, buscando a maximização e o controle adaptativo do índice de satisfação no enlace direto de uma rede de acesso baseado em frequência, OFDMA (do inglês *Orthogonal Frequency Division Multiple Acess*, considerando diferentes modelos de tráfego para serviços de tempo não real, NRT (do inglês *Non-Real Time*), e de tempo real, RT (do inglês *Real Time*); e condições de canal mais realistas, por exemplo, CSI imperfeitas. Com o intuito de resolver o problema de maximização de satisfação com menor complexidade, uma abordagem com otimização de múltiplas camadas usa a teoria da utilidade para formular o problema como uma maximização de soma de taxa ponderada.

Este estudo é focado no desenvolvimento de um *framework* baseado em utilidade empregando a função log-logística deslocada, que devido às suas características permite novas estratégias de escalonamento de priorização baseada em QoS e oportunismo de canal, para uma alocação de potência igualitária entre os recursos de frequência.

Visando a maximização da satisfação de usuários de serviços NRT e RT, dois algoritmos de escalonamento são propostos: MTSM e MDSM, respectivamente. A modificação dos parâmetros da função de utilidade log-logística descolocada permite a implementação de diferentes estratégias de distribuição de recursos.

Buscando controlar os níveis de satisfação dos usuários de serviços NRT, dois algoritmos adaptativos de escalonamento são propostos: ATES e ASC. O algoritmo ATES realiza um controle da satisfação média pela mudança dinâmica do parâmetro de escala, permitindo uma estratégia estável para lidar com o dilema entre satisfação e capacidade. O algoritmo ASC é capaz de garantir uma variação dinâmica do parâmetro de formato, garantindo um controle rigoroso dos níveis de satisfação dos usuários.

Simulações no nível do sistema indicam o cumprimento do objetivo de desenvolvimento de algoritmos de escalonamento eficientes e de baixa complexidade capazes de maximizar e controlar os índices de satisfação. Estas estratégias podem ser úteis para o operador da rede, que se torna capaz de projetar e operar a rede de acordo com um perfil de satisfação de usuário.

Palavras-chave: Teoria da Utilidade, Provimento de QoS, Maximização de Satisfação

List of Figures

List of Tables

Acronyms

The abbreviations and acronyms used throughout this thesis are listed here. The meaning of each abbreviation or acronym is indicated once, when it first appears in the text.

3G	3rd Generation
3GPP	3rd Generation Partnership Project
4G	4th Generation
ATES	Adaptive Throughput-based Efficiency-Satisfaction Trade-Off
ASC	Adaptive Satisfaction Control
BLER	BLock Error Rate
BS	Base Station
CoMP	Coordinated Multi-Point
CQI	Channel Quality Indicator
CSI	Channel State Information
DL	Downlink
DRA	Dynamic Resource Assignment
DSM	Delay-based Satisfaction Maximization
MDSM	Modified Delay-based Satisfaction Maximization
EDF	Earliest Deadline First
eNB	Evolved Node B
FIFO	First In First Out
FER	Frame Erasure Rate
FSB	Fixed Switched Beamforming
HOL	Head Of Line
HSPA	High Speed Packet Access
LTE	Long Term Evolution
LTE-A	Long Term Evolution (LTE)-Advanced
MAC	Medium Access Control
MCS	Modulation and Coding Scheme
MIMO	Multiple Input Multiple Output
MISO	Multiple Input Single Output
MLWDF	Modified Largest Weighted Delay First
MTSM	Modified Throughput-based Satisfaction Maximization
MU	Multi-User
NRT	Non-Real Time

OFDMA	Orthogonal Frequency Division Multiple Access
OFDM	Orthogonal Frequency Division Multiplexing
ORB	Orthogonal Random Beamforming
OSI	Open Systems Interconnection
PF	Proportional Fair
PHY	Physical
QAM	Quadrature Amplitude Modulation
QoE	Quality of Experience
QoS	Quality of Service
RAN	Radio Access Network
RB	Resource Block
RM	Rate Maximization
RRA	Radio Resource Allocation
RT	Real Time
SINR	Signal to Interference-plus-Noise Ratio
SISO	Single Input Single Output
SNR	Signal to Noise Ratio
SORA	Satisfaction Oriented Resource Allocation
SORA-NRT	Satisfaction-Oriented Resource Allocation for Non-Real Time Services
SU	Single-User
TTI	Transmission Time Interval
TSM	Throughput-based Satisfaction Maximization
MTSM	Modified Throughput-based Satisfaction Maximization
TU	Typical Urban
UE	User Equipment
UEPS	Urgency and Efficiency-based Packet Scheduling
UMTS	Universal Mobile Telecommunications System
VoIP	Voice over IP
WCDMA	Wideband Code Division Multiple Access
WFQ	Weighted Fair Queueing
ZMCSCG	Zero Mean Circularly Symmetric Complex Gaussian

Chapter 1

Introduction

This master's thesis proposes efficient and low complexity scheduling techniques able to enhance user satisfaction in different scenarios and traffic models. This introductory chapter aims provide an overview of the studies here performed and has the following organization: Section 1.1 expounds the motivation and open problems considered to develop this study. Section 1.2 provides a literature review of the main issues addressed. Section 1.3 describes the scope of the studies carried out in this thesis. Section 1.4 shows the scientific production resulting of the Master's course. Finally, Section 1.5 describes the organization of the remaining of this master's thesis.

1.1 Motivation

Since its beginning, the wireless communication networks are characterized by changes in the amount of exchanged data and the variety of applications that generate this traffic. In 2008, traditional applications like web browsing, email and file sharing accounted for a preponderant percentual of the total traffic in the Internet. In 2013, Voice over IP (VoIP) and video streaming were responsible for almost half of the total traffic [4].

Mobile data traffic grows continuously, according to [5] the period between 2010 and 2015 is portrayed by a continued and strong increase of 14% quarter-on-quarter and 65% year-on-year. The growth in data traffic is carried both by increased smartphone subscriptions and a continued improvement in average data volume per subscription, fueled by video streaming.

It is expected that this behavior will be maintained over the next decade, with a tenfold increase of global mobile data traffic between 2014 and 2019 [6]. In the end of 2014, the number of mobile-connected devices exceeded the number of people on earth, and by 2019 there will be nearly 1.5 mobile devices per capita.

Therefore, the increasing market demand for wireless services and the scarcity of radio resources calls more than ever for the enhancement of the performance of wireless communication systems. Nowadays, it is mandatory to ensure the provision of better radio services and to improve coverage and capacity, thereby increasing the number of satisfied subscribers [7].

1.2 State of the Art

The scheduling algorithms are responsible for resource allocation among users and impact directly the bandwidth usage efficiency. Many scheduling algorithms have been proposed in the last decade, spanning from the high cell capacity to fairness and the satisfaction of Quality of Service (QoS) requirements [8].

The most common schedulers operate regardless of channel conditions, e.g.: i) First In First Out (FIFO), that serves users according to the order of service requests; ii) round robin, algorithm that schedules users in a circular manner; iii) Earliest Deadline First (EDF), which schedules the packet that will be expired the soonest; iv) Weighted Fair Queueing (WFQ), that assigns resources considering the weights associated with every user. The channel unaware schedulers were first introduced in wired networks, they are very simple, but sometimes can be very inefficient and unfair [7, 8].

Scheduling algorithms that consider Physical (PHY) layer information, like the channel state, are able to exploit more efficiently the resources of the system. The concept of opportunistic scheduling, i.e., consider the channel quality variations and improve the system capacity was first employed in [9], that proposed a power control scheme in which the users are allocated more power when their channels are good, and less when they are bad. This strategy is known in the literature as Maximum Rate [7] or Maximum Throughput [8].

The maximum rate strategy is able to maximize cell throughput, but results in an unfair resource sharing since users with worst channel conditions only get a low percentage of the available resources, in the extreme case they may suffer starvation. Proportional fair scheduling has received much research attention due to its capability on the trade-off between spectral efficiency and fairness [10, 11]. The authors of [12] provide anlytical expressions to evaluate the performance of random access wireless network in terms of user throughput and network throughput subject to a proportional fairness algorithm scheduling resources between users and show the ability of the algorithm to schedule resources avoiding unfairness among users. Other study evaluates a scheduling algorithm which maintains the fairness level in scenarios with fluctuating load. Moreover, shown that the cell throughput can be improved [13].

Maximum throughput and proportional fairness are examples of scheduling algorithms that consider the channel condition. However, channel awareness does not imply QoS provisioning, essential feature to applications such as as video streaming and VoIP. There are several QoS objectives, e.g., throughput, delay, jitter, and latency. Among these QoS metrics, received the most attention delay [14, 15] and throughput [16, 17].

In this work, the problem of scheduling using an utility-based algorithm is investigated. Initially proposed to be used in communications network problems in [18], utility theory quantifies the resources' usage benefits or evaluates the degree to which a network satisfies service requirements of users' applications.

The research carried out in [19] investigated the properties of the optimal sub-carrier allocation associated with utility-based optimization and demonstrated that its resource allocation balances spectral efficiency and fairness. Based on that theoretical framework, the same authors proposed frequency assignment algorithms in order to maximize the average

utility in Orthogonal Frequency Division Multiple Access (OFDMA) wireless networks [20]. Their results indicated that the utility-based cross-layer optimization could enhance the system performance and guarantee a fair resource allocation. The studies performed in [21] also considered a network utility maximization in OFDMA systems to assure a fair and efficient resource allocation. The problem was decomposed into rate control and scheduling problems at the transport and medium access control layers, respectively.

The topic of satisfaction maximization for Non-Real Time (NRT) services was object of study of [22–24]. The works [22] and [23] proposed and evaluated a heuristic downlink scheduling algorithm called Satisfaction Oriented Resource Allocation (SORA) whose main objective is ensure the achievement of a minimum QoS requirement in order to maximize the number of satisfied users. The authors of [24] developed an adaptive scheduling framework. The authors of [25] proposed a downlink scheduling algorithm initially designed for VoIP service, which aims maximize the number of satisfied Real Time (RT) users in the system.

The authors of [26] proposed utility-based algorithms, called Throughput-based Satisfaction Maximization (TSM) and Delay-based Satisfaction Maximization (DSM) which provided a QoS-aware scheduling that maximizes the satisfaction of NRT and RT users, respectively.

The study performed in [27] combined TSM with Fixed Switched Beamforming (FSB) to exploit spatial and multi-user diversity. In [28], DSM is combined with FSB and Orthogonal Random Beamforming (ORB) to evaluate the effect of spatial diversity with this utility-based scheduling algorithm in a scenario with RT services.

Beamforming techniques such as ORB and FSB attracted significant interest because they demand only a very small amount of Channel State Information (CSI) (i.e., Channel Quality Indicators (CQIs)) to be fed back to the Evolved Node B (eNB), mostly Signal to Interference-plus-Noise Ratio (SINR)-related measurements for each candidate beam at the eNB. Since CQIs are simply scalar values, the signaling demand is relatively low. Measurement and signaling can also be kept almost transparent to the users if the eNB carefully coordinates the processing of acquiring CQIs from their served users. Since only a few beams are expected to be active at each period, the user could also report CQIs corresponding only to their best beams. Moreover, these strategies can improve system performance by exploiting multiuser diversity and spatial multiplexing gains, offering feasible coverage and capacity extension without a massive feedback load [29].

According to the beamforming technique, a set of precoding vectors (beamformers) will be generated at the eNB, which will schedule users based on their achievable rates (representing users' CQI) and on utility-based weights [30]. Thus, it will be possible to investigate capacity, fairness and QoS trade-offs of the combination of the scheduling and beamforming techniques. Whereas the optimum beam selection algorithm needs an exhaustive search over the entire set of beams and users, the beamforming schemes present low computational complexity by using suboptimal beam selection procedures [31].

In [32], the TSM algorithm is evaluated considering imperfections of CSI and interference. The scheduling algorithms ought to ensure that users achieve their QoS requirements,

regardless their channel conditions. Other studies in the literature have already addressed the issue of resource allocation assuming perfect CSI at the transmitter [21, 33]. However, the perfect CSI assumption (without estimation errors nor channel feedback delay) can significantly deteriorate the system performance [34,35]. Unsuccessful transmissions can occur when the BS assigns a certain rate to a user based on a nominal CSI that cannot be supported by the true channel state [36].

It was demonstrated in [37] that the introduction of a noise term in the CSI estimation yields significant performance degradation. The statistical description of the CSI uncertainty can be exploited aiming at maximizing the system capacity, as illustrated in [36]. Besides the throughput metric, fairness can also be considered on resource allocation schemes taking into account imperfect CSI, which has already been investigated in [38].

1.3 Thesis Scope

In this study we consider the problem of improving and controlling the percentage of satisfied users in the downlink of an OFDMA system. The contributions of the present work include:

i. development of a generalized utility-based scheduling framework using the shifted log-logistic function;

ii. development and evaluation of scheduling algorithms to maximize user satisfaction, considering different scenarios and NRT and RT traffic models;

iii. development and evaluation of scheduling algorithms to control user satisfaction percentuals;

1.4 Contributions and Scientific Production

The content and contributions presented in this Master's thesis were published and submitted with the following information:

- Monteiro, V. F., Sousa, D. A.,**Costa Neto, F. H**, Maciel, T. F. and Cavalcanti, F. R. P., Throughput-Based Satisfaction Maximization for a Multi-Cell Downlink OFDMA System Considering Imperfect CSI. Brazilian Telecommunications Simposium, September 2015.

- **Costa Neto, F. H**, Guerreiro, I. M., and Maciel, T. F.,Toeplitz-Structured Sequences for Rendezvous in Dynamic Spectrum Access. European Wireless Conference. May, 2014.

- Rodrigues, E. B., **Costa Neto, F. H**, Maciel, T. F., Lima, F. R. M. and Cavalcanti, F. R. P., Utility-Based Resource Allocation with Spatial Multiplexing for Real Time Services in Multi-User OFDM Systems. IEEE Vehicular Technology Conference (VTC - Spring). May 2014.

- Rodrigues, E. B., **Costa Neto, F. H**, Maciel, T. F., Lima, F. R. M. and Cavalcanti, F. R. P., Utility-Based Scheduling and Fixed Switching Beamforming for User Satisfaction Improvement in OFDMA Systems. European Wireless Conference. May 2014.

In parallel to the work developed during the master's course, I have been working on other research projects, which are in the context of analysis and control of trade-offs involving QoS provision. In the context of these projects, I have participated on the following technical reports:

- **F. Hugo C. Neto**, Emanuel B. Rodrigues, Diego A. Sousa, Tarcisio F. Maciel and F. Rodrigo P. Cavalcanti, "Generalized Utility-Based Scheduling Framework for Adaptive Satisfaction Control in OFDMA Systems", GTEL-UFC-Ericsson UFC.40, Tech. Rep., Sep. 2015, Second Technical Report.

- **F. Hugo C. Neto**, Emanuel B. Rodrigues, Diego A. Sousa, Tarcisio F. Maciel and F. Rodrigo P. Cavalcanti, "Generalized Utility-Based Scheduling Framework to Improve User Satisfaction in OFDMA Systems", GTEL-UFC-Ericsson UFC.40, Tech. Rep., Mar. 2015, First Technical Report.

- **F. Hugo C. Neto**, Victor F. Monteiro, Diego A. Sousa, Emanuel B. Rodrigues, Tarcisio F. Maciel and F. Rodrigo P. Cavalcanti, "A Novel Utility-Based Resource Allocation Technique for Improving User Satisfaction in OFDMA Networks", GTEL-UFC-Ericsson UFC.33, Tech. Rep., Aug. 2014, Fourth Technical Report.

- Rodrigues, E. B., **Costa Neto, F. H.**, Lima, F. R. M, Sousa, D. A., Maciel T. F. and Cavalcanti, F. R. P. "Adaptive QoS Control Using Utility-Based Dynamic Resource Assignment with Beamforming for OFDMA Systems", GTEL-UFC-Ericsson UFC.33, Tech. Rep., Feb. 2014, Third Technical Report.

1.5 Thesis Organization

Chapter 2 provides a description of the main assumptions and the overall scenario considered to the development of this thesis. It provides important concepts and features of the key technologies considered, describes the simulation scenario, performance metrics and the comparison algorithms.

Chapter 3 investigates the problem of maximization of the user satisfaction. This chapter presents the general optimization formulation and the utility-based scheduling framework, details the studied algorithms with the description of the different utility functions considered to develop the framework and the evaluation the proposed algorithms by means of system level simulations according to the criteria described previously on Chapter 2.

Chapter 4 studies the control of the user satisfaction levels. It provides a general description of the shifted log-logistic utility function, presents and evaluates two adaptive algorithms.

Chapter 5 provides the main conclusions of this master's thesis.

Appendix A addresses the CQI-based beamforming techniques in the Downlink (DL) of a Multi-User (MU)-Multiple Input Single Output (MISO) system, where one eNB is equipped with multiple antennas and serves several single-antenna mobile users.

Chapter 2

System Model

This chapter describes the main assumptions and the overall scenario considered to develop this thesis. Initially, Section 2.1 presents concepts and features that are important to the development of the ideas here presented. Next, Section 2.2 describes the general scenario and Section 2.3 defines the performance metrics considered in the evaluation of the proposed algorithms. Section 2.4 shows the algorithms used for comparison and Section 2.5 describes the simulation model.

2.1 Key Technologies

The increasing demand to provide high data rates, low latency and improved spectral efficiency compared to previous 3rd Generation (3G) networks lead to the development of the Long Term Evolution (LTE) standard, which is expected to support a wide range of multimedia and Internet-based services even in high mobility scenarios. LTE has been designed as a flexible radio access technology in order to support different system bandwidth configurations (from 1.4 MHz up to 20 MHz). Considering a spectrum allocation of 20 MHz, the targets for uplink and downlink peak data rate requirements are set, respectively, to 50 Mbit/s and 100 Mbit/s [39].

The LTE standard has been specified by the 3rd Generation Partnership Project (3GPP) in Release 8, offering significant improvement over previous technologies such as Universal Mobile Telecommunications System (UMTS) and High Speed Packet Access (HSPA) by introducing a novel physical layer and modifying the core network [40].

The LTE standard considers the radio spectrum access based on the Orthogonal Frequency Division Multiplexing (OFDM) scheme. In particular, Orthogonal Frequency Division Multiple Access (OFDMA) is used in the downlink direction. Differently from basic OFDM, it allows multiple access by assigning sets of sub-carriers to each individual user. OFDMA can exploit sub-carriers distributed on the entire spectrum, being able to provide high scalability, simple equalization, and high robustness against the time-frequency selective nature of radio channel fading [8].

OFDMA converts the wide-band frequency selective channel into a set of several flat fading subchannels. The flat fading subchannels allow the implementation of optimum receivers with reasonable complexity, in contrast to Wideband Code Division Multiple Access (WCDMA)

systems [39]. Moreover, as an inheritance of the HSPA, OFDMA allows large throughput gains in the downlink due to multi-user diversity, since it tries to assign the best subchannels to the individual users.

The increase in the data traffic demanded by the wireless networks led to further improvements in the LTE performance, motivating the development of the LTE-Advanced (LTE-A) networks. The LTE-A standard improves the overall throughput and latency by the introduction of various functionalities, such as Coordinated Multi-Point (CoMP).

Several studies investigated how to improve LTE features with the help of Multiple Input Multiple Output (MIMO). MIMO communication employs multiple transmit and receive antennas to enhance the system performance by exploiting spatial diversity to improve communication reliability and/or spatial multiplexing to improve throughput. Over the same radio channel, spatial multiplexing can be used to simultaneously transmit multiple data streams separated in space, thus enabling to obtain huge system throughput gains [41]. In this way, high spectral efficiency values can be achieved without requiring additional frequency resources.

There are two types of MIMO in LTE systems. On the one hand, there is the Single-User (SU)-MIMO, which considers that every resource block should be given to no more than one User Equipment (UE) at a time. On the other hand, the Multi-User (MU)-MIMO employs different spatial streams that may be assigned to multiple UE, allowing them to share the same resource block. Therefore, MU-MIMO gets better system performance in comparison with SU-MIMO, but incurs a higher design complexity and specific hardware.

2.2 Scenario Description

This study considers the downlink of an LTE access network composed of a single cell in which an Evolved Node B (eNB) is deployed to serve a set of UE $\mathcal{J} = \{1, 2, \cdots, J\}$ distributed within its coverage area.

The system employs OFDMA as the multiple access scheme. Due to signaling constraints, the radio resources are assigned in blocks to the UE. The smallest radio resource unit that can be allocated to an UE for data reception corresponds to a time/frequency chunk spanning over two time slots in the time domain and over one sub-channel in the frequency domain, being termed Resource Block (RB). The system has a set $\mathcal{S} = \{1, 2, \cdots, S\}$ of RBs. The RB comprises 14 symbols in time domain and 12 contiguous OFDM sub-carriers spaced of 15 kHz in the frequency domain. The total power of each eNB is equal to P_t and is evenly distributed among all RBs, then the power allocated to RB s is $p_s = \frac{P_t}{S}$.

The time duration corresponding to the time basis at which resources are allocated to the UE by the scheduling algorithms is denominated Transmission Time Interval (TTI), and it is equal to the time duration of an RB. The TTI is set to 1 ms. Moreover, it is considered that each RB can be allocated to only one UE at each TTI.

The channel coefficient $h_{j,s}$ between the eNB and the UE j on RB s at a TTI n is approximated by the coefficient associated with the middle sub-carrier and first OFDM symbol of the RB. Channel coherence bandwidth is assumed larger than the bandwidth of RB leading to flat fading over each RB. The channel coefficient takes into account the main propagation aspects

on the wireless channel, namely path loss, shadowing (slow fading), and small-scale fading (fast fading).

In this thesis, two path loss models are considered to a carrier frequency of 2 GHz. The first one is a macro cell path loss model based on the propagation model determined by [3, Table A.2.1.1-3], given by

$$PL = 15.3 + 37.6 \cdot \log_{10}(d) \tag{2.1}$$

where d is the distance between the transmitter and receiver antenna, given in meters.

The second model is a modified COST231 Hata urban propagation model based on [2, Table 5.1] and is given by

$$PL = 34.5 + 35 \cdot \log_{10}(d) \tag{2.2}$$

The slow fading (shadowing) is modeled as a log-normal random variable, with mean equal to zero and standard deviation equal to 8 dB [42]. No spatial correlation for shadowing is considered in the simulator.

The fast fading follows a time-and frequency-correlated Rayleigh distribution taking into account the power delay profile of the Typical Urban (TU) channel from [43]. There is a fading map in the simulator and the samples are taken by choosing a random initial position (in time and frequency axes) in the map that is unique for a receiver-transmitter pair. Then, at each TTI, an offset is chosen according to the current time. This assures a degree of decorrelation between the fading samples of different links. The attributed offset depends on the relation between the Doppler spread used in the generation of the map and the one that corresponds to the mobile terminal speed. It becomes an integer value that is used to jump in samples inside the map.

The eNB antenna radiation pattern is modeled as 3-sector cell sites with fixed antenna patterns in accordance with [44]. The horizontal gain is modeled as

$$G_h(\theta_h) = -min\Big(12 \cdot \Big(\frac{\theta_h}{HPBBW_h}\Big)^2, FRB_h\Big) + G_m \tag{2.3}$$

where $-180^\circ \leq \theta_h \leq 180^\circ$ is the horizontal angle relative to the main beam pointing direction, $HPBBW_h = 65^\circ$ is the horizontal half-power beamwidth degree, $FRB_h = 18$ dB is a front back ratio and $G_m = 18$ dBi is a maximum gain.

The vertical gain model is given by

$$G_v(\theta_v) = max(-12 \cdot \Big(\frac{(\theta_v - \theta_{etilt})}{HPBBW_h}\Big)^2, SLL_v) \tag{2.4}$$

where $-180^\circ \leq \theta_v \leq 180^\circ$ is the negative angle relative to horizontal plane, $\theta_{etilt} = 8^\circ$ is the electrical tilt, $HPBBW_v$ is the vertical half-power beamwidth degree, $SLL_v = -18$ dB is a side lobe level relative the max gain of the main beam.

Then, the two gain components are added:

$$G(\theta_h, \theta_v) = G_h(\theta_h) + G_v(\theta_v). \tag{2.5}$$

The eNB must have some knowledge about the channel and the Signal to Noise Ratio (SNR)

of its UE for each RB to be able to determine suitable receive and transmit filter and to perform the scheduling. The instantaneous SNR $\gamma_{j,s}$ of UE j in RB s at TTI n is given by

$$\gamma_{j,s}[n] = \frac{p_s |h_{j,s}|^2}{\sigma^2}, \tag{2.6}$$

where σ^2 denotes the thermal noise power, which is considered constant for all UE.

In practice, the channel is estimated by the UE using pilot symbols transmitted by the eNB. The estimated channel can be modeled according to the model described in [45]:

$$\hat{h}_{j,s}[n] = \sqrt{v} \cdot h_{j,s}[n] + \sqrt{(1-v)} \cdot \eta[n] \tag{2.7}$$

where v is a real number between $(0, 1)$ that represents the quality of the channel estimation ($v = 1$ indicates perfect channel estimation); and $\eta[n]$ models the channel estimation error, modeled as a Zero Mean Circularly Symmetric Complex Gaussian (ZMCSCG) random variable, with $\mathbb{E}|\eta[n]|^2 = \mathbb{E}|h_{j,s}[n]|^2$.

All UE report in periods of θ TTIs and the eNB receives the measure delayed of Δn TTIs. The Channel State Information (CSI) used by the eNB is given by

$$\tilde{h}_{j,s}[n] = \hat{h}_{j,s}[n - \Delta n - (n \mod \delta)] \tag{2.8}$$

In this thesis, we study the CSI imperfections regarding the delay of the measurements. Hence, it is considered that the channels can be perfectly estimated $(v = 1)$ and that the reports are performed at every TTI $(\delta = 1)$.

The Signal to Interference-plus-Noise Ratio (SINR) information available in the eNB is

$$\Gamma_{j,s}[n] = \frac{p_s |\tilde{h}_{j,s}[n]|^2}{\tilde{I}_{j,s} + \sigma^2}, \tag{2.9}$$

where $\tilde{I}_{j,s}$ is the estimation of the interference reported by each UE j to the eNB.

Since it is prohibitive to obtain information about all interference links, thus it is considered that the UE can estimate the instantaneous total interference power, and filter these results along ω TTIs. Interference is estimated regardless of the RBs and is smoothed using an exponential moving average post-filter estimator, which has low complexity. Thus, the estimation of the interference power reported by each UE j to its eNB can be written as

$$\tilde{I}_{j,s}[n] = \left(1 - \frac{1}{\omega}\right) \tilde{I}_{j,s}[n-1] + \frac{1}{\omega} I_{j,s}[n] \tag{2.10}$$

The transmission can fail due to bad channel conditions, wherein the whole information block is lost. Considering $\varphi[n]$ as a binary variable that equals 1 if the transmission fails and 0, otherwise, the BLock Error Rate (BLER) is defined as

$$P_e = \frac{1}{NS} \sum_{k=1}^{N} \sum_{j \in \mathcal{J}} \sum_{s \in \mathcal{S}} \varphi[n] \tag{2.11}$$

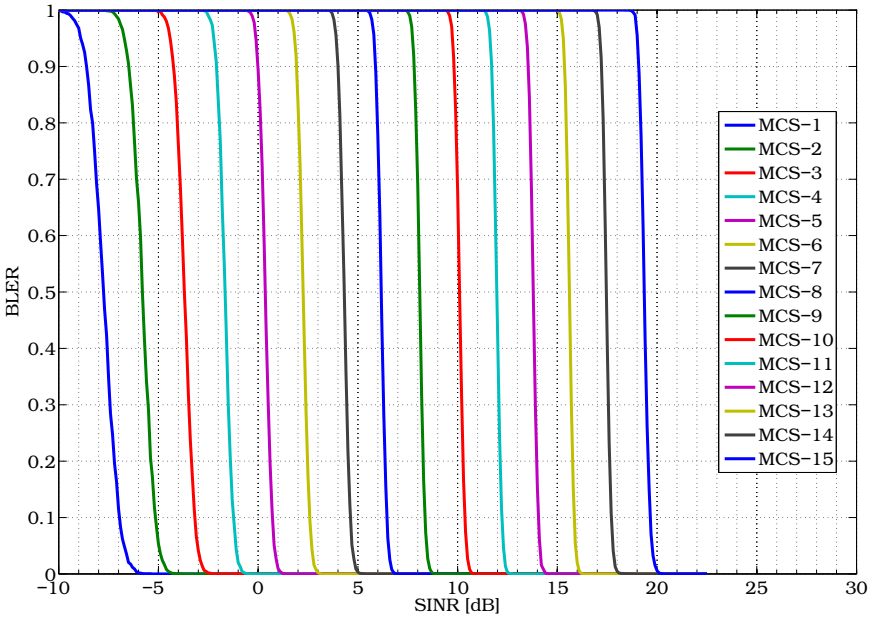

(a) BLER.

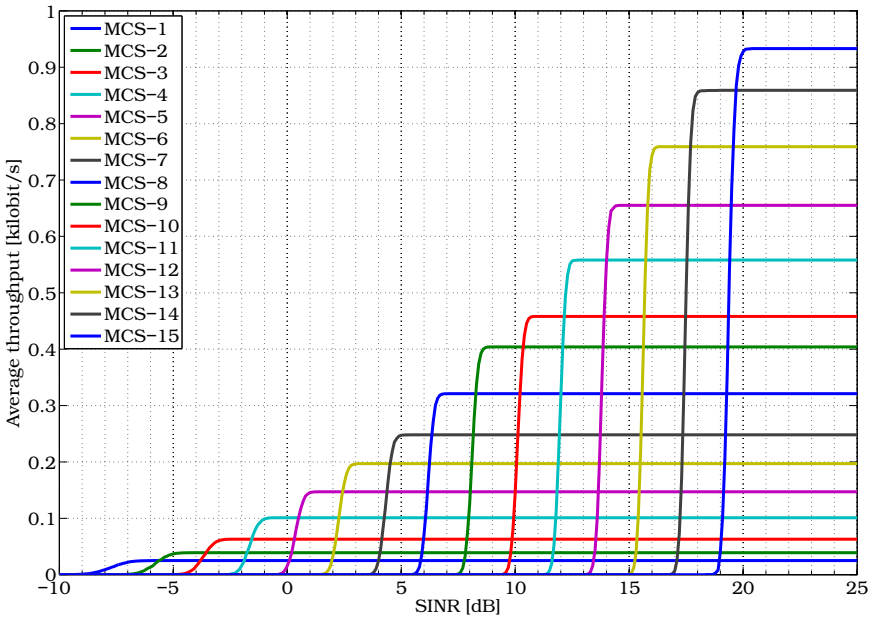

(b) Normalized average throughput.

Figure 2.1: Curves of link-level used for link adaptation.

where N is the number of TTIs of a snapshot.

The link-to-system interface maps the SINR into link-level performance figures of merit, like BLER. The link adaptation scheme selects a proper Modulation and Coding Scheme (MCS) for each link aiming to maximize the throughput for each transmission based on effective gains achieved by the scheduling algorithm. The eNB selects MCS m from a set $\mathcal{M}$ of fifteen MCSs based on different combinations of Quadrature Amplitude Modulation (QAM) and coding rates [39]. Figure 2.1 depicts the BLER and the average throughput curves available for link adaptation, from MCS-1 to MCS-15.

Table 2.1: SINR thresholds for link adaptation [46].

MCS	**Modulation**	**Code rate** [$\times 1024$]	**Rate** [Bits/symbol]	**SINR threshold** [dB]
MCS-1	4-QAM	78	0.1523	-6.2
MCS-2	4-QAM	120	0.2344	-5.6
MCS-3	4-QAM	193	0.3770	-3.5
MCS-4	4-QAM	308	0.6016	-1.5
MCS-5	4-QAM	449	0.8770	0.5
MCS-6	4-QAM	602	1.1758	2.5
MCS-7	16-QAM	378	1.4766	4.6
MCS-8	16-QAM	490	1.9141	6.4
MCS-9	16-QAM	616	2.4062	8.3
MCS-10	64-QAM	466	2.7305	10.4
MCS-11	64-QAM	567	3.3223	12.2
MCS-12	64-QAM	666	3.9023	14.1
MCS-13	64-QAM	772	4.5234	15.9
MCS-14	64-QAM	873	5.1152	17.7
MCS-15	64-QAM	948	5.5547	19.7

The link adaptation interface selects the MCS that yields the maximum average throughput. As defined in [43], a given MCS requires a certain SINR to operate with an acceptably low BLER. By fixing a target desirable value of BLER, the minimum values can be achieved from the link adaptation curves that ensure maintaining the required target BLER. Table 2.1 summarizes the MCSs and their respective SINR thresholds. Observe that the lowest SINR value of -6.2 dB was determined in order to obtain a BLER of 1% on transmissions with MCS-1.

It is regarded different multi-antenna configurations for wireless links: Single Input Single Output (SISO) and Multiple Input Single Output (MISO).

The application layer is the highest layer in the Open Systems Interconnection (OSI) reference model. One important aspect of the application layer is the statistic nature of each traffic type, which is emulated by a suitable traffic model. The traffic models are important for the performance analysis of the network. Several traffic types are envisaged for evaluation within the simulator each one with distinct characteristics. The services considered are full-buffer traffic (Non-Real Time (NRT)) and VoIP (Real Time (RT)). The performance of scheduling algorithms in OFDMA system depends on the considered traffic model.

The full buffer model simulates the worst case scenario, i.e., all users are greedy for resources. The number of users in the cell is constant in each simulation snapshot and the buffers of the users' data flows always have unlimited amount of data to transmit [47]. The full-buffer traffic is a simple and idealized traffic model where the transmit buffer associated with each user has always data to be sent. This model is useful to simulate high loads since the traffic associated to each user has 100% of activity.

The evaluation of RT services is based on the Voice over IP (VoIP) traffic model. It is a conversational service that is an evolution of the old circuit-switched voice service. In this service is assumed that a user within the cellular network is communicating with another user outside the cellular network. The traffic model considers that an average voice activity of 50% where speech and silence periods alternate following a two-state Markov chain depicted in Figure 2.2.

In this figure, ζ and ξ are the transition probabilities from speech to silent and from silent

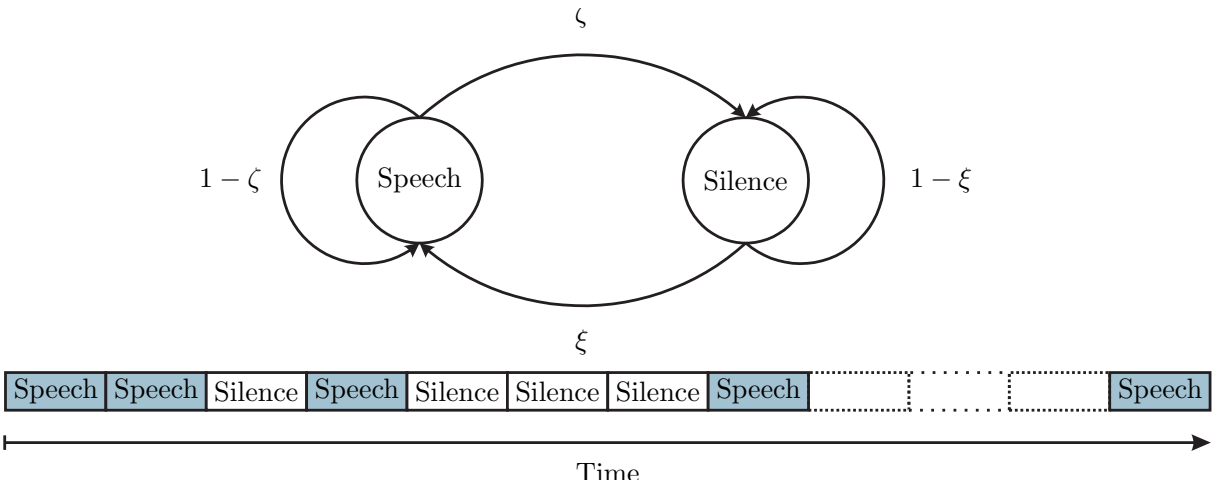

Figure 2.2: VoIP Traffic Model [1].

to speech states, respectively. Note that the call lasts for the whole simulation time since we consider a semi-dynamic simulation paradigm.

Therefore, we consider a 2-state voice activity model to analyze and initially estimate the talk spurt arrival statistics [48]. A talk spurt is the time period between the entering active state and leaving the active state. Table 2.2 provides the parameters of the VoIP traffic that is assumed in the simulations.

Table 2.2: Parameters of the VoIP Traffic Model.

Parameter	Value
Number of States	2 (speech and silent)
Average duration of speech period (t_{on})	3s
Average duration of silent period (t_{off})	3s
Call duration	Simulation time
Encoder frame length	20 ms
Voice activity factor	50%
Average delay requirement	40 ms
Average Frame Erasure Rate (FER) requirement	0.02
Average packet duration	3s
Total voice payload on air interface	320 bits

2.3 Performance Metrics

Defining $t_{j,s,m}$ as the throughput of UE j transmitting on RB s and using MCS m, the total throughput T_j of UE j is given by

$$T_j = \sum_{s=1}^{S} \sum_{m=1}^{M} t_{j,s,m} \kappa_{j,s,m}, \tag{2.12}$$

where $\kappa_{j,s,m} \in \{0, 1\}$ is the binary assignment variable indicating whether the RB s is allocated to UE j using the MCS m.

In order to evaluate the proposed scheduling algorithms in terms of satisfaction, the percentage Y of satisfied users is written as

$$\mathrm{Y} = \frac{J^{\mathrm{sat}}}{J}, \tag{2.13}$$

where J^{sat} is the number of satisfied users in the cell. An NRT user is considered satisfied if its session throughput is equal or higher than a threshold ($T_j[n] \geq T_j^{\text{req}}$). An RT user is considered satisfied if its FER is equal or lower than a threshold ($d_j[n] \leq d_j^{\text{req}}$). It is assumed that a frame is lost if a packet arrives at the receiver later than the delay budget [26]. According to [48], a VoIP user is considered not satisfied if 98% radio interface tail latency of the user is greater than 50 ms. This assumes an end-to-end delay below 200 ms for mobile-to-mobile communications.

The Jain's index is used to evaluate the scheduling techniques in terms of fairness. For a generic Quality of Service (QoS) metric $\mathbf{x} = [x_1, \cdots, x_j, \cdots, x_J]$, Jain's fairness index can be written as

$$F(\mathbf{x}) = \frac{\left(\sum_{j=1}^{J} x_j\right)^2}{J \cdot \sum_{j=1}^{J} x_j^2}, \tag{2.14}$$

Jain's fairness index is independent of scale and is bounded between $1/J$ and 1. A totally fair allocation (with all x_j's equal) has fairness equal to 1, while a totally unfair allocation (with all resources given to only one user), has fairness equal to $1/J$. For NRT services, x_j is given by the throughput $T_j[n]$. For RT services, x_j corresponds to the Head Of Line (HOL) delay.

2.4 Comparison Algorithms

The Rate Maximization (RM) [49] algorithm for OFDMA systems aims to maximize the sum of data rates of the users subject to a maximum transmission power constraint. The user with index $j^\star$ is chosen to receive on resource s in TTI n if it satisfies

$$j^\star = \arg\max_j \{t_{j,s}\}. \tag{2.15}$$

This algorithm assigns each resource to the user that has the highest channel gain on it and, therefore, it is a pure opportunistic policy.

The Proportional Fair (PF) scheduler performs a trade-off between fairness and throughput [18].It tries to serve users with favorable radio conditions in order to provide a high instantaneous throughput relative to their average throughput. The user with index $j^\star$ is chosen to receive on resource s in TTI n according to

$$j^\star = \arg\max_j \left\{ \frac{t_{j,s}[n]}{T_j[n]} \right\}. \tag{2.16}$$

The Modified Largest Weighted Delay First (MLWDF) [50] policy selects the users to receive on resource s in TTI n according to

$$j^\star = \arg\max_j \left\{ d_j^{\text{hol}}[n] \frac{t_{j,s}[n]}{T_j[n]} \right\}. \tag{2.17}$$

This resource allocator is specially suitable for RT services, since it regards the HOL packet delay in its formulation.

The Urgency and Efficiency-based Packet Scheduling (UEPS) [51] algorithm is utility-based. It uses the relative status of the current channel to the average one as an efficiency indicator of

radio resource usage and the time utility as a urgency factor. For the UEPS criterion, the user with index $j^\star$ is chosen to receive on resource s on TTI n according to

$$j^\star = \arg\max_j \left\{ \left| U'(d_j^{\text{hol}}[n]) \right| \cdot \frac{t_{j,s}[n]}{T_j[n]} \right\}. \tag{2.18}$$

more details about the utility function U are given in the next chapter.

2.5 Simulator Description

This section presents the architecture of a semi-dinamic system-level simulator developed to evaluate an OFDMA-based Radio Access Network (RAN). The simulator is composed of three parts: initialization, main loop and results processing. In the initialization, all the simulation objects and data structures are created, such as UE, eNB, cellular grid and channel fading maps. In the main loop the simulation time is advanced and the state of simulation parameters are updated according to the dynamics of the system. Finally, in the results processing the simulation objects are processed in order to obtain statistics necessary to analyse the system's performance. Through the evaluation of these statistics the system performance can be optimized by the proposal of new RRM strategies.

Figure 2.3 depicts the main elements of the simulation. In the beginning of the flow-chart, there are the steps 01 and 02 that create the simulator objects (e.g., the set of UE $\mathcal{J} = \{1, 2, \cdots, J\}$) and generate the channel fading map ($h_{j,s}$). The steps inside the main loop (04 to 09) are the core of the simulator. The essential tasks performed are:

- step 04: take the channel state and CSI available at the transmitter and receiver to provide fundamental information to scheduling procedures, perform data reception and verify if there were errors in the received data packets;
- steps $05 - 06$: check traffic state aiming to evaluate if new packects should be generated. The packet size and packet generation frequency depends of the type of service, like NRT or RT;
- step 07: exploiting the available information of channel and traffic, the scheduling algorithm define the distribution of resources according to QoS requirements;
- step 08: after the assignment of resources, the data reception is performed to evaluate if the data packets were successfully transmitted; the received SINR is calculated according to (2.9) and mapped to the link-to-system curves to estimate packet error probabilities;
- step 09: according to the amount of data that was correctly received, the transmitter buffer of the eNB with respect to each connected UE is updated.

Finally, step 10 processes and step 11 saves the simulation data in order to obtain statistics that will be useful to analyse the system performance.

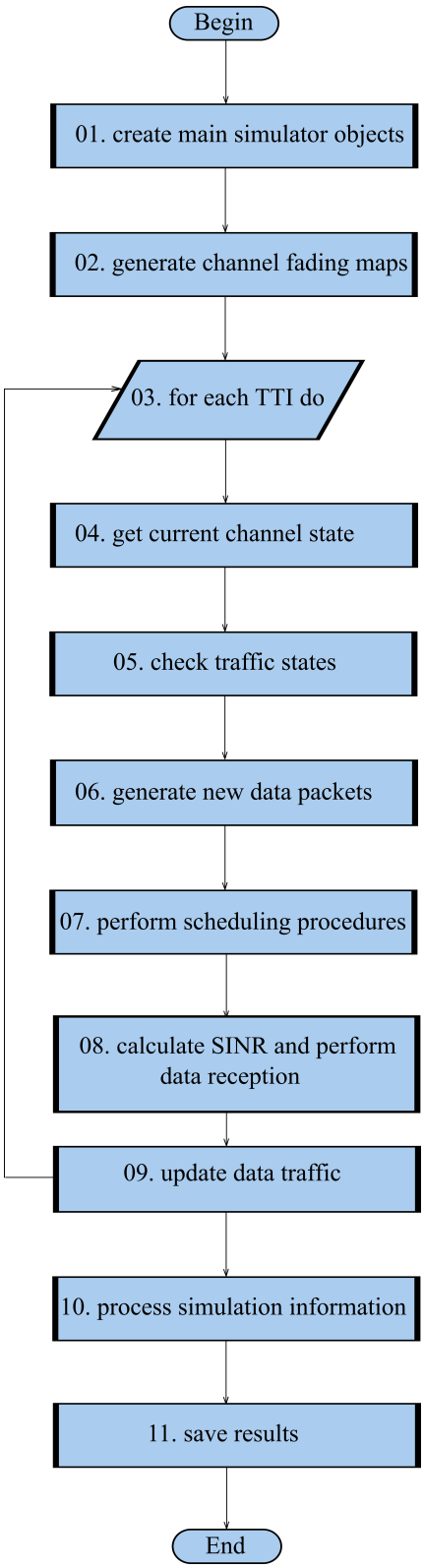

Figure 2.3: Simulator flow-chart.

Chapter 3

Scheduling Framework to Improve User Satisfaction

In this chapter, the problem of maximizing the user satisfaction is investigated. Section 3.1 presents the general optimization formulation and the utility-based scheduling framework. Section 3.2 details the studied algorithms, describing the different utility functions considered to develop the framework. Sections 3.3 and 3.4 evaluate the proposed algorithms and Section 3.5 provides a partial conclusion based on the observed performance results.

3.1 General Utility-Based Scheduling Framework

Utility theory allows to connect the Physical Layer (PHY) and the Medium Access Control (MAC) sublayer to achieve cross-layer optimization [19]. This theory is a flexible tool to deal with different trade-offs, like capacity versus fairness or capacity versus satisfaction.

In this study, we consider a general scheduling framework that is able to maximize the degree to which a network satisfies service requirements of users' applications in terms of throughput and delay. The general optimization problem is formulated as

$$\max_{\mathcal{S}_j} \sum_{j=1}^{J} U\left(x_j[n]\right), \tag{3.1a}$$

$$\text{subject to} \quad \bigcup_{j=1}^{J} \mathcal{S}_j \subseteq \mathcal{S}, \tag{3.1b}$$

$$\mathcal{S}_i \bigcap \mathcal{S}_j = \emptyset, \quad i \neq j, \forall i, j \in \{1, \ldots, J\}, \tag{3.1c}$$

where $\mathcal{S}$ is the set of all resources in the system, J is the total number of User Equipment (UE), $\mathcal{S}_j$ is the subset of resources assigned to the UE j, and $U\left(x_j[n]\right)$ is a utility function based on a generic Quality of Service (QoS) metric $x_j[n]$ measured in the Transmission Time Interval (TTI) n.

The constraints (3.1b) and (3.1c) state that the union of all subsets of resources allocated to different users must be limited to the total set of resources available in the system and that the same resource cannot be shared by two or more users in the same TTI, respectively.

It is demonstrated in [20] that a simplified optimization problem can be derived from the

original one given by (3.1). According to this simplification, the objective function of (3.1) becomes linear in terms of the instantaneous user's data rate and the problem is characterized as a weighted sum rate maximization, whose weights are adaptively controlled by the marginal utilities. The objective function of the simplified problem is given by

$$\max_{S_j} \sum_{j=1}^{J} U'(x_j[n]) \cdot R_j[n], \tag{3.2}$$

where $R_j[n]$ is the instantaneous data rate of UE j and $U'(x_j)$ is the first derivative of the utility function of the UE j with respect to the QoS metric.

The study in [20] established that if we consider a fixed power allocation, the scheduling is based on the selection of the user with index $j^\star$ to receive on the resource s in TTI n according to

$$j^\star = \arg\max_j \left\{ w_j \cdot r_{j,s}\,[n] \right\}, \tag{3.3}$$

where w_j is the utility-based weight of UE j and $r_{j,s}$ is the instantaneous achievable transmission rate of user j with respect to Resource Block (RB) $s \in \mathcal{S}$.

This work aims to formulate general scheduling algorithms suitable for maximizing the satisfaction of different types of services. Therefore, the variable x_j can be either the users' average data rates (throughput) or the users' Head Of Line (HOL) packet delay, which are QoS metrics suitable for Non-Real Time (NRT) and Real Time (RT) services, respectively.

In the one hand, if the UE j has NRT service, the marginal utility is given by

$$w_j^{NRT} = \frac{\partial U}{\partial T_j}\Big|_{T_j = T_j[n-1]} \tag{3.4}$$

where $T_j[n-1]$ is the average throughput of UE j calculated up to the previous TTI, i.e., TTI $n-1$. On the other hand, if j has a RT service, the marginal utility is obtained by

$$w_j^{RT} = \Big| \frac{\partial U}{\partial d_j^{HOL}}\Big|_{d_j^{HOL}[n] = d_j^{HOL}[n]} \Big|, \tag{3.5}$$

where d_j^{HOL} is the HOL packet delay of UE j in the TTI n.

Therefore, the utility-based weights (3.4) and (3.5) provide sufficient information to allocate the resources to the users leading to a QoS-based scheduling with low complexity. In fact, all necessary computations to allocate resources according to these equations are simple operations:

i. calculation of the marginal utility per user,

ii. calculation of the product between the marginal utility per user and instantaneous data rate, and

iii. sorting the users by this product value in (3.3) on each resource.

If more than one user has the same priority, a tiebreaker process selects the user with the highest Signal to Noise Ratio (SNR).

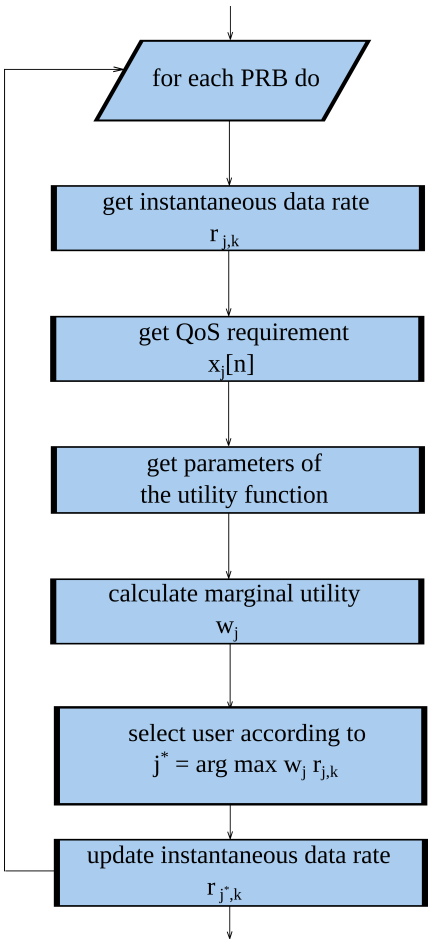

Figure 3.1: Utility-based scheduling algorithm flow-chart.

Figure 3.1 depicts the utility-based scheduling procedure mentioned on the simulator flow-chart described on Chapter 2.

3.2 Maximization of User Satisfaction Using Suitable Utility Functions

3.2.1 TSM/DSM Based on the Logistic Function

The authors of [26] proposed two utility-based scheduling algorithms able to maximize the number of satisfied users in a 4$^{\text{th}}$ Generation (4G) cellular system. The first one is the Throughput-based Satisfaction Maximization (TSM) algorithm , whose formulation is based on the users' throughput and which is suitable for NRT services. The second one is the Delay-based Satisfaction Maximization (DSM) algorithm, whose formulation is based on the users' HOL packet delay and which is suitable for RT services.

The TSM and DSM algorithms originally used a sigmoid utility function based on a generic QoS metric $x_j[n]$ of the UE j. In this work, the sigmoid is written as the logistic function. This change wants to consider a function continuously differentiable over the interval of $x_j[n]$ and limited between 0 and 1. The logistic function is given by

$$U^{\text{Lo}}(x_j^\star[n]) = \frac{1}{1 + e^{\mu(x_j^\star[n] - x_j^{\star\text{req}})/\sigma}}, \tag{3.6}$$

where $x_j^\star$ is the current QoS metric; σ is a nonnegative parameter that sets the shape of the logistic function and μ is a constant which determines if the function is ascending ($\mu = -1$) or

descending ($\mu = 1$).

Without loss of generality, it is established that x_j is normalized by the QoS requirement. Considering NRT services $x_j = T_j^{\star}/T_j^{\star\text{req}}$ and $T_j^{\text{req}} = T_j^{\star\text{req}}/T_j^{\star\text{req}} = 1$. Considering RT services, it is established that $x_j = d_j^{\star}/d_j^{\star\text{req}}$ and $d_j^{\text{req}} = d_j^{\star\text{req}}/d_j^{\star\text{req}} = 1$. Therefore, $U^{\text{Log}}(x_j^{\star}[n])$ is simply replaced by $U^{\text{Log}}(x_j[n])$ hereafter.

The TSM algorithm employs an increasing step-shaped utility curve centered at x_j^{req}. As indicated on Figure 3.2(a) by the solid line, a user becomes satisfied rapidly if its throughput approaches the requirement. The opposite occurs when the user throughput decreases to values lower than the requirement. This behavior is in accordance with the definition of satisfaction for NRT services generally found in the literature [26].

The DSM algorithm employs a decreasing step-shaped function, as indicated on Figure 3.2(a) by the dashed line. A given user becomes unsatisfied rapidly if the HOL packet delay approaches or exceeds the delay requirement. The opposite occurs when the user delay decreases to values below the requirement.

In this study, we establish that the logistic is equal to a given value δ when the QoS metric x_j achieves a proportion ρ of the QoS requirement x_j^{req}. Therefore, the shape parameter of the logistic function is given by

$$\sigma = \frac{\mu \cdot (\rho - 1) \cdot x_j^{\text{req}}}{\log\left(\frac{1}{\delta} - 1\right)}. \tag{3.7}$$

Regarding the NRT utility function, we achieved satisfactory results when $\delta = 0.01$, $\rho = 0.50$ and $x_j^{\text{req}} = 1$. The NRT function starts to increase noticeably, i.e., $U(x_j) = \delta = 0.01$, when x_j is half of the QoS requirement, i.e., $x_j = \rho \cdot x_j^{\text{req}} = 0.50$. Using (3.7), we have that $\sigma_{\text{TSM}} = 0.1088$. For the case of RT services, the utility function starts to decrease noticeably, i.e., $U_j(x_j) = 0.99$, when x_j is half of the QoS requirement, i.e., $x_j = \rho \cdot x_j^{\text{req}} = 0.50$. Using (3.7), we also obtained $\sigma_{\text{DSM}} = 0.1088$. Figure 3.2(a) shows the curves obtained using this strategy to determine the parameter adjustment.

The utility-based weight performs an important function in the scheduling algorithm, once

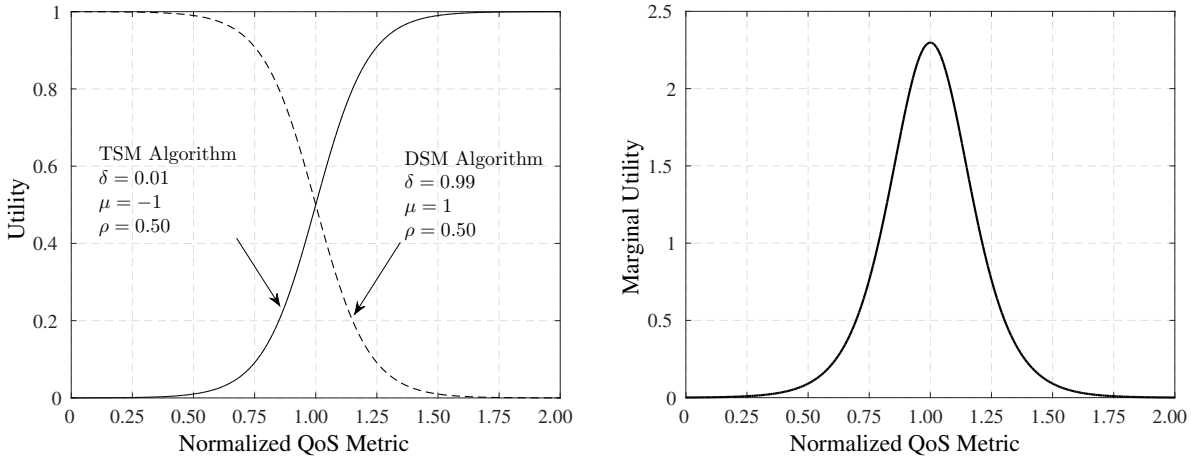

(a) Utility functions **(b)** Marginal utility function

Figure 3.2: Original curves of TSM and DSM algorithms using the parameter adjustment described by (3.7).

the priority of a given user to get a resource is directly proportional to this weight. The utility-based weight in (3.3), based on a generic QoS metric x_j of the UE j, is given by the marginal utility, which is the first derivative of the utility function $U(x_j[n])$ with respect to the QoS metric $x_j[n]$, i.e., $w_j = \dfrac{\partial U(x_j[n])}{\partial x_j[n]}$. Therefore, the logistic marginal utility is given by

$$w_j^{\text{Lo}} = \frac{\mu e^{\mu(x_j[n]-x_j^{\text{req}})/\sigma}}{\sigma(1+e^{\mu(x_j[n]-x_j^{\text{req}})/\sigma})^2}. \tag{3.8}$$

The particular expression of w_j^{Lo} must be used in the corresponding scheduler algorithm given by (3.3). The marginal utility represented by (3.8) is a bell-shaped function, which is a symmetric function centralized at the $x_j^{\text{req}} = 1$. Figure 3.2(b) indicates the marginal utility function achieved with this parametrization. Since we use normalized values of x_j and the adjustment of the parameter results in the same value $\sigma = 0.1088$ for RT and NRT services, the utility-based weight curve is equal for TSM and DSM algorithms. The users who have a higher priority in the scheduling process are the ones experiencing QoS levels close to the QoS requirement.

The study performed in [26] demonstrates that it is possible to provide high user satisfaction for NRT and RT users with low complexity if we consider the logistic function as the utility function in the scheduling. The present work extends the utility-based framework, employing a new utility function, called shifted log-logistic, which has more parameters and provides conditions to manage the resources more efficiently.

3.2.2 MTSM/MDSM Based on the Shifted Log-Logistic Utility Function

Utility functions are used to solve scheduling optimization problems for different applications, building a bridge among several layers of the wireless communication system [19]. Previous studies employed different utility functions, like exponential and logarithm [52]. After an extensive research of utility functions with different properties, like laplace, cauchy, dirichlet, beta [53], the author achieved interesting results with the shifted log-logistic utility function, a continuously differentiable function of the QoS metric x_j, represented by

$$U^{\text{S-Log}}(x_j[n]) = \frac{1}{1+\left(1+\dfrac{\theta\eta}{\lambda}(x_j[n]-x_j^{\text{req}})\right)^{-1/\theta}}, \tag{3.9}$$

where $x_j[n]$ is the normalized QoS metric and x_j^{req} is the QoS requirement of the UE j; θ is a real parameter which determines the shape of the curve; λ is a real parameter that sets the scale of the function; and η is a constant which asserts if the function is ascending ($\eta = 1$) or descending ($\eta = -1$).

According to the value of the shape parameter θ, the shifted log-logistic utility function is determined at different $x_j[n]$ intervals:

i. $x_j[n] \geq x_j^{\text{req}} - \dfrac{\lambda}{\theta}$, if $\theta > 0$;

ii. $x_j[n] \in (-\infty, \infty)$, if $\theta = 0$;

iii. $x_j[n] \leq x_j^{\text{req}} - \dfrac{\lambda}{\theta}$, if $\theta < 0$.

Exploiting the properties of the shifted log-logistic utility function, the new scheduling schemes called Modified Throughput-based Satisfaction Maximization (MTSM) and Modified Delay-based Satisfaction Maximization (MDSM) are able to deal with the scheduling more efficiently, giving more flexibility to the framework and making possible to improve of the user satisfaction for NRT and RT services, respectively.

It is important to consider the reasons of the choice of the shifted log-logistic utility function. Firstly, this function is continuously differentiable over the range $x_j[n]$ and limited between 0 and 1, i.e., $0 \leq U^{\text{S-Log}} \leq 1$. Secondly, it has two parameters, θ and λ that clearly impact its behavior, allowing different Radio Resource Allocation (RRA) strategies to be configured by a suitable parameter setting, as it will be shown in this study.

The MTSM algorithm employs an increasing step-shaped utility curve centered at T_j^{req}. This behavior is in conformity with the definition of satisfaction for NRT services used previously in the TSM algorithm: a user is quickly satisfied if its throughput approaches to the requirement; or its satisfaction decreases to lower values when distant from the requirement. However, this new function has a different range of variation in comparison with the original sigmoid, as shown in Figure 3.3(a). As it can be seen, the proposed utility function has constant values when the values of x becomes distant of the required value, x_{req}.

The MDSM algorithm employs a decreasing step-shaped function, since users' utility derived from the network is lower when the delay is higher. As previously defined for the DSM algorithm, a given user becomes unsatisfied rapidly if the HOL packet delay approaches and exceeds the delay requirement. The opposite occurs when the user delay decreases to values below the requirement. Figure 3.3(b) indicates that for RT services we also have intervals where the utility has constant values.

In this study, we establish a rule to determine the scale parameter λ as function of the QoS requirement. The shifted log-logistic is equal to a given value δ when the QoS metric x_j achieves

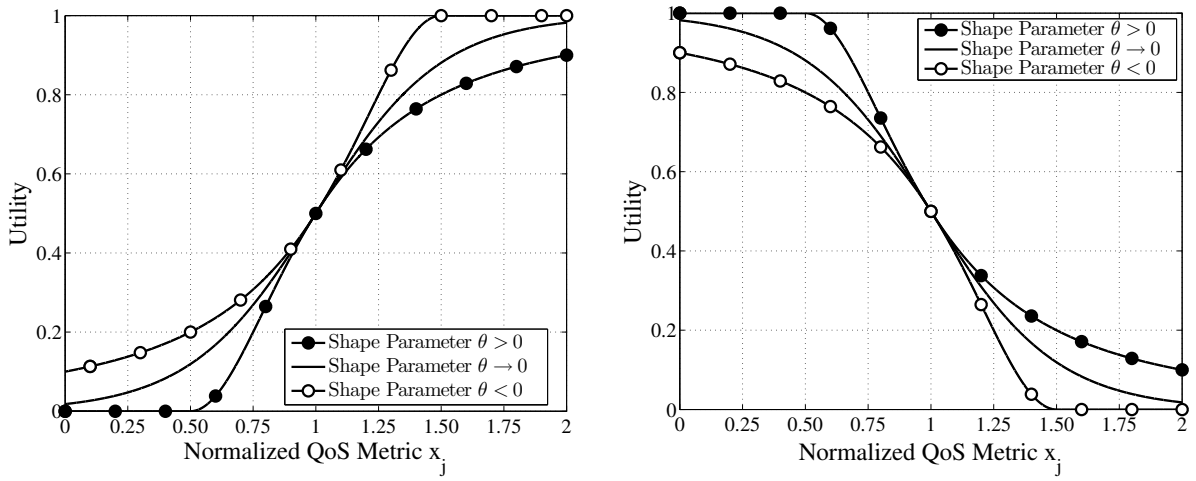

(a) NRT services. **(b)** RT services.

Figure 3.3: Utility functions with scale parameter $\lambda = 1$ and using different values of shape parameter.

a proportion ρ of the QoS requirement x_j^{req}. Therefore, the scale parameter is given by

$$\lambda = \frac{\theta\eta x_j^{\text{req}}(\rho - 1)}{\left(\frac{\delta}{1-\delta}\right)^{\theta} - 1}. \tag{3.10}$$

Considering the NRT utility function, satisfactory results have been achieved when the curve starts to increase noticeably, i.e., $U_j(x_j) = \delta = 0.01$, when x_j is half of the QoS requirement, i.e., $x_j = \rho \cdot x_j^{\text{req}} = 0.50$. Using $\theta \to 0$ in (3.10), follows that $\lambda_{\text{MTSM}} = 0.1088$. Regarding RT services, the utility function starts to decrease significantly, i.e., $U_j(x_j) = 0.99$, when x_j is half of the QoS requirement, i.e., $x_j = \rho \cdot d_j^{\text{req}} = 0.50$. Using $\theta \to 0$ in (3.10), is obtained that $\lambda_{\text{MDSM}} = 0.1088$.

The shifted log-logistic function has the marginal utility given by

$$w_j^{\text{S-Log}} = \frac{\frac{\eta}{\lambda}\left(1 + \frac{\theta\eta}{\lambda}(x_j[n] - x_j^{\text{req}})\right)^{-1-1/\theta}}{\left(1 + \left(1 + \frac{\theta\eta}{\lambda}(x_j[n] - x_j^{\text{req}})\right)^{-1/\theta}\right)^2}. \tag{3.11}$$

It is important to observe that the shifted log-logistic is a generalization of the logistic function, since $w_j^{\text{S-Log}} \to w_j^{\text{Lo}}$ when $\theta \to 0$. More details are provided in Appendix B.

The format of marginal utility functions impacts the scheduling algorithms, determining suitable arrangements to improve the users' satisfaction. For comparison purposes and without loss of generality, the symmetric format achieved when $\lambda = 0.1088$ and $\theta \to 0$ is established as the standard marginal utility, i.e., the TSM/DSM original bell-shaped curve, as indicated in Figure 3.4. This particular set of parameters ensures that the curves are equivalent to that considered in [26].

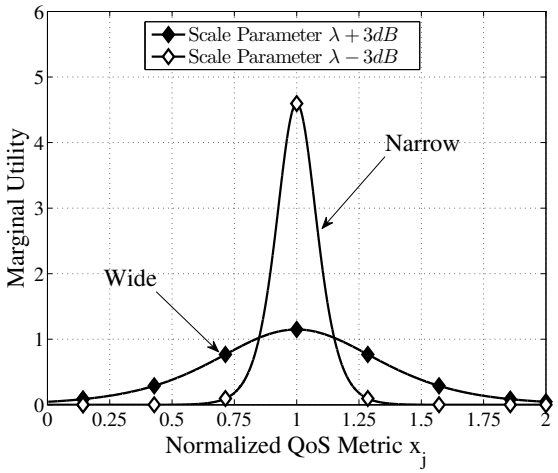

Figure 3.4: Symmetric marginal utility functions, narrower or wider, $\lambda + 3dB$ and $\lambda - 3dB$, respectively.

To simplify the analysis, we consider separately the effect of variation of each parameter in the marginal utility curve. Firstly, the shape parameter is fixed at lower values, $\theta \to 0$. The reference value of λ is given by 0.1088. When this value is increased, the curve becomes more flattened. In the opposite, smaller values of λ impose a narrower function. These parameter adjustments allow the proposed algorithms (MTSM and MDSM) to prioritize users in different

ways, thereby avoiding them to become unsatisfied. Secondly, the scale parameter is fixed in $\lambda = 0.1088$ and the shape parameter θ is varied between -1 and 1. When $\theta = 1$, the curve is right-tailed, i.e, extremely aligned to the right side and $w_j = 0$ when $x_j < x_j^{req}$. Oppositely, if $\theta = -1$, the curve is left-tailed, extremely aligned to the left side and $w_j = 0$ when $x_j > x_j^{req}$, as indicated in Figure 3.5(a). When the shape parameter has the absolute value 1, the curve has a sharp edge. Whth intermediary values of the shape parameter, $|\theta| = 0.5$, smoother edges in the curves are achieved, and also skewed to the left and right. The resultant functions are shown in Figure 3.5(b).

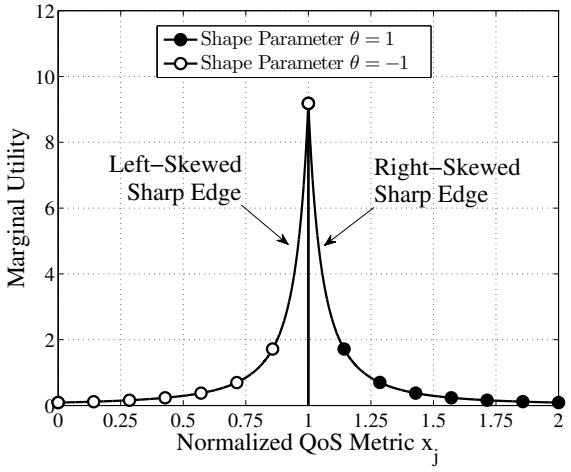

(a) Asymmetric marginal utility functions with sharpe edges, right-skewed $\theta = 1$; and left-skewed $\theta = -1$.

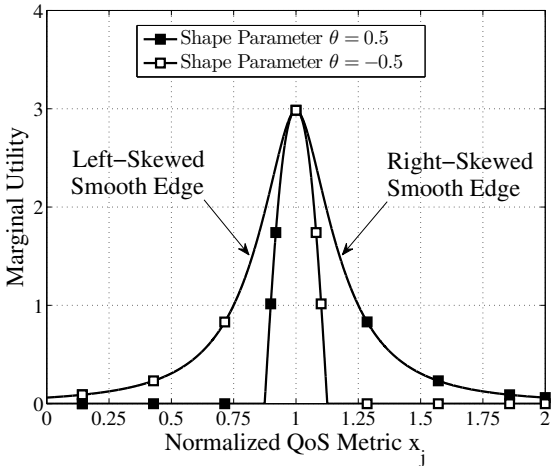

(b) Asymmetric marginal utility functions with soft edges, right-skewed $\theta = 0.5$, and left-skewed $\theta = -0.5$.

Figure 3.5: Shifted log-logistic marginal utility functions with different values of shape parameter θ. The scale parameter is fixed at $\lambda = 0.1088$.

3.3 Performance Evaluation of MTSM Algorithm

Initially, we evaluate the MTSM scheduler considering the effect of the changes of the shifted log logistic function parameters, extending the analysis made in [26]. Table 3.1 presents the main parameters of the simulated Long Term Evolution (LTE)-like system network.

3.3.1 Perfect CSI

The MTSM algorithm is analyzed considering the effect of the scale parameter λ in symmetric marginal utilities. In order to carry out this analysis, consider the shape parameter fixed at $\theta \rightarrow 0$. The effect of the variation of the scale parameter is shown in Figure 3.4. The increment of λ results in a more flattened curve. On the other hand, the decrement of λ results in a narrower curve. Therefore, five different marginal utility curves are simulated: *wider* ($\lambda = 90\,dB$), *wide* ($\lambda = 30\,dB$), TSM (original) ($\lambda = -10\,$dB), *narrow*($\lambda = -30\,dB$), *and narrower* ($\lambda = -60\,dB$). Since the range of values of the scale parameters is very large, we use dB to represent them.

Figures 3.6(a) and 3.6(b) depict the percentage of satisfied users as function of the number of NRT users in the system. Variations in a smaller range of the scale parameter do not cause significant changes in the users' satisfaction levels in comparison with the original TSM. Only huge variations of the scale parameter λ are capable of modifying the level of satisfaction.

Table 3.1: Simulation Parameters of MTSM Evaluation

Parameter	**Value**
Maximum BS transmit power	20 W
BS antenna radiation pattern	Three-sectored
Cell radius	1 km
UE speed	3 km/h
Carrier frequency	2 GHz
System bandwidth	5 MHz
Sub-carrier bandwidth	15 kHz
Number of RBs	25 NRT
Path loss - macro cell scenario [3]	$PL = 15.3 + 37.6 \cdot \log_{10}(d)$ [a]
Path loss - urban macro scenario [2]	$PL = 34.5 + 35 \cdot \log_{10}(d)$ [a]
Channel coherence time	90 ms
Antenna gain[b][44]	$G_h(\theta_h) + G_v(\theta_v)$
Downtilt angle	8 degrees
Log-normal shadowing st. dev.	8 dB
Small-scale fading [43]	3GPP Typical Urban
AWGN power per sub-carrier	-123.24 dBm
Noise figure	9 dB
Link adaptation	Link level curves from [39]
SNR threshold of MCS 1 [39]	-6.9 dB
Transmission Time Interval	1 ms
NRT traffic model	Full buffer
User throughput requirement	512 kbps
Multi-antenna configuration	SISO
Simulation time span	10 s
Number of simulation runs	50
Confidence Interval	95%

[a] d is the distance to the BS in km.
[b] θ_h and θ_v represent the horizontal and vertical angles related to the Base Station (BS), respectively.

However wider and narrower curves cannot achieve gains. Oppositely, these modifications of λ resulted in reductions of the satisfaction levels. This behavior occurs because the values of marginal utility of the users distant of the requirement became of the same order, consequently the scheduling of resources is determined by channel conditions, only the users with the higher instantaneous rates are chosen.

Different channel propagation conditions are considered, a macro cell scenario [3] and an urban macro scenario [2]. As expected, there are impacts on the satisfaction levels achieved by the different algorithm configurations. The worsening of channel conditions decreases the satisfaction levels and the proposed MTSM algorithm is more impacted than TSM. They start from a tie situation in Figure 3.6(a) to a difference of 20% in Figure 3.6(b).

Figures 3.6(c) and 3.6(d) show the system capacity in terms of total throughput as a function of the number of NRT users. A small increase of scale parameter λ provides a gain for lower loads that disappears with the increasing number of users, as it can be seen in the wide curve. The wider curve, which is achieved with a huge value of λ, has a flat marginal utility function, and consequently users have utility weights of approximately the same order. Since the scheduling also depends on the instantaneous data rate, this factor becomes more significant than the marginal utility in the allocation process, which tends to a less equitable distribution of resources, concentrating them with the users with best radio link quality.

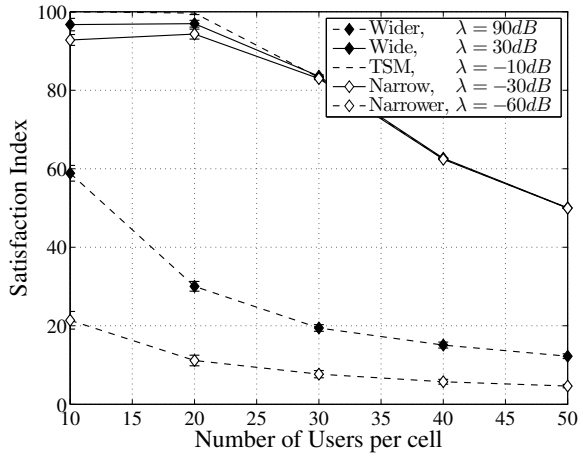

(a) User Satisfaction - macro cell scenario [3].

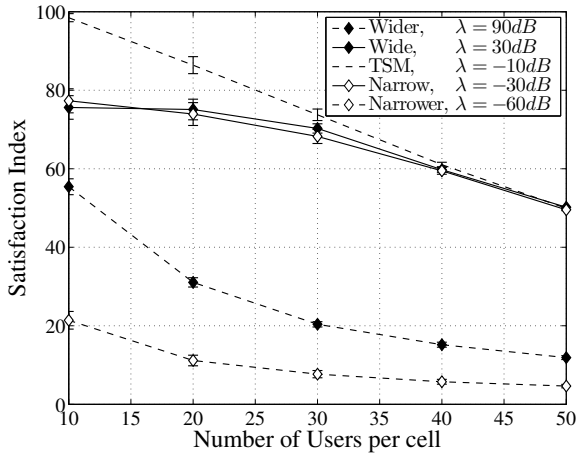

(b) User Satisfaction - urban macro scenario [2].

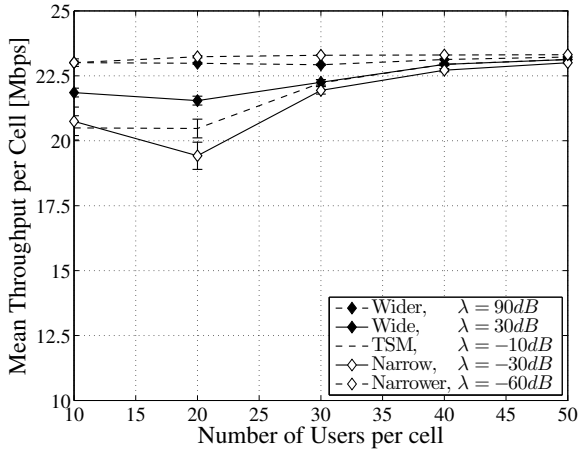

(c) Total cell throughput - macro cell scenario [3].

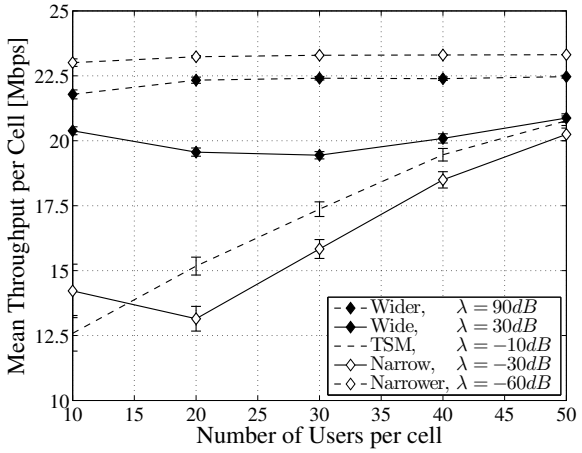

(d) Total cell throughput - urban macro scenario [2].

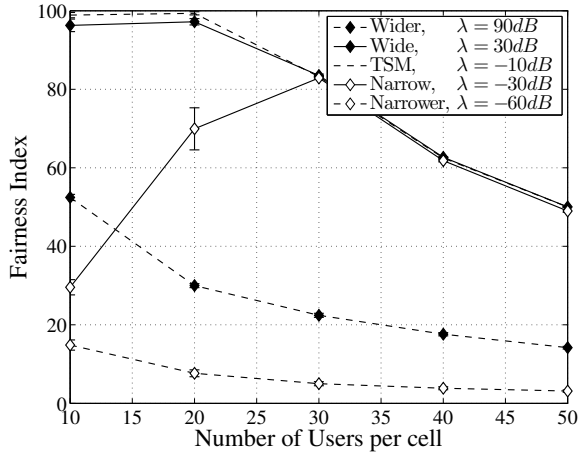

(e) Mean cell fairness index - macro cell scenario [3].

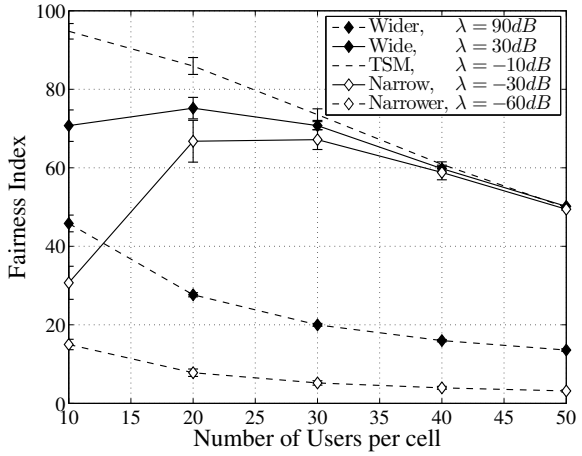

(f) Mean cell fairness index - urban macro scenario [2].

Figure 3.6: Performance metrics of the MTSM algorithm as a function of the number of NRT users with different values of scale parameter, λ.

The decrease of λ causes a narrowing of the marginal utility curve. The narrow curve allocates resources only to users near to the QoS requirement, penalizing users with lower values of throughput . For example, users that present high throughput will not be selected because their utility-based weights tends to zero. The narrower curve is an extreme situation, because only users with the exact QoS requirement have non-zero utility. In this case, almost

all users are tied and the tiebreaker is based on the SNR. Therefore, the scheduling algorithm is similar to Rate Maximization (RM).

As mentioned in the discussion of the results of satisfaction, the system capacity also is impacted by the channel propagation conditions. The configurations with extreme values of scale parametes (wider and narrower) suffer little impact since these settings schedule users with the best conditions. But the other configurations (wide and narrow) are clearly more affected, with a decrement of 50% of the mean throughput per cell for small loads from Figure 3.6(c) to 3.6(d).

The fairness of the TSM algorithm followed the behavior observed for the satisfaction levels, as it can be seen in Figure 3.6(e) and 3.6(f). As verified for the other metrics, there is a decrement with the change of channel condition from macro cell scenario [3] to urban macro scenario [2]. The wider and narrower configurations of MTSM are little affected, maintaining low values compared with the other ones. The configuration with $\lambda = -30dB$ (narrow) distributes resources to users near to the requirement. With a small number of users this results in an uneven distribution of resources that is reduced with the increment of the system load. This behavior can be observed in both propagation scenarios.

Therefore, the results showed that the modification of the scale parameter λ of the shifted log-logistic utility function (i.e., symmetric marginal utility curves) allows the observation of different behaviors of the scheduling algorithm , however it is not able to provide an improvement of the satisfaction index of the system in comparison with the original TSM algorithm.

From now on, we analyze the effect of the change of the shape parameter θ of the marginal utility function given by (3.11). Positive values of the shape parameter, $\theta > 0$, result in a curve with the tail directed to the right side. In the opposite, negative values $\theta < 0$ imply in a tail directed to the left side. The magnitude of the scale parameter, θ, also determines the behavior of the function when the values are near the QoS requirement: higher values of the shape parameter, $|\theta| = 1$, result in curves with sharper edges; lower values, $|\theta| = 0.5$, imply in smoother peaks.

TSM uses a symmetric bell-shaped curve according to Figure 3.2(b). The scale parameter is fixed at $\lambda = 0.1088$. The simulated configurations of MTSM are given by the curves shown in the Figures 3.5(a) and 3.5(b). Thus, five different marginal utility curves are analyzed: right skewed with sharp edge ($\theta = 1$), right skewed with soft edge ($\theta = 0.5$), bell-shaped ($\theta \to 0$), left skewed with soft edge ($\theta = -0.5$), left skewed with sharp edge ($\theta = -1$).

Figures 3.7(a) and 3.7(a) depict the percentage of satisfied users as a function of the number of NRT users in the system. The symmetric configuration (TSM) avoids the users to become unsatisfied because it gives the same priority to users with QoS levels just above or just below the QoS requirement. The asymmetric curves give different priority to such users. That difference in the distribution of priorities allows us to obtain an increase in the satisfaction levels. While right skewed curves benefit users with the highest throughputs, left skewed ones benefit users with throughput below the requirement. The highest gains in the satisfaction levels are achieved with the left skewed configurations, hence giving more

resources to users with low throughput improves their condition to get resources. The right skewed and symmetric configurations have similar users' satisfaction behavior, since they benefit users with the best channel conditions.

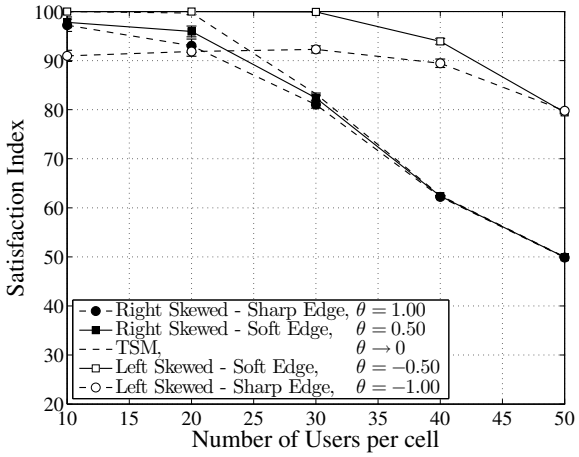

(a) User Satisfaction - macro cell scenario [3].

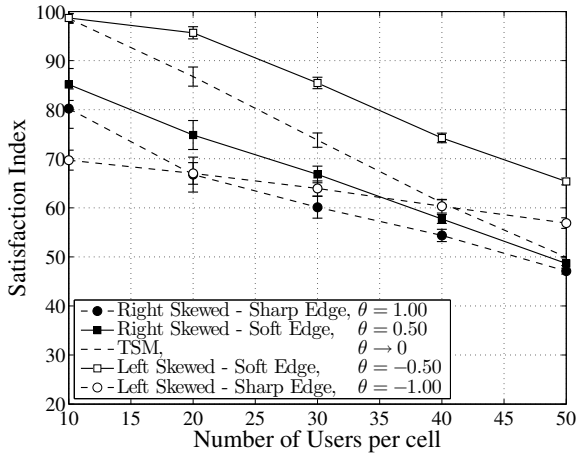

(b) User Satisfaction - urban macro scenario [2].

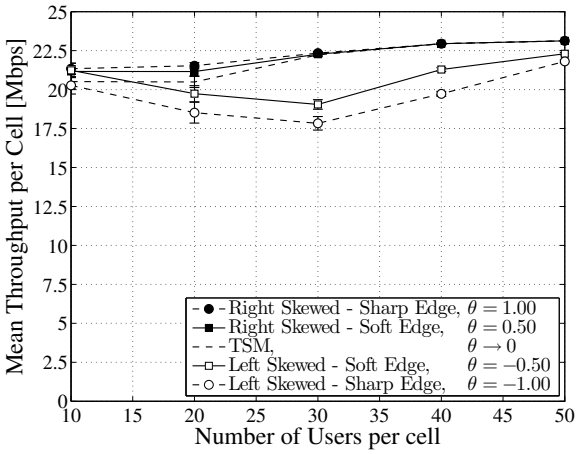

(c) Total cell throughput - macro cell scenario [3].

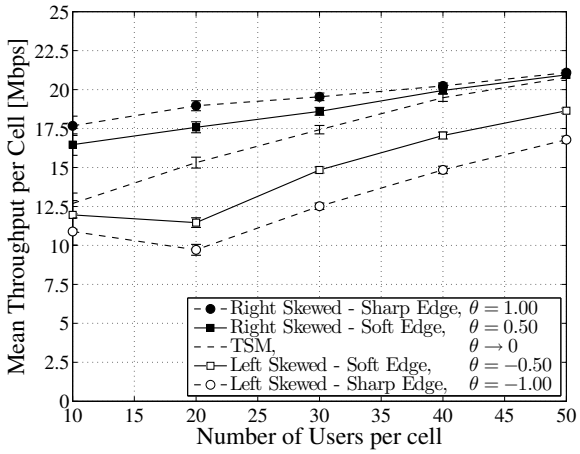

(d) Total cell throughput - urban macro scenario [2].

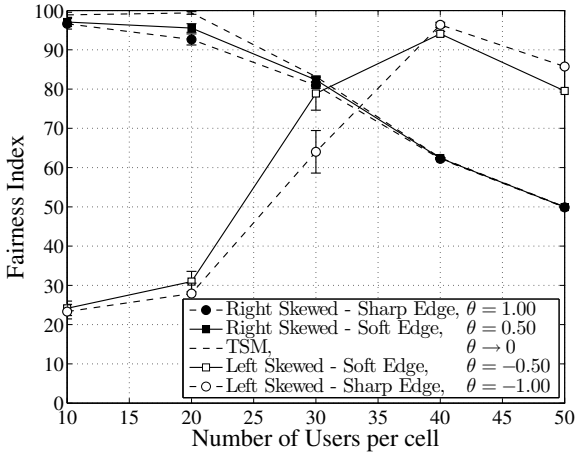

(e) Mean cell fairness index - macro cell scenario [3].

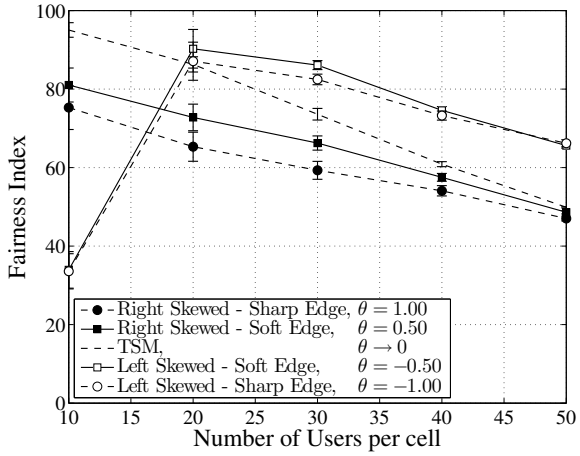

(f) Mean cell fairness index - urban macro scenario [2].

Figure 3.7: Performance metrics of the MTSM algorithm as a function of the number of NRT users with different values of shape parameter, θ.

The peakedness of the marginal utility function also influences users' satisfaction levels. The left skewed curve with sharp edge gives zero priority to users with throughput higher than

the requirement while the left skewed curve with soft edge also gives priority to a portion of the users with throughput higher than the QoS requirement. This means that left skewed with soft edge curve also gives priority to users with better channel conditions, that can surely transmit efficiently and explore more successfully the resources in comparison with the configuration that only chooses users below the requirement.

In the macro cell scenario (results indicated by the Figure 3.7(a)) the left skewed soft edge configuration ($\theta = -0.50, \lambda = 0.1088$) improves the users' satisfaction in 30% for higher loads and increases in almost 75% the number of users with satisfaction level above 90% in comparison with TSM, as it can be seen in Figure 3.7(a). Similarly, in the urban macro scenario, the left skewed soft edge configuration still achieves gains in comparison with TSM. Figure 3.7(b) indicates that the satisfaction level is improved in 15% for higher loads and the number of users with satisfaction level above 90% is increased in 50% in comparison with TSM. Therefore, the asymmetric format of the marginal utility function (left skewed soft edge configuration) is capable to improve the user satisfaction in different scenarios.

The system capacity in terms of total throughput as a function of the system load expressed in number of users is shown in Figures 3.7(c) and 3.7(d). The total cell throughput provided by the TSM and right skewed MTSM increases with the system load, meaning that these algorithms exploit multi-user diversity. The right skewed sharp edge configuration achieved the highest throughput levels because it selects only the users with best channels conditions. However, the effect becomes less significant with the increasing load, since the maximum capacity of the cell is achieved with higher loads.

The left skewed marginal utility functions initially decrease the cell throughput with the increasing load. This happens due to the algorithm of benefiting the users below the QoS requirement, who have channel conditions poorer than those selected with the symmetric and right skewed marginal utility functions. Consequently, the selected users achieve lower throughputs. However, this behavior changes when the system load increases, once the scarcity of resources forces the scheduler to select users with better channel conditions. The difference between the throughput of the right skewed sharp edge MTSM and the left skewed soft edge MTSM decreases with the increment of the system load, achieving 5% with a load of 50 users. Therefore, the decrease of throughput of the left skewed and soft edge configuration justifies the great improvement of satisfaction level.

The urban macro scenario is more challenging than macro cell scenario, consequently the total system throughput has a decrement. However, the relative behavior between the different configurations remains the same. Since the left skewed configuration selects the users with worst channel conditions, these configurations have the highest decrement of throughput.

Figures 3.7(e) and 3.7(f) depict the mean fairness for different loads. The symmetric and the right skewed marginal utility functions provide a balanced distribution of resources with lower loads. The left skewed curves begin with low fairness because the system load is small in comparison with the number of resources, consequently there is a great variability of the throughput of the selected users. With the increasing number of users the distribution of resources becomes more equitable, and the variability is reduced. Since Jain's fairness index

is inversely proportional to the variability of the measures, it tends to increase. However, when the system load increases to a given value, the left skewed curves tend to provide a more balanced resource distribution, since the resource contention tends to be won by users with QoS near the requirement. Consequently, the trend observed in other cases starts to be verified in this configuration.

Finally, we compare the best configuration of MTSM with TSM and the classical algorithms Proportional Fair (PF) and RM. Based on the previous comments, the best results are achieved when MTSM is a left skewed curve, with a soft edge. This configuration is obtained considering the scale parameter $\lambda = 0.1088$ and the shape parameter $\theta = -0.50$.

Figures 3.8(a) and 3.8(b) compare the user satisfaction of MTSM with classical algorithms. In general, RM provides an overall degraded satisfaction level, since it selects only the users with best channel conditions and PF presents good satisfaction results, but it is strongly degraded at higher loads. The MTSM algorithm shows the best satisfaction results for all considered system loads, which demonstrates the advantage of using asymmetric utility functions to maximize user satisfaction. Figure 3.8(b) indicates that the MTSM algorithm provides a scheduling algorithm that maintains the highest satisfaction levels compared with all other algorithms, even in challenging channel conditions. Despite the fact that PF gets a good result in the macro cell scenario [3], it suffers a major breakdown in urban macro scenario [2].

Besides the lower degraded levels, the RM algorithm provides the best throughput results, achieving the maximum system capacity for all system loads by assigning resources to the users that can transmit at the highest Modulation and Coding Scheme (MCS), as can be seen in Figures 3.8(c) and 3.8(d) .

Since TSM and MTSM are focused at achieving high satisfaction levels, they show the worst performance in terms of efficiency in the resource usage in comparison with RM. MTSM is an algorithm that tries to select users below the QoS requirement or just above its value, which is not so efficient in terms of system capacity when the system has few users. However, the increasing of load implies the scarcity of resources and the selection of the users made by the MTSM scheduler becomes more opportunistic. The algorithm explores more efficiently the multi-user diversity, selecting the users with better channel conditions. In the urban macro scenario this feature is clearer, since the throughput has an improvement of 40% with the increase of the system load. The PF algorithm presents an almost flat behavior for different traffic loads.

An intrinsic trade-off between system capacity and user fairness can be noticed. Figures 3.8(e) and 3.8(f) demonstrate that the PF algorithm achieves good fairness levels, being capable to provide high levels for all loads considered. The RM algorithm is able to use the resources very efficiently but is unfair in the QoS distribution. As a consequence, it achieves the worst fairness levels. MTSM is not so good as RM in terms of system capacity but compensates it by providing high fairness among users with the increment of load.

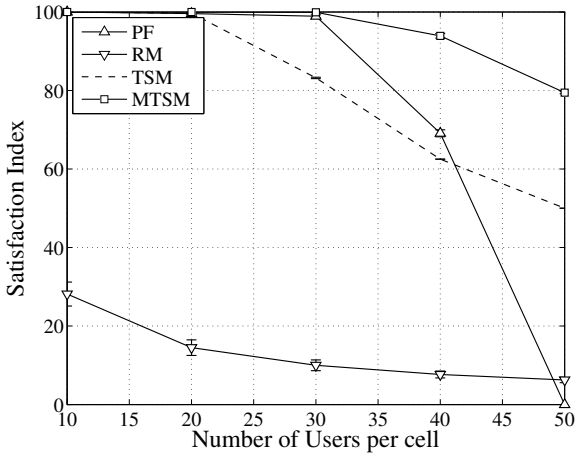

(a) User Satisfaction - macro cell scenario [3].

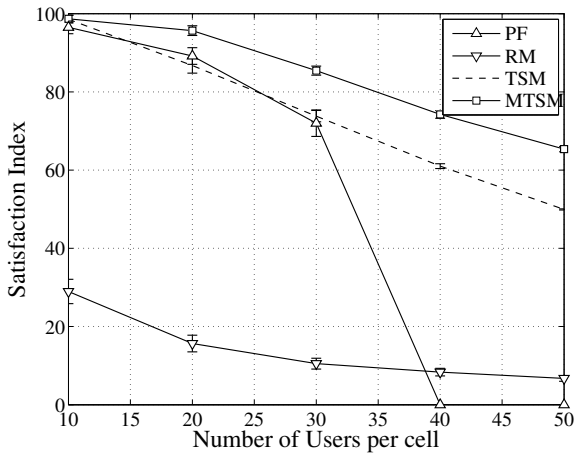

(b) User Satisfaction - urban macro scenario [2].

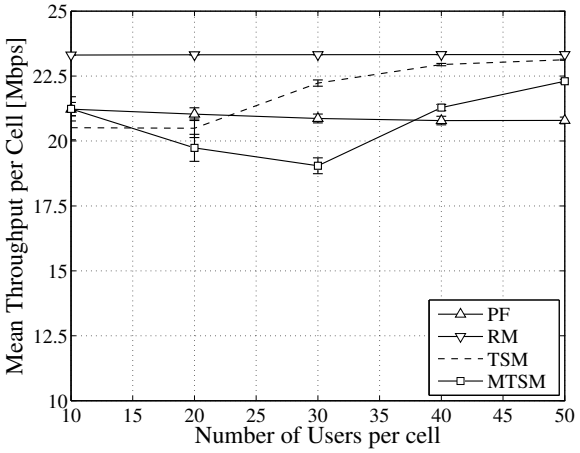

(c) Total cell throughput - macro cell scenario [3].

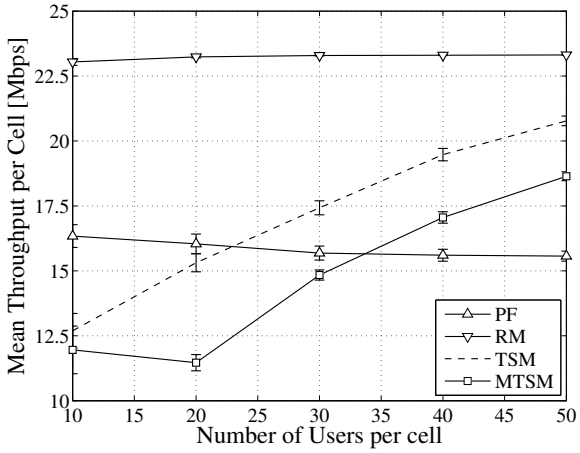

(d) Total cell throughput – urban macro scenario [2].

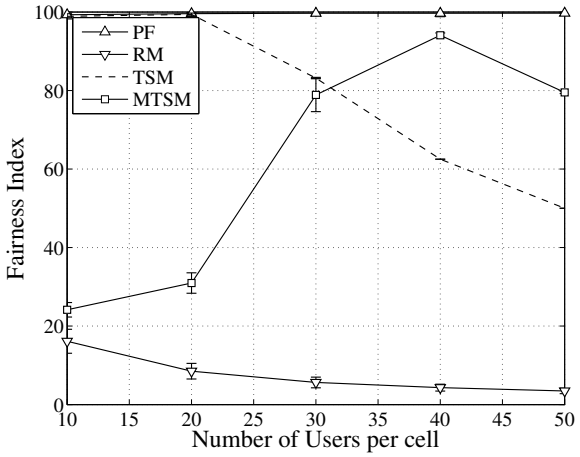

(e) Mean cell fairness index - macro cell scenario [3].

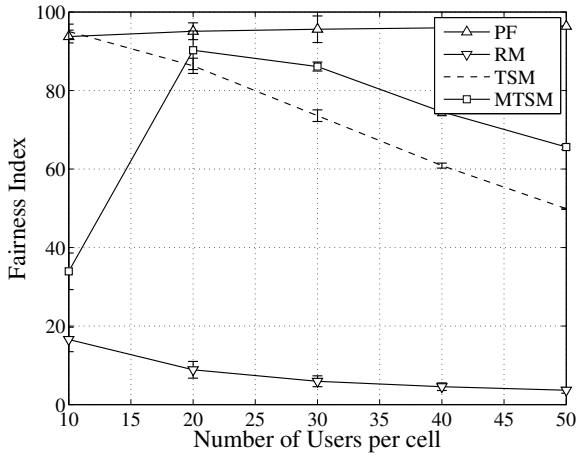

(f) Mean cell fairness index - urban macro scenario [2].

Figure 3.8: Performance metrics of the MTSM algorithm compared with the classical algorithms PF, RM and TSM.

3.3.2 Imperfect CSI

The previous section established the perfect knowledge of Channel State Information (CSI) to evaluate the performance of different scheduling algorithms. This section extends this study, considering imperfect CSI: the UE are able to estimate their channels perfectly, but the Evolved Node B (eNB) receives their measurements delayed by Δn TTIs.

This work broadens the analysis carried out by [32], that analyzed the impacts of CSI imperfections on the performance of the TSM algorithm.

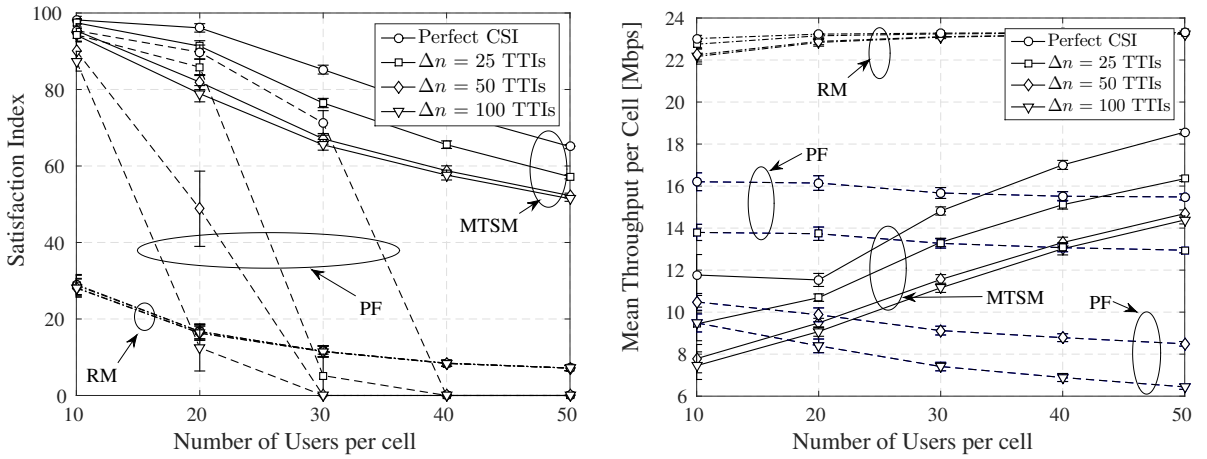

(a) User Satisfaction index. **(b)** Total Cell Throughput.

Figure 3.9: Performance metrics of the MTSM algorithm compared with classical algorithms considering imperfect CSI in an urban macro scenario [2].

Figure 3.9(a) presents the satisfaction index as a function of the number of UE attended per cell, considering PF, RM, and MTSM algorithms with different measurement delays in the CSI. It can be noticed that the satisfaction index obtained with the MTSM scheduler is sensitive to the CSI imperfections, with a decrement of 15% of the satisfaction index. The MTSM algorithm schedules UE considering their QoS parameter. Therefore, CSI delay can incur in an improper scheduling decision of that algorithm. The increasing CSI delay has no considerable effects on the satisfaction index obtained by the RM algorithm, even when the delay is higher than the channel coherence time, i.e., a scenario with low correlation between the CSI and the actual channel. The RM tends to select UE that are close to the eNB, so that the SNR is dominated by the large-scale fading. This fact makes the RM algorithm less sensitive to CSI measurement delays.

The mean cell throughput is depicted in Figure 3.9(b). For higher delays, the total system capacity is not reached by the MTSM algorithm even for a high number of UE. When the delay increases the CSI becomes less correlated to real channel information. This leads to incorrect precoding, incurring in a higher BLock Error Rate (BLER), as shown in Figures 3.10(a).

Since RM algorithm is less sensitive to CSI imperfections, it reaches the total system capacity as can be seen in Figure 3.9(b) and has lower BLER, as indicated by the Figure 3.10(b). In the MTSM scheduler, when the number of UE increases, the difference between the mean eNB throughput also increases, as a consequence of the high number of UE that the algorithm tries to satisfy with its limited number of resources. Furthermore, the eNB is more likely to incur in errors when transmitting to UE more distant from it, as shown in Figure 3.10(a).

The impact of imperfect CSI on the algorithms can be neglected for small measurement delays, such as Δn = 25 TTIs. However, if the delay is greater than half the channel coherence time, the CSI and the real channel become almost uncorrelated. This fact decreases the satisfaction index and the eNB throughput drastically by increasing the BLER to unacceptable

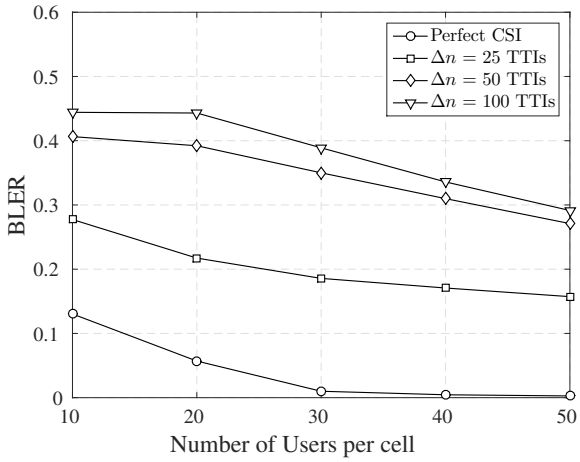

(a) MTSM Algorithm.

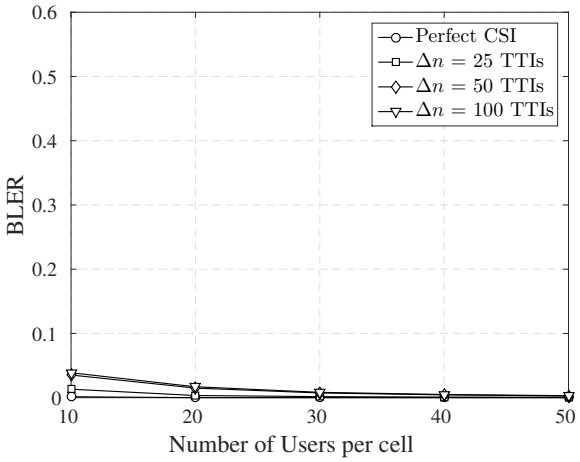

(b) RM Algorithm.

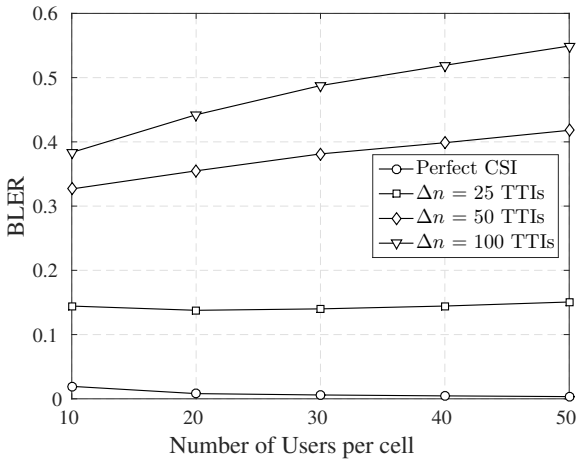

(c) PF Algorithm.

Figure 3.10: BLER with imperfect CSI in an urban macro scenario [2].

values.

3.4 Performance Evaluation of MDSM Algorithm

This section evaluates the MDSM algorithm with different configurations according to Table 3.2, which shows the main parameters of the simulated LTE-like system network.

Table 3.2: Simulation Parameters

Parameter	Value
Maximum BS transmit power	20 W
BS antenna radiation pattern	Three-sectored
Cell radius	1 km
UE speed	3 km/h
Carrier frequency	2 GHz
System bandwidth	5 MHz
Sub-carrier bandwidth	15 kHz
Number of RBs	6
Path loss - macro cell scenario [3]	$PL = 15.3 + 37.6 \cdot \log_{10}(d)$ [a]
Path loss - urban macro scenario [2]	$PL = 34.5 + 35 \cdot \log_{10}(d)$ [a]
Channel coherence time	90 ms
Antenna gain[b][44]	$G_h(\theta_h) + G_v(\theta_v)$
Downtilt angle	8 degrees
Log-normal shadowing st. dev.	8 dB
Small-scale fading [43]	3GPP Typical Urban
AWGN power per sub-carrier	-123.24 dBm
Noise figure	9 dB
Link adaptation	Link level curves from [39]
SNR threshold of MCS 1 [39]	-6.9 dB
Transmission Time Interval	1 ms
RT traffic model	VoIP
HOL packet delay requirement	40 ms
VoIP packet size	320 bits
Multi-antenna configuration	SISO
Simulation time span	30 s
Number of simulation runs	10
Confidence Interval	95%

[a] d is the distance to the BS in km.
[b] θ_h and θ_v represent the horizontal and vertical angles related to the BS, respectively.

3.4.1 Perfect CSI

The MDSM algorithm is initially analyzed considering the effect of the scale parameter λ in symmetric marginal utilities. The shape parameter fixed at $\theta \to 0$. The effect of the variation of the scale parameter is shown in Figure 3.4. We consider three different curves: *wide* ($\lambda = 30\,dB$), DSM (original, $\lambda = -10$ dB) and *narrow*($\lambda = -20\,dB$).

Figures 3.11(a) and 3.11(b) indicate the percentage of satisified users. The wide MDSM configuration tends to allocate resources giving more importance to the channel conditions, consequently it is less sensitive to the system load variation, since it always selects users with the highest instantaneous data rate. As the load increases, higher gains are observed in comparison to the other configurations. The wide configuration achieves an improvement of 20% compared with the symmetric curve (DSM) for higher loads in the macro cell scenario. It achieves an improvement of 50% compared with the symmetric curve (DSM) for higher loads in the urban macro scenario.

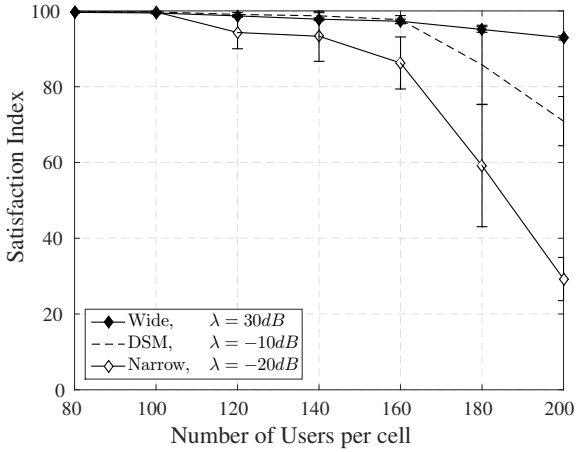

(a) User Satisfaction - macro cell scenario [3].

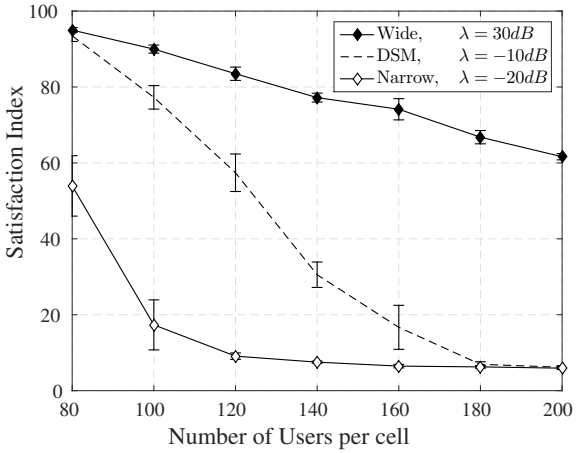

(b) User Satisfaction - urban macro scenario [2].

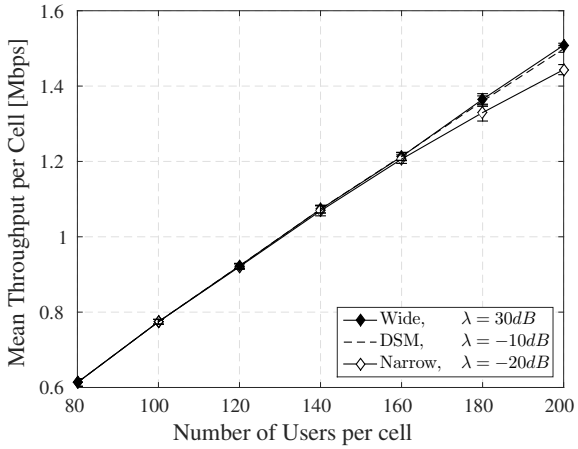

(c) Total cell throughput - macro cell scenario [3].

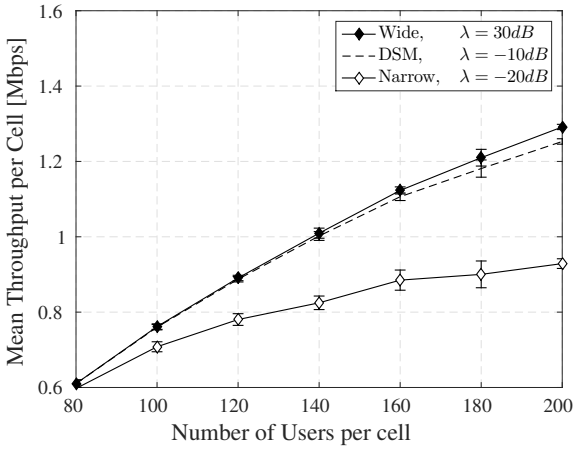

(d) Total cell throughput - urban macro scenario [2].

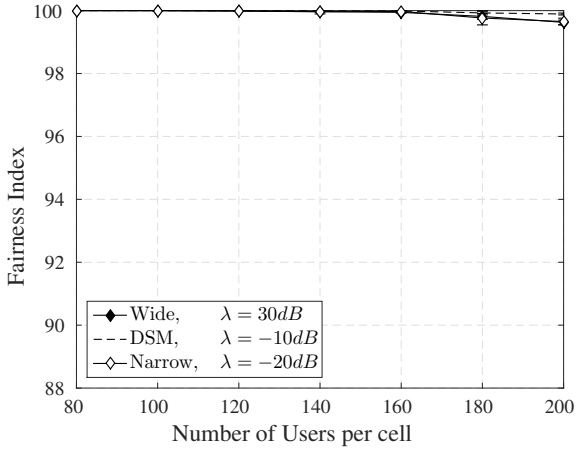

(e) Mean cell fairness index - macro cell scenario [3].

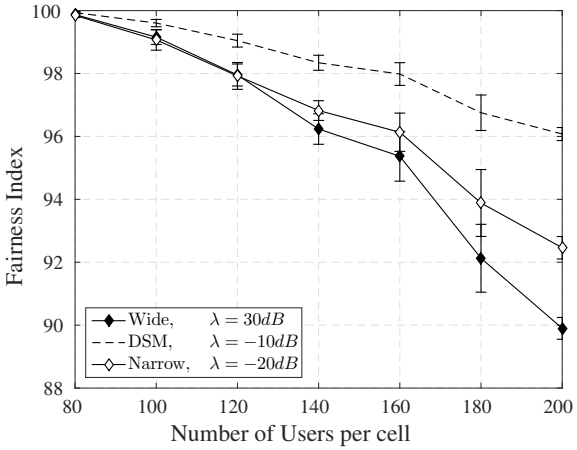

(f) Mean cell fairness index - urban macro scenario [2].

Figure 3.11: Performance metrics of the MDSM algorithm as a function of the number of RT users with different values of scale parameter, λ.

The narrow configuration has the lowest satisfaction indexes because penalizes users in extreme conditions, i.e., very good or very bad users have low priority. With this, users with better channel conditions, despite having the lowest HOL delays, are discarded since their marginal utility tends to zero. In contrast, the wide configuration is able to distribute resources among users with better conditions, achieving gains comparable to that observed in DSM. The

change of channel conditions from macro cell to urban macro impacts directly the satisfaction levels achieved by the algorithms, with a significant decrement of DSM, which decays from 70% to 10% with higher loads. The wide configuration of MDSM offers a greater resistance to more critical channel conditions, since it distributes resources to users which are to a greater delay in relation to the delay requirement.

The system capacity in terms of total throughput as a function of the system load is depicted in Figure 3.11(c) and 3.11(d). The total cell throughput provided by the MDSM increases as the system load raise for all considered configurations. The same behavior is observed with DSM.

The mean fairness index behavior as a function of the system load is depicted by Figures 3.11(e) and 3.11(f) . The fairness levels in the macro cell scenario have the same order, almost 1, for all loads considered. The worsening channel conditions of the urban macro scenario result in a deterioration of fair indices, which decay to values of the order of 95% for DSM or 90% for MDSM.

Proceeding with the evaluation, we consider the effect of the marginal utility' asymmetry in the MDSM algorithm. Thus, we evaluate the scheduling algorithm for RT services, extending the study of [26], that considered a symmetric bell-shaped curve.

Therefore, we evaluate the effect of the change of the shape parameter θ of the marginal utility function given by (3.11). Once packets with HOL packet delay higher than the delay requirement are discarded at the transmitter, we consider negative values of the shape parameter, $\theta < 0$ because we are interested in curves skewed to the left side, benefiting users with delay equal or below the requirement. The magnitude of the scale parameter θ, also determines the behavior of the function when near the QoS requirement: higher values of the shape parameter, in this study $\theta = -1$, result in curves with sharper edges; lower values, here considered $\theta = -0.5$, imply smoother peaks. Therefore, we consider three different curves: bell-shaped $(\theta \to 0)$, left skewed with soft edge $(\theta = -0.5)$, and left skewed with sharp edge $(\theta = -1.0)$. The simulated curves are shown in Figures 3.5(a) and 3.5(b).

The behavior of the satisfaction index of the system as a function of RT users is shown at Figures 3.12(a) and 3.12(b). The results indicate that the left skewed configurations are able to provide gains in the satisfactions levels in comparison with the original symmetric curve, hence they improve the conditions of transmission of users with low HOL delay.

The left skewed with soft edge curve gives priority to a portion of users with HOL delay higher than the requirement, while left skewed curve with sharp edge, gives zero priority to users with HOL delay higher than the requirement. This means that the soft edge configuration gives priority to users which will have delay higher than the requirement. Consequently, this configuration distributes resources to users that will be unsuccessful. This is a clear disadvantage of that configuration that results in satisfaction levels lower than those achieved by the sharp edge configuration. In spite of this disadvantage, the left skewed soft edge MDSM achieves gains of 15% in the satisfaction levels in comparison with DSM for a load of 200 users. In the considered scenario, the left skewed sharp edge is the most efficient configuration to maximize users' satisfaction, obtaining an improvement of 20% compared with the symmetric curve (DSM) for higher loads (200 users). Figure 3.12(b) show us that the DSM algorithm

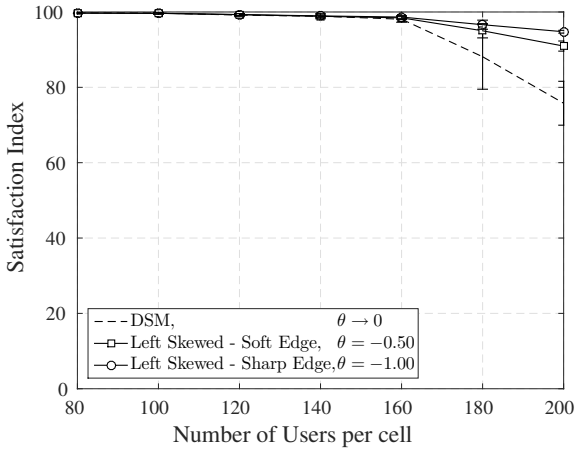

(a) User Satisfaction - macro cell scenario [3].

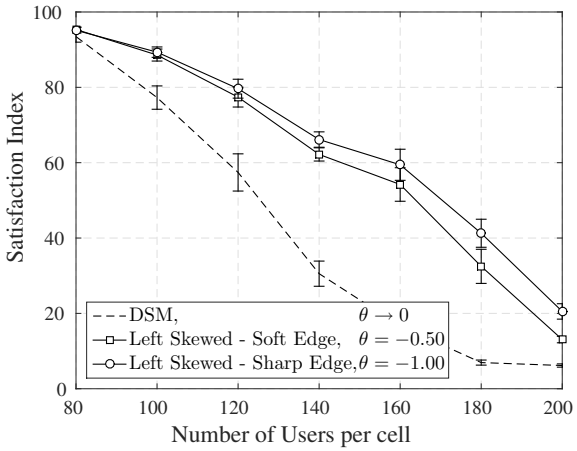

(b) User Satisfaction - urban macro scenario [2].

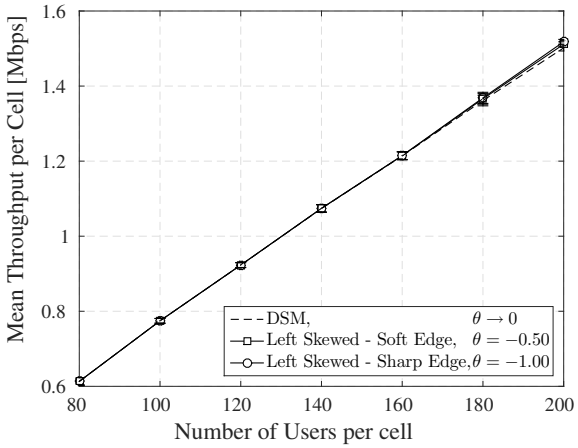

(c) Total cell throughput - macro cell scenario [3].

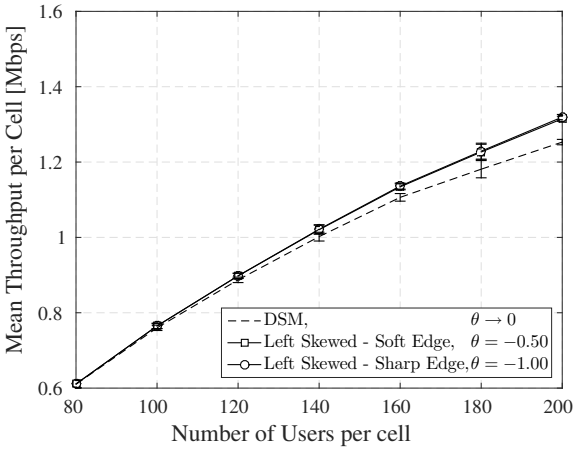

(d) Total cell throughput - urban macro scenario [2].

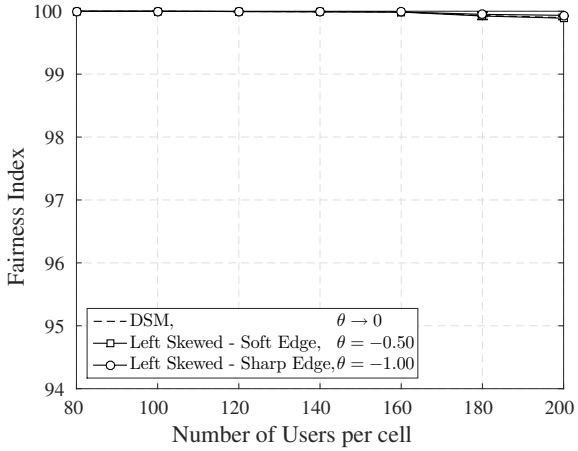

(e) Mean cell fairness index - macro cell scenario [3].

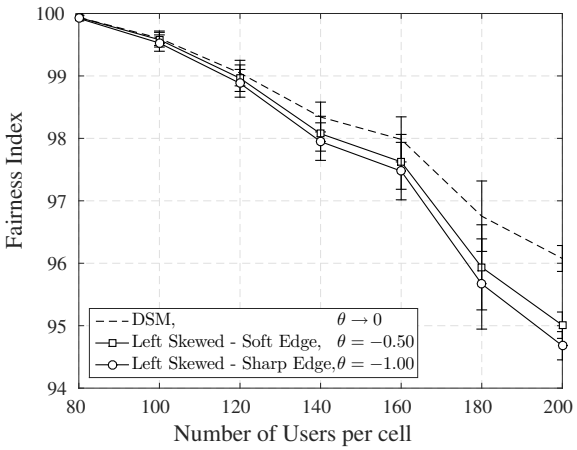

(f) Mean cell fairness index - urban macro scenario [2].

Figure 3.12: Performance metrics of the MDSM algorithm as a function of the number of RT users with different values of shape parameter, θ.

is more impacted by the worsening of channel conditions, while the asymmetric curves of the MDSM configurations are able to provide a distribution of resources that improve user satisfaction.

The system capacity in terms of total throughput is shown at Figures 3.12(c) and 3.12(d). The proposed MDSM configurations achieved total cell throughput of the same order of

DSM, the average data rate improvement becomes more noticeable only at higher loads. It is also observed that the total cell throughput provided by the MDSM configurations raise as the number of users become higher. Therefore, the proposed RRA exploit successfully the multi-user diversity.

The mean fairness index as a function of the number of RT users is indicated in Figures 3.12(e) and 3.12(f). The fairness levels obtained have the same order, almost 1 in the macro cell scenario and a little bit smaller in the urban macro scenario. Therefore, the symmetric and the left skewed marginal utility functions provide a balanced distribution of resources.

From the discussion of the performance metrics achieved by the different shifted log-logistic marginal utilities, we conclude that the wide configuration achieved the best results of user satisfaction and resource efficiency. Therefore, in order to evaluate this MDSM configuration we compare it with classical RRA algorithms found in the literature, i.e., Modified Largest Weighted Delay First (MLWDF), Urgency and Efficiency-based Packet Scheduling (UEPS) and DSM.

In the macro cell scenario, there is a tie between satisfaction levels achieved by MLWDF, UEPS and MDSM algorithms, Figure 3.13(a). However, when the urban macro scenario is considered, the MDSM achieves the highest levels of satisfaction compared with all other algorithms, which demonstrates the advantage of using a wide marginal utility function when satisfaction maximization is desired, as can be seen in Figure 3.13(b).

The MDSM algorithm provides good capacity results, achieving throughput of the same order of MLWDF and UEPS, with an almost uniform behavior for different traffic loads, as can be seen in Figures 3.13(c) and 3.13(d).

According to Figure 3.13(e), all the considered algorithms are in equal manner fair in the macro cell scenario. The difficulties encountered in distributing resources so that users meet the minimum requirements due to more challenging channel conditions of urban macro scenario, implies a uneven allocation and decreases the Jains' fairness index, as can be seen in Figure 3.13(f)

3.4.2 Imperfect CSI

This section analyses the impacts of CSI imperfections on the performance of the DSM algorithm. As well as done in Section 3.3.2, the CSI imperfection is modeled as a delay of the channel measurements received by the eNB.

The MDSM algorithm is the less susceptible to CSI imperfections and maintains the highest satisfaction levels, as indicated in Figure 3.14(a). The UEPS and MLWDF show a significant fall in satisfaction indexes. The UEPS and MLWDF algorithms use the status of the current channel as an indicator of the resource usage and directs the distribution of resources among users. Therefore, they are strongly affected by a delayed CSI. With lower loads, the delay of 25 TTIs reduces the satisfaction levels of UEPS and MLWDF in 50% while MDSM has its satisfaction index only decreased by 10%. Considering higher loads, the decrement of satisfaction of UEPS and MLWDF is even worse, going quickly to zero with 120 UE, and MDSM achieves levels near to 70%.

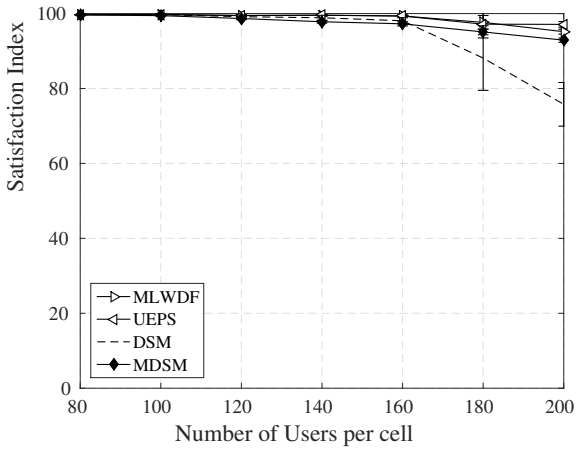

(a) User Satisfaction - macro cell scenario [3].

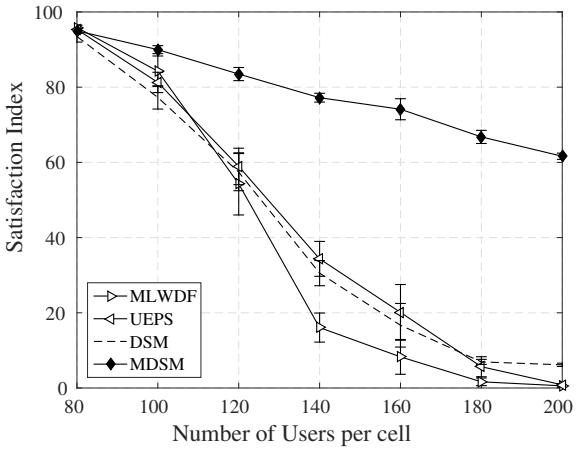

(b) User Satisfaction - urban macro scenario [2].

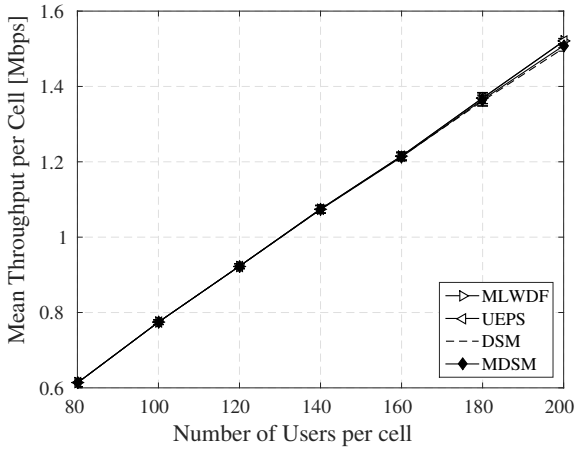

(c) Total cell throughput - macro cell scenario [3].

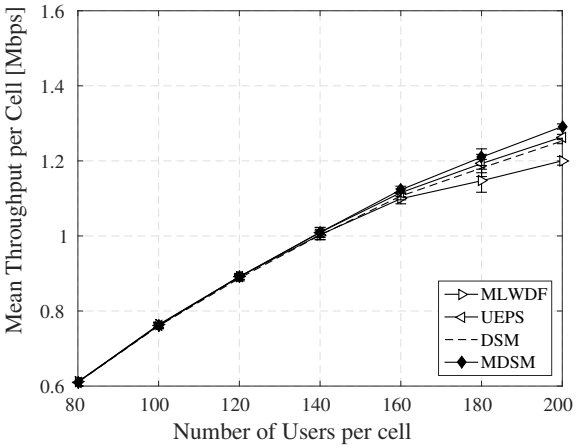

(d) Total cell throughput – urban macro scenario [2].

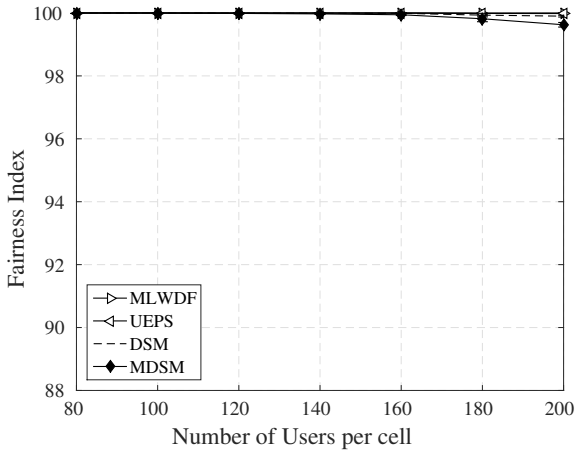

(e) Mean cell fairness index - macro cell scenario [3].

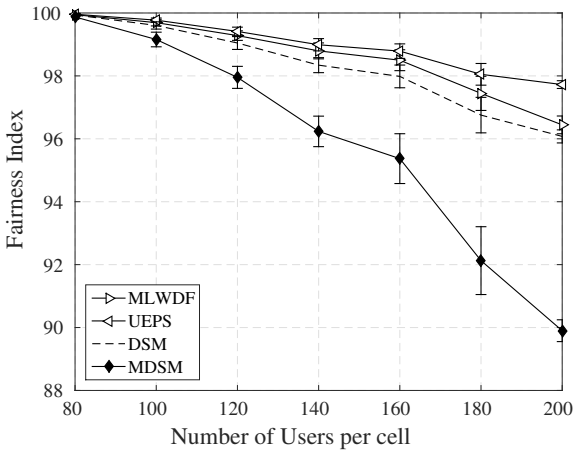

(f) Mean cell fairness index - urban macro scenario [2].

Figure 3.13: Performance metrics of the MDSM algorithm compared with the algorithms MLWDF, UEPS and DSM.

The considered model of RT services implies low data traffic demand. Therefore, the imperfection of CSI has low impact over the mean throughput per cell, as can be seen in Figure 3.14(b). The impact of imperfect CSI on the algorithms can be neglected for small measurement delays, such as Δn = 25 TTIs or Δn = 50 TTIs . However, if the delay is greater than half the channel coherence time, the CSI and the real channel become almost uncorrelated. This fact

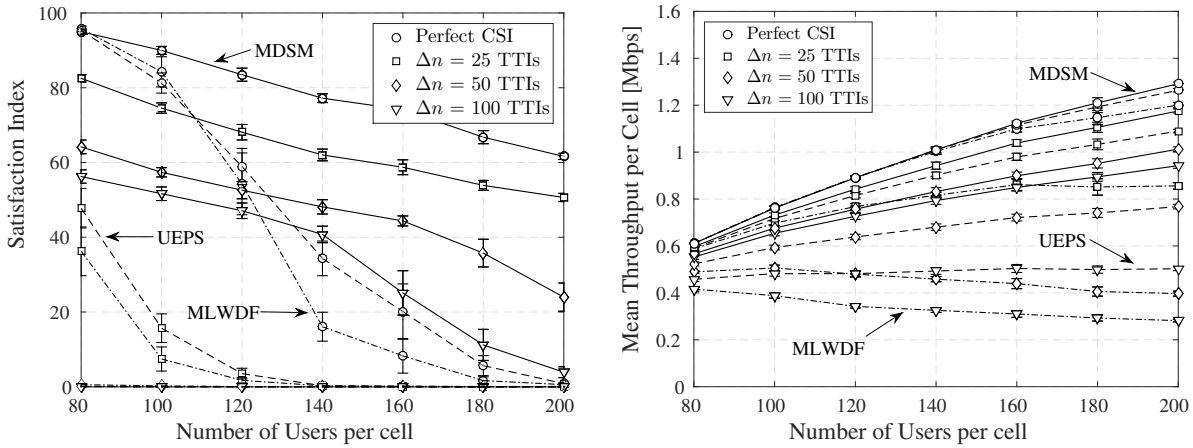

(a) User Satisfaction index. **(b)** Total Cell Throughput.

Figure 3.14: Performance metrics of the MDSM algorithm compared with classical algorithms considering imperfect CSI in an urban macro scenario [2].

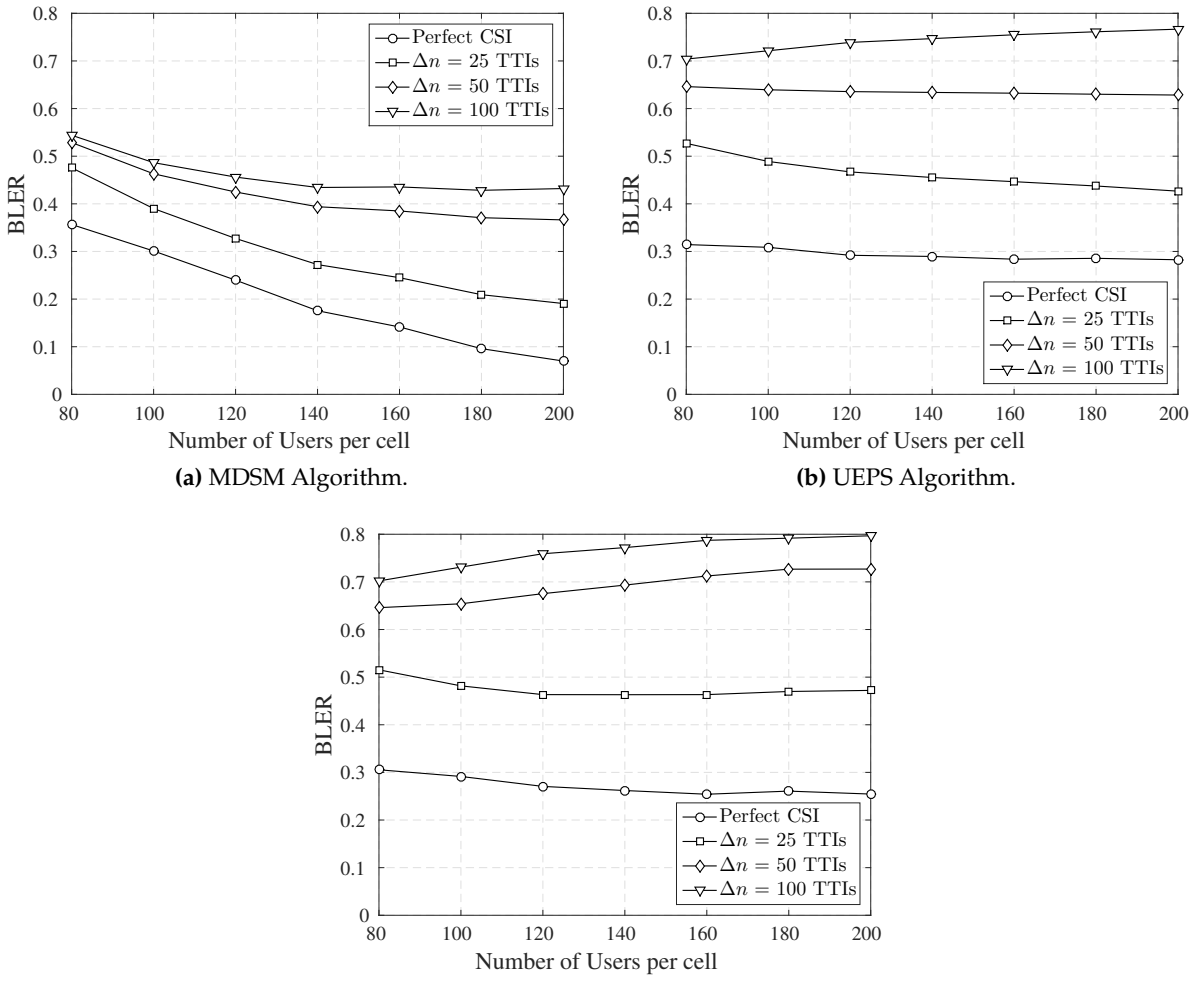

(a) MDSM Algorithm. **(b)** UEPS Algorithm.

(c) MLWDF Algorithm.

Figure 3.15: BLER with imperfect CSI in an urban macro scenario [2].

decreases the eNB throughput moderately by increasing the BLER to unacceptable values.

3.5 Partial Conclusions

The determination of the function to be used in a utility-based scheduling framework depends on the goal the one wants to achieve. This study demonstrated by means of system-level simulations that the shifted log-logistic function is effective towards the objective of user satisfaction maximization, achieving gains in comparison with classical algorithms.

The MTSM algorithm obtains significant gains when employing asymmetric marginal utility functions, enabling a stable strategy maximize user satisfaction and keep the spectral efficiency at satisfactory levels for the entire load range considered. The best performance results, achieved with a left skewed and soft edge curve, indicate an increment of 30% of the users' satisfaction levels for higher loads.

The MDSM algorithm also attained gains with the use of asymmetric marginal utility functions. Differently from previously noticed with MTSM, variations in the aperture of the function, i.e., a more flattened curve also provided gains in the users' satisfaction. The best performance results, achieved with a wider curve, indicate an increment of 20% of the users' satisfaction levels for higher loads.

Chapter 4

Scheduling Framework for Adaptive Satisfaction Control

In this chapter, the problem of controlling the user satisfaction is further investigated considering the dynamic and adaptive variation of the parameters of the shifted log-logistic function. Section 4.1 provides a general description of the shifted log-logistic utility function. Sections 4.2 and 4.3 present two adaptive algorithms, describing the extension of the utility-based framework described previously and Section 4.4 evaluate the proposed algorithms. Finally, Section 4.5 provides a partial conclusion based on the system-level simulation results.

4.1 Shifted Log-Logistic Utility Function

In this study, we develop a general scheduling framework that is able to control the degree to which a network satisfies service requirements of users' applications in terms of throughput. In other words, this research investigates novel ways to control the satisfaction level of users of Non-Real Time (NRT) services. In this context, we evaluate different methods to solve this problem extending the framework based on utility theory proposed in [26] and described in details in Chapter 3.

The present study extends the investigation of utility-based scheduling algorithms, analyzing adaptive policies using the shifted log logistic utility function. This function is represented by

$$U^{\text{S-Log}}(T_j^{\star}[n]) = \frac{1}{1+\left(1+\dfrac{\theta(T_j^{\star}[n]-T_j^{\star\text{req}})}{\lambda}\right)^{-1/\theta}}, \tag{4.1}$$

where $T_j^{\star}$ is the throughput of user j and $T_j^{\star\text{req}}$ is the required throughput; θ is a real parameter which determines the shape of the function and λ is a real parameter that sets the scale of the function.

Without loss of generality, it is considered T_j normalized by the Quality of Service (QoS) requirement, i.e., $T_j = T_j^{\star}/T_j^{\star\text{req}}$ and $T_j^{\text{req}} = T_j^{\star\text{req}}/T_j^{\star\text{req}} = 1$ and $U^{\text{S-Log}}(T_j^{\star}[n])$ is simply replaced by $U^{\text{S-Log}}(T_j[n])$ hereafter.

The shifted log-logistic utility function is limited by $T_j[n]$ intervals, according to the values of θ, λ and T_j^{req}. Given $\theta > 0$, $U^{\text{S-Log}} = 1$ if $T_j[n] < T_j^{\text{req}} - \frac{\lambda}{\theta}$. Considering $\theta < 0$, $U^{\text{S-Log}} = 1$ if $T_j[n] > T_j^{\text{req}} - \frac{\lambda}{\theta}$.

The function indicated by (4.1) is continuous, differentiable over the range $T_j[n]$, and limited between 0 and 1, i.e. $0 \leq U^{\text{S-Log}} \leq 1$.

The utility-based weight performs an important function in the scheduling algorithm, once the priority of a given user to get a resource is directly proportional to this weight. The shifted log-logistic marginal utility is given by

$$w_j^{\text{S-Log}} = \frac{\frac{1}{\lambda}\left(1 + \frac{\theta(T_j[n] - T_j^{\text{req}})}{\lambda}\right)^{-1-1/\theta}}{\left(1 + \left(1 + \frac{\theta(T_j[n] - T_j^{\text{req}})}{\lambda}\right)^{-1/\theta}\right)^2}, \tag{4.2}$$

As mentioned previously, the marginal utility function has two parameters, θ and λ, that clearly impact its behavior, allowing different scheduling strategies to be configured by an adequate parameter setting. The shape parameter, θ, impacts the symmetry of the marginal utility curve, while the scale parameter λ, influences the peakedness of symmetric curves.

This study explores the dynamic variation of the two parameters of the shifted log-logistic function in the scheduling, showing that it is possible to control the satisfaction levels by suitable arrangements of these parameters. The proposed algorithms that are obtained by the variation of each of these parameters separately are called Adaptive Throughput-based Efficiency-Satisfaction Trade-Off (ATES) and Adaptive Satisfaction Control (ASC) and are described in the following sections. Figure 4.1 depicts the extension on the scheduling procedure described by [26].

The considered algorithms exploit in a widely way the multi-user diversity, since the shifted log-logistic utility function covers a larger range of variations for the considered QoS metric. System level simulation results demonstrate that it is possible to mimic different scheduling algorithms by modifying the framework parameters while maintaining user satisfaction at defined levels for different system loads considering NRT services.

4.2 Adaptive Throughput-Based Efficiency-Satisfaction Trade-Off Algorithm

The ATES algorithm aims to deal with the trade-off between resource efficiency and satisfaction planned by the network operator in a scenario with NRT services. This is done by means of a dynamic control of the scale parameter of the marginal utility function.

The ATES technique dynamically adapts the scale parameter of the shifted log-logistic rule framework aiming to achieve a desired throughput-based satisfaction distribution among users. This strategy provides a strict control of the network QoS and has a good prediction in terms of system capacity.

To keep satisfaction around a target value, the λ parameter is calculated using a control

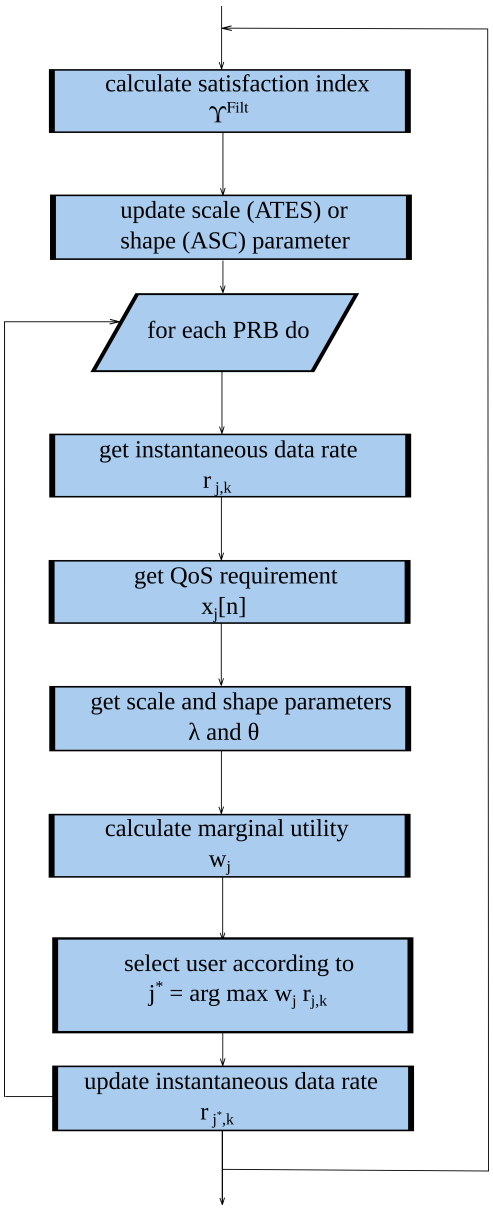

Figure 4.1: Adaptive scheduling algorithms flow-chart.

loop of the form

$$\lambda[n] = \lambda[n-1] - \eta(\mathrm{Y}^{\mathrm{Filt}} - \mathrm{Y}^{\mathrm{Target}}), \tag{4.3}$$

where η is a step size that determines the speed of adaptation of λ; $\mathrm{Y}^{\mathrm{Filt}}$ is a filtered satisfaction percentage and $\mathrm{Y}^{\mathrm{Target}}$ is the target satisfaction. To ensure the convergence, the λ parameter is limited by an interval given by $[\lambda_{\min}, \lambda_{\max}]$. A block diagram representation of the scale parameter control loop is depicted in Figure 4.2.

Modifications of the scale parameter vary the format of the utility function as indicated in Figure 4.3(a). The increase of λ, indicated by the arrows, makes the step less abrupt. This

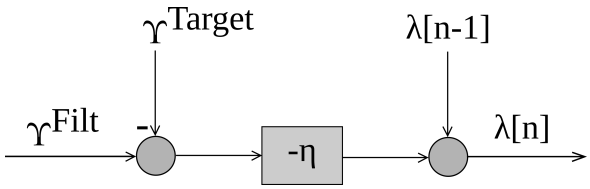

Figure 4.2: Block diagram representation of (4.3).

behavior means that the user becomes satisfied more slowly if the user throughput approaches the requirement. The marginal utility function, represented in Figure 4.3(b), has its peakedness reduced by the increase of λ, as indicated by the arrow in the figure. Lower values of the scale parameter imply a scheduling process that give higher priority to users experiencing throughput levels close to the requirement.

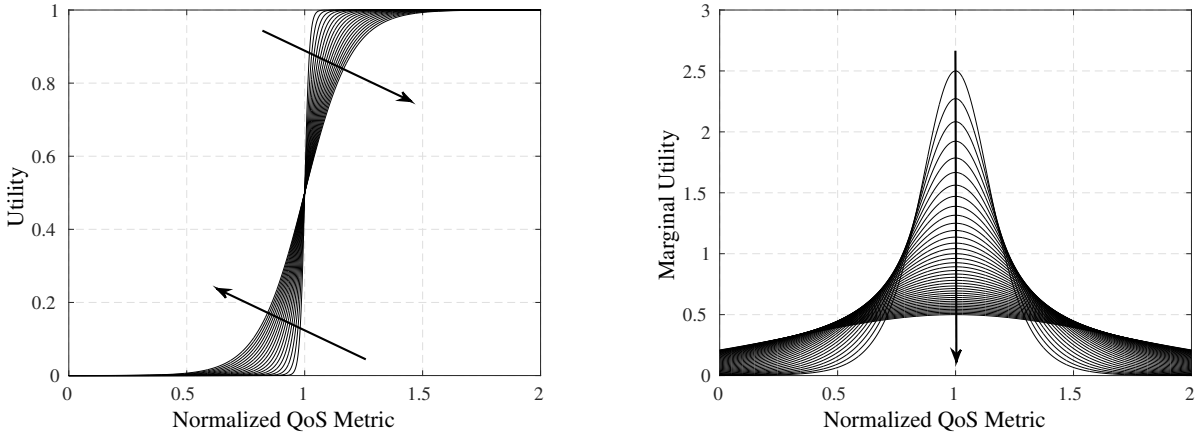

(a) Utility function **(b)** Marginal utility function

Figure 4.3: Behavior of $U^{\text{S-Log}}$ and $w^{\text{S-Log}}$ with a fixed shape parameter ($\theta \to 0$) and different values of the scale parameter λ.

4.3 Adaptive Satisfaction Control Algorithm

The ASC algorithm controls the shape parameter of the shifted log-logistic function. The adaptive equation is given by

$$\theta[n] = \theta[n-1] - \epsilon(\mathrm{Y}^{\text{Filt}} - \mathrm{Y}^{\text{Target}}), \tag{4.4}$$

where ϵ is a constant that establishes the speed of adaptation of θ; Y^{Filt} is a filtered satisfaction percentage and $\mathrm{Y}^{\text{Target}}$ is the target satisfaction percentage. The θ parameter is limited to the range $[\theta_{\text{min}}, \theta_{\text{max}}]$ to prevent dispersion of the algorithm. The scale parameter is fixed at $\lambda = 0.1088$, the standard value previously established on Chapter 3. A block diagram representation of the shape parameter control loop is depicted in Figure 4.4.

The shape parameter allows a different control of the format of the marginal utility function in comparison with the changes determined by (4.3). The ASC algorithm considers the absolute value and the sign of the shape parameter. As a consequence, it makes possible prioritizing users through different manners and it improves the conditions of the algorithm to control the satisfaction of the users in the system.

The signal of the θ parameter determines the direction of the marginal utility curve. Positive values of θ imply right tailed curves while negative values determine left tailed curves. Figure 4.5(a) indicates the changes in the format of the utility function with the variation of the absolute value of θ, considering only negative values of the shape parameter, $\theta < 0$. In this study, only negative values of θ are considered because the evaluation of Modified Throughput-based Satisfaction Maximization (MTSM) demonstrated that this configuration provides the maximum satisfaction level for a large amount of users in comparison with

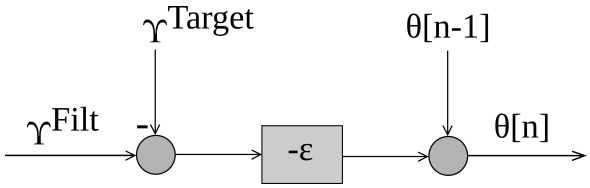

Figure 4.4: Block diagram representation of 4.4.

positive values.

Figure 4.5(b) shows different instances of the marginal utility curve considering several magnitudes of the θ parameter. The increase of the absolute value of θ impacts the sharpness of the curve. Higher values determine sharp edges while smaller ones establish soft curves, as indicated by the arrows. Another effect is the point where the marginal utility becomes zero, since it is a function of λ/θ. Given a constant value of λ, increasing θ reduces the distance between the maximum point of the marginal utility and the point at which it is zero. Consequently, this format of the curve determines that the scheduler gives priority to users with throughput strictly below the requirement. However, smaller values of the modulus of θ allow give some priority to users with throughput higher than the requirement. Therefore, the ASC algorithm explores the asymmetry of the marginal utility function, allowing a different scheduling in comparison with the previous studies based on the logistic function.

4.4 Performance Evaluation

In this section, we analyze the ATES and ASC algorithms by means of simulations considering the different adapative parameter adjustments described previously. The analyses are based on the results of system-level simulations conducted for NRT services in a single-cell scenario. Table 4.1 showns the considered parameters of the Long Term Evolution (LTE)-like simulated system. Initially, each algorithm will be evaluated separately, seeking a description of their behavior. Then, they will be compared with each other, seeking to establish their advantages and disadvantages.

Figures 4.6(a) and 4.6(b) depict the satisfaction index achieved by the ATES technique considering different targets of satisfaction percentage, $\mathrm{Y}^{\mathrm{Target}} = \{100, 90, 80, 70, 60\}\%$.

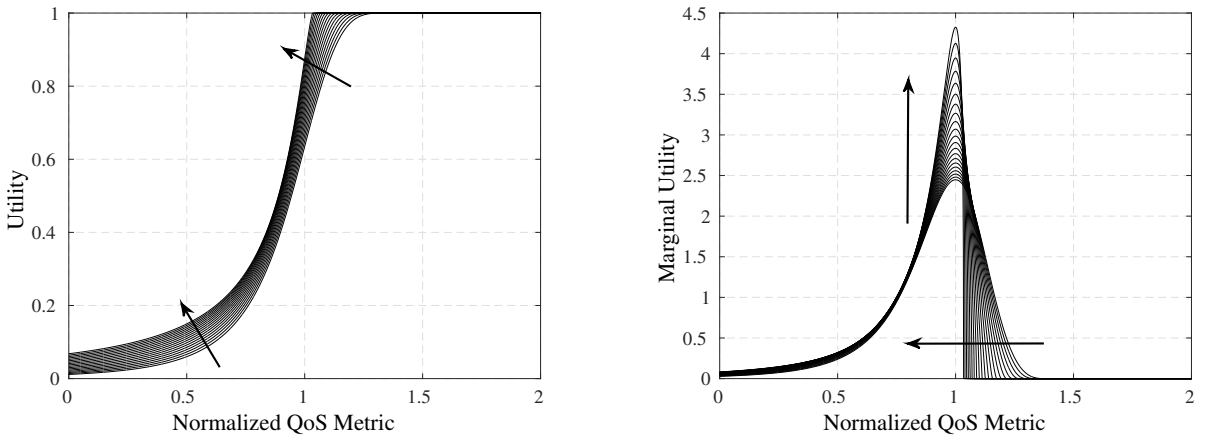

(a) Utility function **(b)** Marginal utility function

Figure 4.5: Behavior of $U^{\text{S-Log}}$ and $w^{\text{S-Log}}$ with a fixed scale parameter and different absolute value of the shape parameter, $\theta < 0$.

Table 4.1: Simulation Parameters of ASC and ATES Evaluation

Parameter	Value
Maximum BS transmit power	20 W
BS antenna radiation pattern	Three-sectored
Cell radius	1 km
UE speed	3 km/h
Carrier frequency	2 GHz
System bandwidth	5 MHz
Sub-carrier bandwidth	15 kHz
Number of Resource Blocks (RBs)	25 NRT
Path loss - macro cell scenario [3]	$PL = 15.3 + 37.6 \cdot \log_{10}(d)$ [a]
Path loss - urban macro scenario [2]	$PL = 34.5 + 35 \cdot \log_{10}(d)$ [a]
Channel coherence time	90 ms
Antenna gain[b][44]	$G_h(\theta_h) + G_v(\theta_v)$
Downtilt angle	8 degrees
Log-normal shadowing st. dev.	8 dB
Small-scale fading [43]	3GPP Typical Urban
AWGN power per sub-carrier	-123.24 dBm
Noise figure	9 dB
Link adaptation	Link level curves from [39]
SNR threshold of MCS 1 [39]	-6.9 dB
Transmission Time Interval	1 ms
NRT traffic model	Full buffer
User throughput requirement	Variable
Multi-antenna configuration	SISO
Satisfaction target (Y^{Target})	Variable
Minimum scale parameter (λ_{min})	-50 dB
Maximum scale parameter (λ_{max})	-10 dB
ATES step size (η)	0.10
Minimum shape parameter (θ_{min})	-5.0
Maximum shape parameter (θ_{max})	-0.5
ASC step size (ϵ)	0.10
Simulation time span	10 s
Number of simulation runs	75
Confidence Interval	95%

[a] d is the distance to the BS in km.
[b] θ_h and θ_v represent the horizontal and vertical angles related to the Base Station (BS), respectively.

The ATES technique is capable of reaching levels of satisfaction around the planned value in the macro cell scenario, as can be seen in Figure 4.6(a). If worst channel conditions are considered like the urban macro scenario, as depicted in Figure 4.6(b) , only the smaller targets are achieved for a wide range of users.

Therefore, ATES technique keeps the satisfaction percentage near the requirement in the macro cell scenario, but in all cases the target is not met exactly. These results show that the dynamic variation of peakedness of symmetric curves cannot explore successfully the resources, since it gives the same priority to users with QoS near the throughput requirement and does not consider a large set of users with worse conditions. This explains the decrease of the accuracy observed for higher loads (above 30 users), when the satisfaction levels decay almost 15%.

Figures 4.6(c) and 4.6(d) show the mean throughput per cell as a function of the number of users in the system. The ATES algorithm provides different throughput values depending

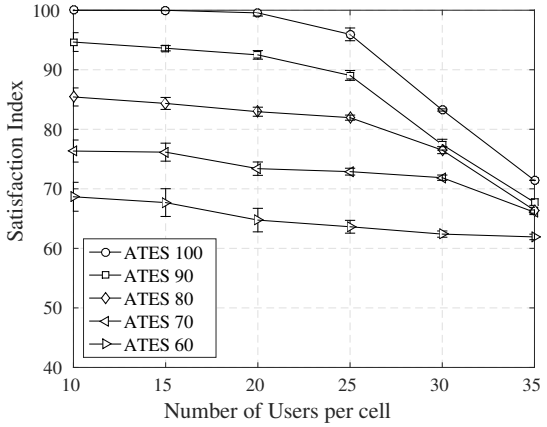

(a) User satisfaction - macro cell scenario [3].

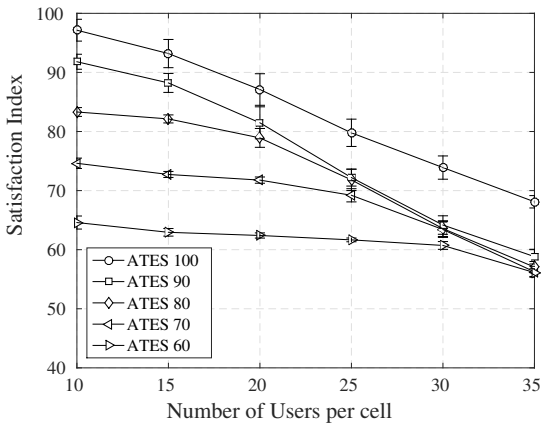

(b) User satisfaction - urban macro scenario [2].

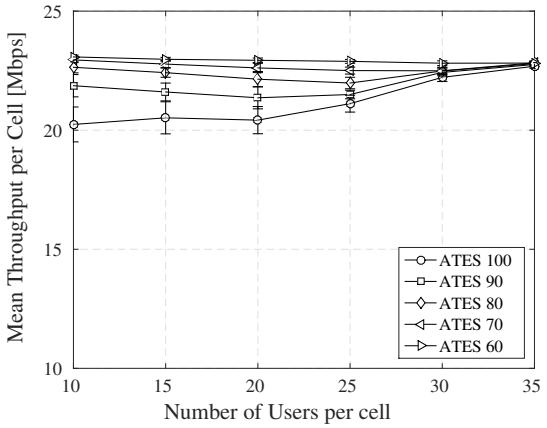

(c) Mean throughput per cell - macro cell scenario [3].

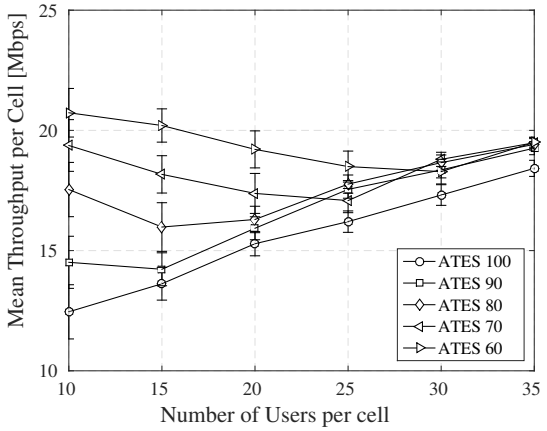

(d) Mean throughput per cell - urban macro scenario [2].

Figure 4.6: Performance metrics of the ATES algorithm as a function of the number of NRT users.

on the chosen satisfaction target, and the change from one target to another has different impact on the throughput, capacity improvement achieved changing Y^{Target} from 100 to 90% is higher than modifying it from 90 to 80%. Observe that $Y^{Target} = 60\%$ provides the maximum throughput levels.

Figures 4.7(a) and 4.7(b) show the satisfaction levels achieved using the ASC algorithm with different targets, $Y^{Target} = \{100, 90, 80, 70, 60\}\%$.

The ASC technique is very successful at reaching and maintaining the levels of satisfaction next to the targets for a large range of users, while ATES algorithm cannot find the target exactly, mainly for higher loads. These results show us that the ASC policy is able to achieve a stable convergence of a specified satisfaction for a higher number of users allowing the network operator to have a good prediction about the system QoS.

The mean throughput per cell achieved by ASC, as indicated in Figures 4.7(c) and 4.7(d), are very similar, independent of the satisfaction target. Also, the values are smaller than those achieved by the ATES. These results indicate the different manner of ASC to deal with the trade-off satisfaction and system capacity.

Figure 4.8 depicts the capacity versus satisfaction plane of a system with 10 User Equipment (UE). This result shows that the ATES algorithm can adjust its utility-based weight in

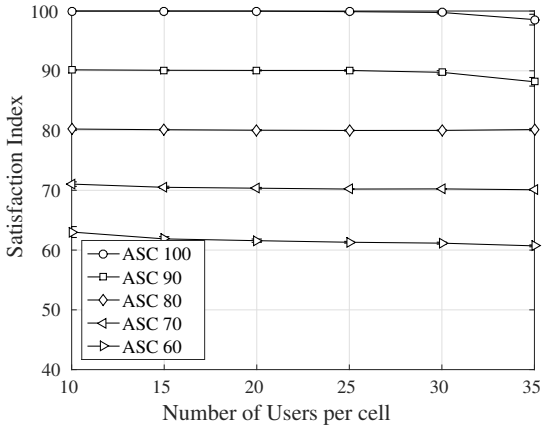

(a) User satisfaction - macro cell scenario [3].

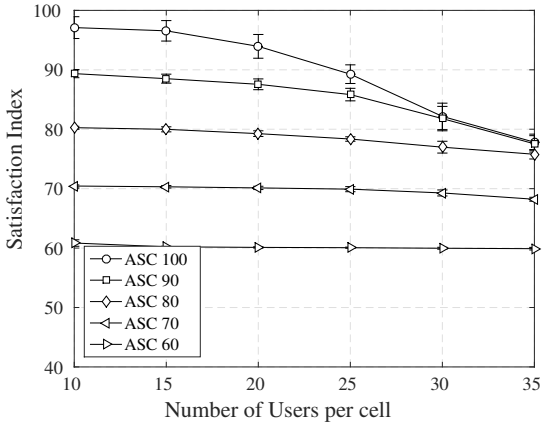

(b) User satisfaction - urban macro scenario [2].

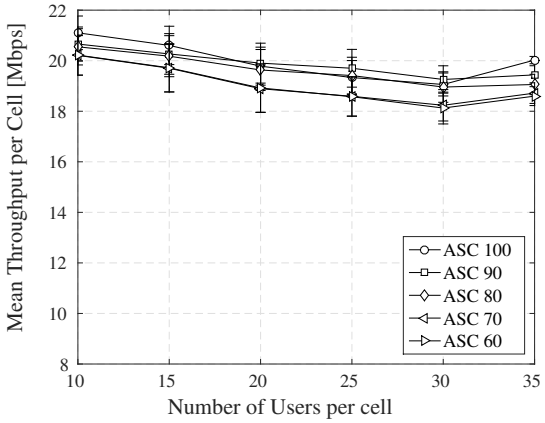

(c) Mean throughput per cell - macro cell scenario [3].

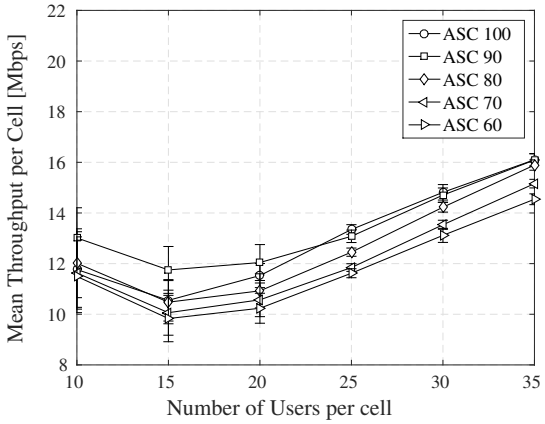

(d) Mean throughput per cell - urban macro scenario [2].

Figure 4.7: Performance metrics of the ASC algorithm as a function of the number of NRT users.

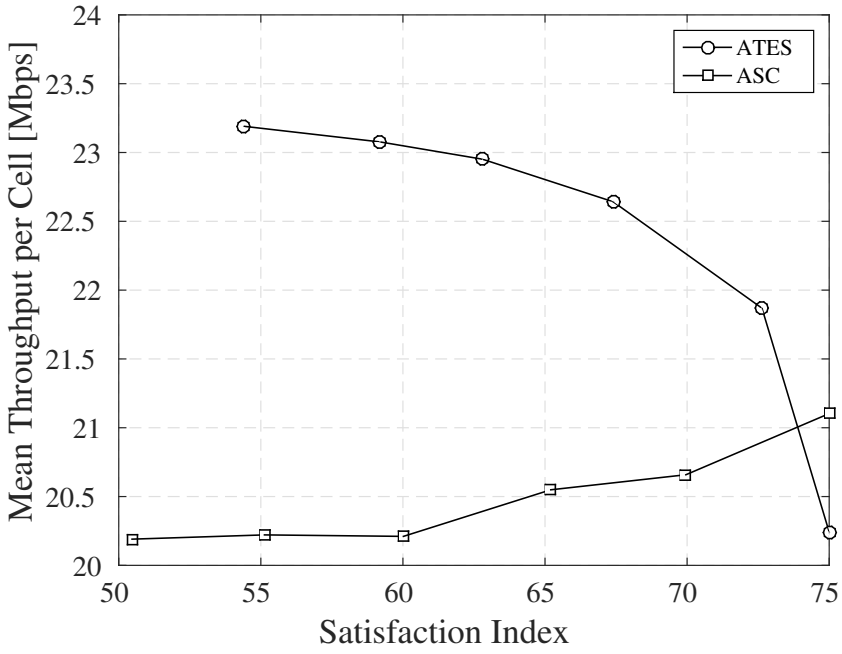

Figure 4.8: Capacity vs Satisfaction plane considering a system load of 10 users - macro cell scenario [3].

order to provide a dynamic trade-off between resource efficiency and user satisfaction - higher requirements of satisfaction percentage are achieved with a decrement of the total cell throughput. The ASC algorithm is not able to deal with this trade-off so efficiently like ATES. ASC aims the strict achievement of the satisfaction levels, since it gives more priority to users with the worst throughput. So, it achieves the satisfaction percentages and has an almost constant throughput.

4.5 Partial Conclusions

The simulations demonstrated that the shifted log-logistic utility function is effective towards the objective of user satisfaction control and make possible employ different strategies. The ATES algorithm adaptively changes the scale parameter λ, enabling a stable strategy to deal with the trade-off between user satisfaction and spectral efficiency. The ASC algorithm is able to ensure a dynamic variation of the shape parameter θ, guaranteeing a strict control of the user satisfaction levels. This feature could be useful in terms of network planning and optimization.

Chapter 5

Conclusions

This thesis deals with scheduling algorithms aiming at the maximization and adaptive control of the satisfaction index in the downlink of an Orthogonal Frequency Division Multiple Access (OFDMA) network, considering different types of traffic models. In order to solve the problem of maximizing the satisfaction with affordable complexity, a cross layer optimization approach uses the utility theory to formulate the problem as a weighted sum rate maximization. Chapter 3 provides some insight on the nature of the mentioned problem, presenting the mathematical formulation of the utility-based scheduling framework.

The determination of the function to be used in the utility-based scheduling framework depends on the desired objectives. This thesis studies two utility functions. Initially, we consider the logistic function, to standardize the framework proposed in [26]. Next, we analyze the shifted log-logistic function, a generalization of the logistic function. The shifted log-logistic function has more parameters, which allows novel scheduling strategies and impacts the distribution of resources among users. Therefore, the new framework considers different strategies of Quality of Service (QoS)-based priorization and channel opportunism, for an equal power allocation among frequency resources.

Chapter 3 considers the problem of improving the percentage of satisfied users. Novel scheduling algorithms that employ different symmetric and asymmetric marginal utility functions are evaluated: Modified Throughput-based Satisfaction Maximization (MTSM) and Modified Delay-based Satisfaction Maximization (MDSM). The various function forms are obtained from the modification of the shape and scale parameters of the shifted log-logistic function. On one hand, MTSM aims to improve satisfaction index among Non-Real Time (NRT) users in a cellular network. On the other hand, MDSM aims to maximize satisfaction among Real Time (RT) users.

The MTSM algorithm obtains significant gains with the use asymmetric marginal utility functions based on throughput with maximum point in the users' throughput requirement, enabling a stable strategy to maximize user satisfaction and keep the spectral efficiency at satisfactory levels for the entire load range considered. The best performance results, achieved with a left skewed and soft edge curve achieved a significant improvement of the users satisfaction levels in comparison with Throughput-based Satisfaction Maximization (TSM) and

the classical algorithms Proportional Fair (PF) and Rate Maximization (RM).

The MDSM algorithm also attained gains with the employment of asymmetric marginal utility functions. Differently from MTSM, uses a marginal utility function based on Head Of Line (HOL) packet delay with maximum point in the users' HOL packet delay requirement, which is usually equal to the RT delay budget of the system. MDSM achieved gains with symmetric and asymmetric curves. In contrast with MTSM, variations in the aperture of the marginal utility curve, i.e., a more flattened curve also provided gains in the users' satisfaction, outperforming Delay-based Satisfaction Maximization (DSM) and classical algorithms Modified Largest Weighted Delay First (MLWDF) and Urgency and Efficiency-based Packet Scheduling (UEPS).

In realistic scenarios, imperfect Channel State Information (CSI) at the transmitter can induce the scheduling of a user whose real channel state cannot support a required data rate, harming the system performance. Chapter 3 also evaluates the impact of the CSI imperfection on the performance of MTSM and MDSM.

Even presenting larger sensitivity to CSI imperfections, since they schedule user considering a QoS-based utility function it is more likely to incur an improper scheduling decisions due to delayed CSI measurements. MTSM and MDSM achieve higher User Equipment (UE) satisfaction percentages than the classical algorithms.

Therefore, the system level simulations indicate the accomplishment of the objective of proposing efficient and low complexity scheduling techniques able to maximize user satisfaction in different scenarios with NRT and RT services.

Chapter 4 investigates novel ways to control the satisfaction level of users of NRT services. This thesis evaluates two algorithms using the shifted log-logistic utility function: Adaptive Throughput-based Efficiency-Satisfaction Trade-Off (ATES) and Adaptive Satisfaction Control (ASC). The ATES algorithm performs an average satisfaction control by adaptively changing the scale parameter, using a feedback control loop that tracks the overall satisfaction of the users and keep it around the desired target value, enabling a stable strategy to deal with the trade-off between satisfaction and capacity. The ASC algorithm is able to ensure a dynamic variation of the shape parameter, guaranteeing a strict control of the user satisfaction levels. This is a strategic advantage to the network operator who is able to design and operate the network according to a planned user satisfaction profile.

Thereby, the system level simulations indicate the accomplishment of the objective of development of adaptive scheduling techniques able to control user satisfaction indexes for different system loads considering NRT services.

Some perspectives of future work include :

- evaluation of others traffic models to broaden our understanding of the applicability of the proposed scheduling algorithms;
- shift to a multi-cellular network and develop inteference management features is a interesting feature to evaluate the algorithms in a more realistic scenario;
- consider the provement of Quality of Experience (QoE): an increasingly number of

studies is focusing on delivering high-quality service experience instead of technical requirements indicated by QoS indicators, like throughput or HOL delay.

Appendix A

Utility-Based Scheduling with Spatial Multiplexing

A.1 Introduction

Efficient and innovative scheduling techniques are essential to provide considerable gains in coverage, capacity and QoS for OFDMA-based broadband wireless networks. In a commercial wireless network, improved coverage, capacity and QoS represent better investment return rates and better radio services. For the customers, this should yield better services, higher fairness and enhanced QoS levels with widespread availability at possibly lower prices. Therefore, it is of utmost importance to investigate innovative means to optimize scheduling techniques that deal with the resources and fully exploit all kinds of diversity offered by an OFDMA-based system, such as time, frequency, space and multi-user.

From the user's point of view, it is relevant to have a fair resource allocation, meet their QoS requirements and maximize their satisfaction independently of their channel situation. Furthermore, network operators want to have the maximum possible number of satisfied clients in order to keep and/or expand its market share and decrease churn.

This appendix consider the problem of user satisfaction maximization using an utility-based scheduling algorithm that uses a sigmoidal utility function combined with either Orthogonal Random Beamforming (ORB) or Fixed Switched Beamforming (FSB) to exploit several kinds of satisfaction, such as time, frequency, space and multi-user, in order to achieve the pursued objective. System level simulations demonstrate that there is an optimal number of spatial beams and that the proposed joint scheduling and beamforming provides higher user satisfaction than other classical techniques found in the literature.

As far as we are concerned, the present study is the first one to propose and evaluate a joint utility-based scheduling and spatial beamforming with the specific objective of improving the percentage of satisfied RT users in an OFDMA system.

The rest of the appendix is organized as follows. Section A.2 presents the system modeling, while section A.3 describes the combination of the beamforming techniques with the utility-based framework described in Chapter 3. System-level simulation results are shown in sections A.4 and A.5. The conclusions of the work are drawn in section A.6.

A.2 System Model

As mentioned earlier, it is considered an OFDMA system where all users form a set $\mathcal{J}$ with size J, and all Resource Blocks (RBs) to be assigned to the users form a set $\mathcal{K}$ with size K. It also assumed a downlink Multiple Input Single Output (MISO) channel with M_T transmit antennas at the Evolved Node B (eNB) and a single receive antenna at the terminals, and $\mathbf{H}_{j,k}$ is an $1 \times M_T$ matrix whose elements $h_{j,k,m}$ consist in the channel transfer function between the receive antenna of terminal j and the transmit antenna m of the Base Station (BS) on RB k. The channel transfer function of the RB is aproximated by the transfer function of the mid sub-carrier that composes the block. Furthermore, it is assumed that the channel coefficients remain constant during the period of a Transmission Time Interval (TTI). Also, perfect channel state information is assumed at both transmitter and receiver.

In a Multi-User (MU)-MISO scenario, the BS can steer a narrow beam b towards a direction of interest by weighting the signal sent by each of its antennas. The complex weights $w_{k,b}$ used to steer beam b on RB k are organized in a beamforming vector. From the whole set of beamforming vectors available for transmission on an RB k, the BS can choose to transmit using a subset $\mathcal{B}_k$ of active beams with size B_k, where $B_k \leq M_T$ in order to limit intercell interference. Using such B_k beams, the BS spatially multiplex different users on RB k.

The total BS transmit power P_t is constant and equally distributed among the RBs. Furthermore, the power p_k of each RB is equally divided between the B_k active beams. Therefore, the power on beam b of the RB k assigned to a terminal j is denoted by $p_{j,k,b}$ and given by p_k/B_k.

It is not considered the intra-cell interference in the scheduling decisions. After resource allocation, terminal j is subject to intra-cell interference from other terminals to which other beams have been assigned on the same resource. Users' data rates are determined using a link adaptation curve considering the Signal to Interference-plus-Noise Ratio (SINR) values after resource allocation [39].

A.3 Spatial Multiplexing

Figure A.1 shows examples of radiation pattern of ORB with 2 beams and FSB with 4 beams. On one hand, ORB creates very large beams, and so a higher coverage can be obtained. This feature is very useful for systems with a large number of users. Notice that where a given beam presents the maximum gain, there is a null on the other beam. On the other hand, FSB produces narrow and directed beams, which reduces the spatial interference. Notice that these beamforming patterns must be combined with the three-sectored radiation pattern of the BS. More details about how the beamforming vectors are generated by ORB and FSB are given in the following.

A.3.1 Orthogonal Random Beamforming

The ORB strategy generates $B_k \leq M_T$ orthogonal random beams on each RB k, where B_k different users can be spatially multiplexed. Random vectors given by $\tilde{\mathbf{w}}_{k,b} \sim \mathcal{CN}(0,1)$ are generated and the beamforming vectors $\mathbf{w}_{k,b}$ in $\mathcal{B}_k$ are obtained by an orthonormalization of $\tilde{\mathbf{w}}_{k,b}$. For $B_k > 1$, the weighting vectors are forced to be orthogonal to each other and to have

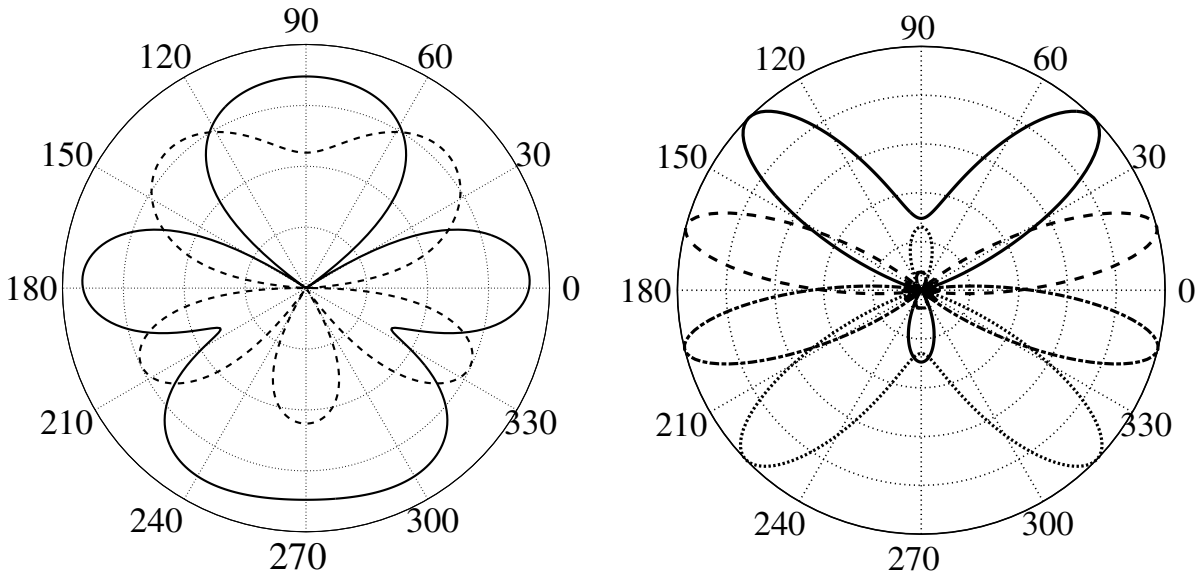

(a) ORB with $B_k = 2$ beams. **(b)** FSB with $B_k = 4$ beams.

Figure A.1: Examples of radiation patterns of ORB and FSB beamforming.

unit norm, i.e., $\mathbf{w}_{k,b}^H \mathbf{w}_{k,b'} = 0$, if $b \neq b'$, or $\mathbf{w}_{k,b}^H \mathbf{w}_{k,b'} = 1$, if $b = b'$.

Thereby, the interference among beams is reduced along the main direction of each beam, i.e., a terminal will receive a signal with higher power whenever aligned with this direction. Besides, new random beams must be periodically generated, thus allowing the whole cell to be covered and giving equal chance to all terminals to profit from the spatial filtering induced by ORB [54]. Due to the orthogonality condition among beams, there is at most M_T beamforming vectors.

A.3.2 Fixed Switching Beamforming

The FSB technique employs fixed steered beams to multiplex several users in space. These beams are formed by applying phase shifts to the individual transmit antenna elements in a uniform linear array, resulting in a evenly distributed arrangement. The desired phase shifts, corresponding to each specific beam, are organized in the phase set $\Theta = \{\theta_1, \ldots, \theta_{M_T}\}$. Therefore, for each phase shift θ_b specified, the weighting vector used to steer the beam b on RB k, is organized as the following steering vector:

$$\mathbf{w}_{k,b} = \frac{1}{\sqrt{M_T}} \left[1 \; e^{j\pi \sin\theta_b} \ldots e^{j\pi(M_T-1)\sin\theta_b}\right]. \tag{A.1}$$

Notice that the beams $w_{k,b}$ are not necessarily orthogonal to each other. FSB offers the flexibility to generate a maximum of M_T beams and to choose afterwards a reduced subset of active beams $\mathcal{B}_k$ in order to limit intra-cell interference.

A.3.3 Joint Scheduling and Beamforming

Based on [54], we consider that the ordering of the beams of the set $\mathcal{B}_k$ is not statistically relevant considering the entire resource assignment process. Therefore, the beams can be processed sequentially, i.e., the algorithms can be applied to beam $b = 1$, then to to beam $b = 2$, and so on.

The scheduling is done on a TTI basis. It is controlled by a priority assignment map $A \in \mathbb{R}^{J \times K \times M_T}$. This map represents the priorities of the users for all RBs and beams, where M_T upper limits $B_k, \forall k$. If more than one user has the same priority for the same RB and beam, a tiebreaker process selects the user with the highest Signal to Noise Ratio (SNR).

An extension of a scheduling algorithm to cope with beamforming techniques was proposed by [54]. Based on that, we adapted our utility-based Dynamic Resource Assignment (DRA) algorithm. Two modifications intended to limit spatial interference were made:

- **Avoidance of self-interference**: whenever a beam b of RB k is allocated to user j, all the other beams $b' \neq b$ on RB k are blocked to user j. This condition prevents user j from being allocated to multiple beams of the same RB, and so user j does not interfere with himself.

- **Locking of beams/resources**: whenever all B_k beams of the RB k are allocated to users, RB k is withdrawn from the set $\mathcal{K}$ of available RBs. Whenever user j is allocated the beam b of RB k, this beam is blocked to all others users $j' \neq j$. However, the other beams $b' \neq b$ of RB k remain free to be assigned to other users $j' \neq j$. This condition avoids that multiple users be allocated to the same beam of a given RB.

A.4 Performance Evaluation of NRT Service Scenario

In this section we firstly investigate the performance of the TSM scheduler with/without the use of FSB beamforming. Next, the TSM+FSB technique is compared with other classical scheduling algorithms found in the literature, such as RM [49], PF [18] and Satisfaction-Oriented Resource Allocation for Non-Real Time Services (SORA-NRT) [23, 54]. Notice that the classical algorithms were also extended to work with FSB. Analyses are based on the results of system-level simulations conducted for NRT services. The simulation parameters are presented in Table A.1.

The performance of the TSM algorithm with/without FSB is evaluated considering different numbers of active beams, in comparison with the Single Input Single Output (SISO) scenario. A total number of $M_T = 8$ transmit antennas is considered at the BS and the number of active beams B_k is varied from 1 to 4. Therefore, the beamforming configurations analyzed are denominated TSM FSB1, FSB2, FSB3 and FSB4.

Figure A.2 shows the system capacity in terms of total cell throughput as a function of the number of NRT users (system load). Considering the SISO case, the total throughput provided by TSM increases as the system load also increases. This means that TSM indeed exploits multi-user diversity while tries to keep all users as satisfied as possible.

The combinations TSM FSB1 and FSB2 also preserve the ability of exploiting multi-user diversity whereas it is benefited by two advantages brought by multiple antennas: i) the array gain that enhances signal quality; and ii) spatial diversity due to spatially distributed beams. Therefore, TSM and FSB are able to improve the system throughput. TSM FSB2 provides meaningful gains (about 20% to 30%) compared to TSM SISO. The performance of TSM FSB3 and TSM FSB4 is worse than the cases with 1 and 2 active beams. The explanation for this behavior is that the power of each RB p_k has to be divided among more beams, which decreases

Table A.1: Simulation Parameters - NRT Service Scenario

Parameter	Value
Number of cells	1
Maximum BS transmit power	1 W
BS antenna radiation pattern	Three-sectored
Cell radius	250 m
UE speed	3 km/h
Carrier frequency	2 GHz
System bandwidth	5 MHz
Sub-carrier bandwidth	15 kHz
Number of RBs	25
Path loss[a]	$L = 128.1 + 37.6 \log_{10} d$
Log-normal shadowing st. dev.	8 dB
Small-scale fading [43]	3GPP Typical Urban
AWGN power per sub-carrier	-123.24 dBm
Noise figure	9 dB
Link adaptation	Link level curves from [39]
Transmission Time Interval	1 ms
NRT traffic model	Full buffer
User throughput requirement	512 kbps
Parameter σ	2.441×10^{-5}
Number of transmit antennas	8
Number of receive antennas	1
Multi-antenna configuration	MU-MISO
Simulation time span	30 s
Number of simulation runs	10

[a] d is the distance to the eNB in km.

the signal quality for each assigned user. Besides that, more active beams lead to additional interference in case the users are not well aligned with the main lobes of their assigned beams.

Figure A.3 depicts the percentage of satisfied users as a function of the number of users in the system. An NRT user is considered satisfied if its session throughput is higher or equal to a threshold ($T_j[n] \geq T^{\text{req}}$). simulation snapshot.

The result shown in Fig. A.3 demonstrates that the TSM FSB1 and TSM FSB2 effectively exploit the spatial dimension of the resource allocation process by keeping the users'

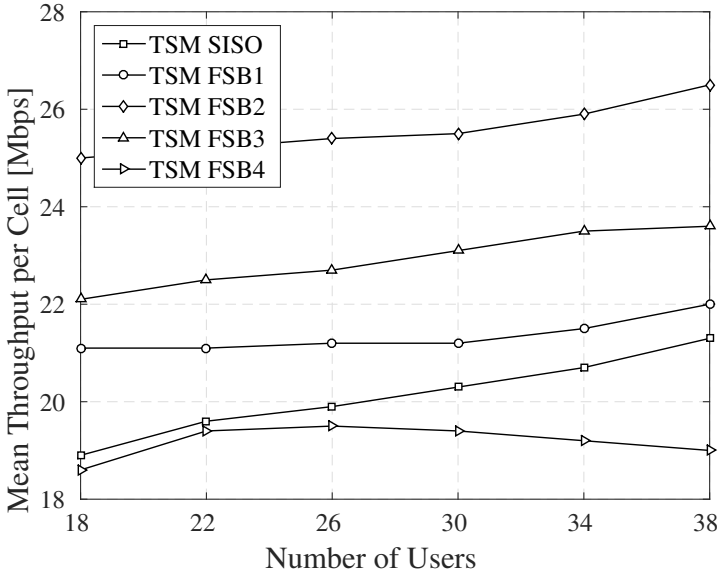

Figure A.2: Mean throughput per cell of the TSM scheduler with FSB and SISO antenna configurations.

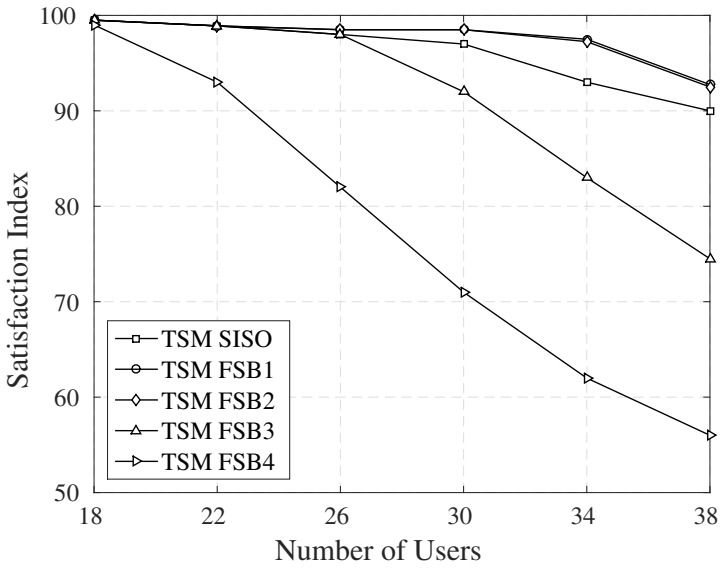

Figure A.3: Satisfaction index of the TSM scheduler with FSB and SISO antenna configurations.

satisfaction as good as or slightly better than that achieved in the SISO configuration while providing considerable throughput gains for the system, as shown in Fig. A.2. Not only does TSM FSB2 show the best trade-off between capacity and satisfaction, but achieves the best balance between multi-user and spatial multiplexing gains, and spatial interference avoidance, as well. Again TSM FSB3 and FSB4 presented the worst results, indicating that the inclusion of more beams in the system is not necessarily translated into a good resource allocation.

The TSM technique with 4 and 3 active beams presents higher user throughputs at the expense of high levels of outage, i.e., many users have no opportunity to transmit. This high outage occurence explains the bad satisfaction and fairness results presented by TSM FSB4 and TSM FSB3 (see Figure A.3).

Let us choose the best FSB configuration ($B_k = 2$ beams), and compare the performance of TSM with other schedulers found in the literature, namely RM, PF and SORA-NRT.

Figure A.4 depicts the system capacity in terms of total cell throughput as a function of the

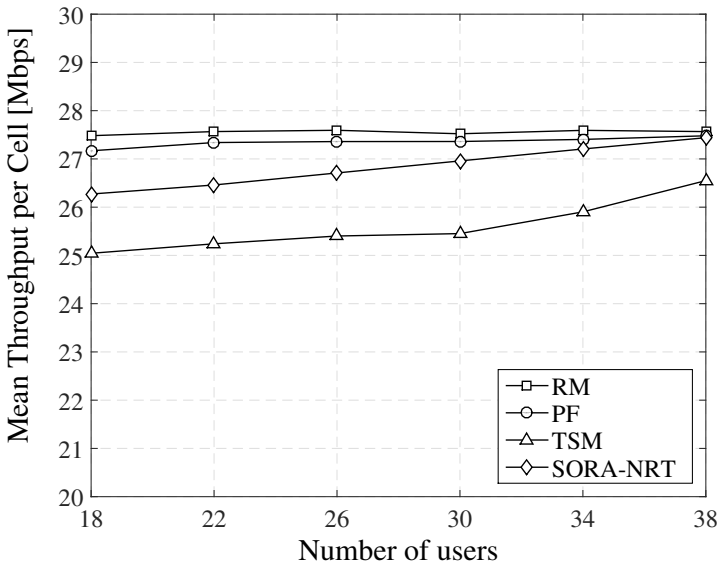

Figure A.4: Mean Throughput considering different schedulers and FSB with 2 beams.

number of NRT users. As expected, the RM scheduler provides the best results. It is able to achieve the highest system capacity for all system loads by assigning each beam within the RBs to the user that can transmit at the highest rate. PF presents good total system throughput with an almost flat behavior for different traffic loads. Moreover, the SORA-NRT scheduler presents a reasonable performance in terms of capacity for low and moderate loads because it tries to satisfy the users as much as possible. However, SORA-NRT achieves very good results for high offered loads, because it is able to opportunistically exploit the multi-user diversity by allocating the remaining resources to the flows with the best channel conditions. Finally, TSM tries to keep the throughput of the satisfied flows as close as possible from each other, which is not so efficient in terms of system capacity. However, notice that TSM also approaches the performance of RM when the system load increases. This happens because it is also able to exploit multi-user diversity in order to achieve higher system capacity.

Figure A.5 depicts the percentage of satisfied users as a function of the system load. TSM shows the best satisfaction results for all considered system loads, which demonstrates the advantage of using sigmoidal utility functions when satisfaction maximization is desired. RM provides an overall degraded QoS because it leaves many users in outage situations. PF and SORA-NRT also present good satisfaction results, but the latter outperforms the former for high loads. It is important to highlight the satisfaction gain provided by the proposed TSM technique compared with SORA-NRT, since the latter was specially designed to provide the highest satisfaction levels.

Another advantage of the TSM technique is the low computational complexity. Its complexity is in the same order of PF and lower than SORA-NRT (heuristics). The complexity of TSM depends only on the calculation of the users' weights with dimension J, and K sorting operations of a scheduling metric with dimension J (K and J are the numbers of resources and users, respectively). The computational complexity of the FSB beamforming is the same for all schedulers.

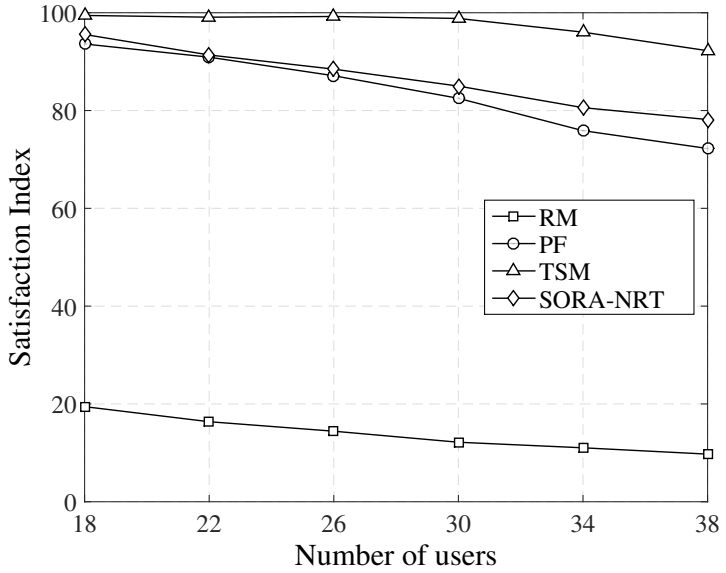

Figure A.5: Satisfaction index considering different schedulers and FSB with 2 beams.

A.5 Performance Evaluation of RT Service Scenario

Sections A.5.1 and A.5.2 investigate the performance of the DSM algorithm with/without the use of ORB and FSB beamforming, respectively. It is also compared the joint DSM/beamforming with other classical scheduling algorithms found in the literature, such as RM [49], MLWDF [50], and UEPS [51]. Details about these scheduling algorithms are provided in Chapter 2. Notice that the classical algorithms were also extended to work with ORB or FSB. Section A.5.3 discusses which is the best beamforming strategy to be used in conjunction with DSM. Analyses are based on system-level evaluations of RT services.

A total number of $M_T = 8$ transmit antennas is considered at the BS for the ORB and FSB cases. A different numbers of active beams B_k are considered, which is varied from 1 to 4 in both cases. The simulation parameters are shown in Table A.2.

The simulation results presented in the following is the percentage of satisfied RT users. If the user's Frame Erasure Rate (FER) is lower than or equal to a requirement, the user is considered satisfied; otherwise it is assumed unsatisfied.

A.5.1 ORB Results

The percentage of satisfied users as a function of the system load is depicted in Figure A.6. Notice that the DSM ORB1 has the highest satisfaction values, which surpass those of the SISO configuration, because the antenna array directivity enhances the SINR. However, when

Table A.2: Simulation Parameters - RT Service Scenario

Parameter	Value
Number of cells	1
Maximum BS transmit power	1 W
BS antenna radiation pattern	Three-sectored
Cell radius	250 m
UE speed	3 km/h
Carrier frequency	2 GHz
System bandwidth	5 MHz
Sub-carrier bandwidth	15 kHz
Number of RBs	25
Path loss[a]	$L = 128.1 + 37.6 \log_{10} d$
Log-normal shadowing st. dev.	8 dB
Small-scale fading	3GPP Typical Urban
AWGN power per sub-carrier	-123.24 dBm
Noise figure	9 dB
Link adaptation	Link level curves from [39]
Transmission Time Interval	1 ms
RT packet size	256 bits
RT packet interarrival time	2 ms
FER threshold	2%
HOL delay requirement	100 ms
RT delay budget	100 ms
Parameter σ	138.135
Number of transmit antennas	8 (ORB/FSB)
Number of receive antennas	1
Multi-antenna configuration	MU-MISO
Simulation time span	15 s
Number of simulation runs	10

In s

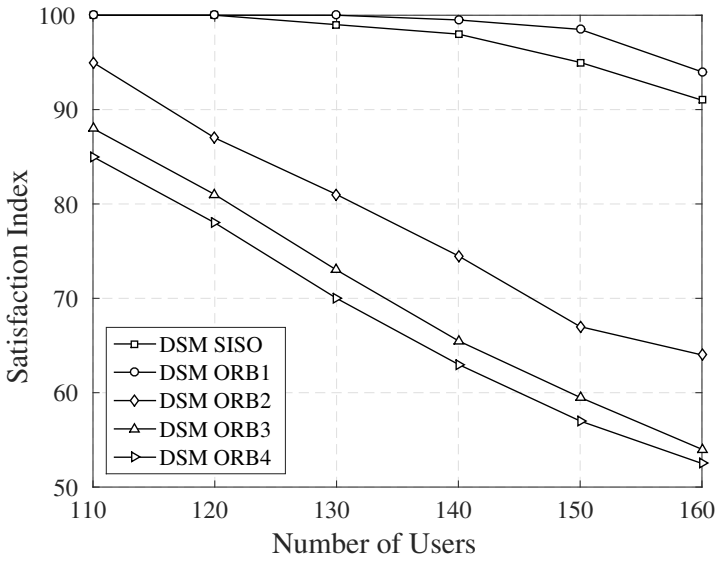

Figure A.6: Evaluation of the DSM technique with ORB.

the number of active beams is further increased, the performance of DSM ORB decreases considerably. These results indicate a trade-off between spatial multiplexing and spatial interference when ORB is used, because of the nature of the beams that are generated by this strategy, which are orthogonal, but very wide. Thus, cross-interference between beams can be eliminated only for users perfectly aligned with the main lobes of the random beams. Since this situation is highly improbable, the increased number of beams leads to the scheduling of users that highly interfere with each other, which causes the performance losses shown in Fig. A.6.

Let us choose the best ORB configuration ($B_k = 1$ beam), and compare the performance of DSM with other classical scheduling algorithms in Figure A.7. The algorithms that take into account the HOL delay in their formulations are those ones that provide the highest user satisfaction. The resource allocation criteria of these algorithms are based on the combination of two indicators: a QoS indicator that is a function of the HOL delay, and an efficient indicator that can be the achievable transmission rate (DSM) or the ratio between the transmission

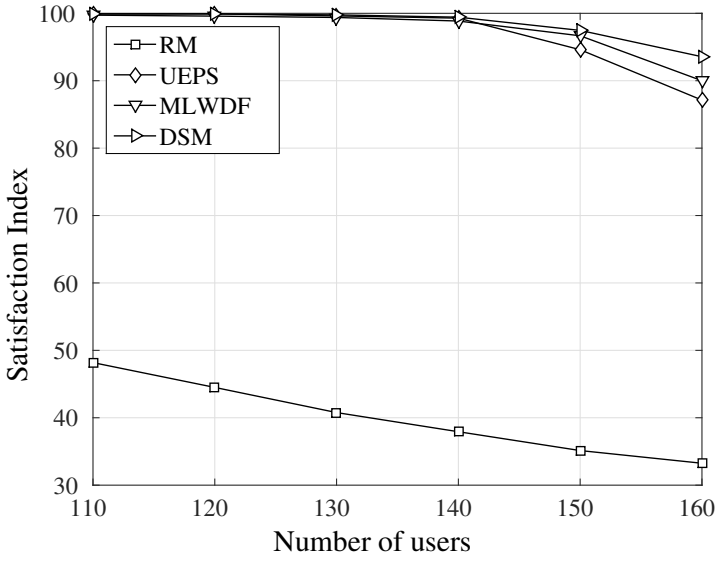

Figure A.7: Evaluation of different RRA techniques using ORB with 1 beam.

rate and the user throughput (MLWDF and UEPS). As can be noticed, the proposed DSM technique achieved its objective of maximizing user satisfaction. The combination of the bell-shaped delay-based indicator and the achievable transmission rate indicator proved to be the best option. Furthermore, its computational complexity is in the same order of the classical algorithms, except RM, which presents the lowest complexity.

A.5.2 FSB Results

According to Figure A.8, there is also an optimal number of beams to be used by FSB. In comparison with DSM SISO, the use of one beam in DSM FSB1 is not advantageous. However, when 2 beams are activated, there is a remarkable satisfaction improvement. The use of one additional beam is not beneficial anymore, causing a slight satisfaction degradation. DSM FSB4 degrades the system performance even more, but is still better than DSM SISO. When more beams are used, we still have the benefit of enhanced quality due to the array gain, but this gain is limited by the reduction of the transmit power per beam. Moreover, the spatial multiplexing gain is linear with the number of beams. However, these two advantages are overcome by the interference caused by the overlap of adjacent beams, which degrades performance.

Choosing the best FSB configuration ($B_k = 2$ beams), and comparing the performance of DSM with RM, MLWDF, and UEPS, we can see that DSM still outperforms the other techniques (see Figure A.9). The reasons behind this behavior were already explained in section A.5.1 for the ORB case.

A.5.3 Comparison between ORB and FSB

In this section, we assess the configurations of DSM ORB and DSM FSB that achieve the highest gains in terms of user satisfaction, namely ORB1 and FSB2.

Assessing Figures A.6 and A.8, one can notice that DSM FSB2 provides better user satisfaction than both DSM ORB1 and DSM SISO. When the system load is low, the user satisfaction is high for all schemes. As the load increases, the satisfaction of SISO and ORB1 decreases quickly, while FSB2 maintains high satisfaction values. This behavior is a consequence of the DSM FSB resource allocation, which minimizes the interference and exploits

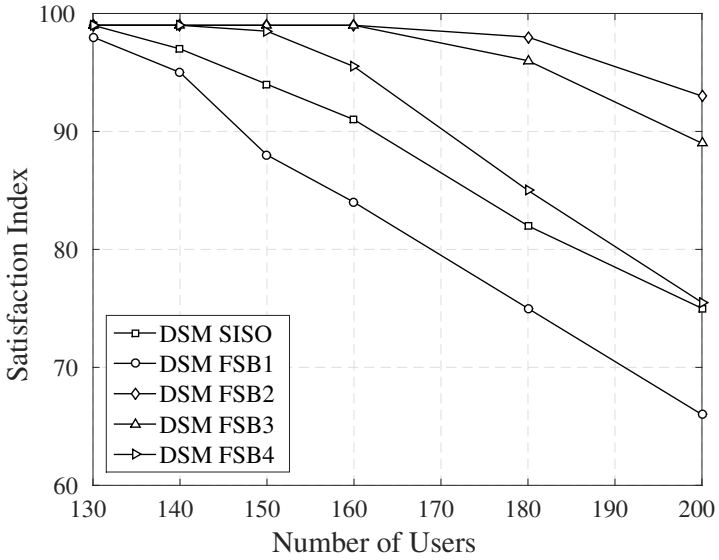

Figure A.8: Evaluation of the DSM technique with FSB.

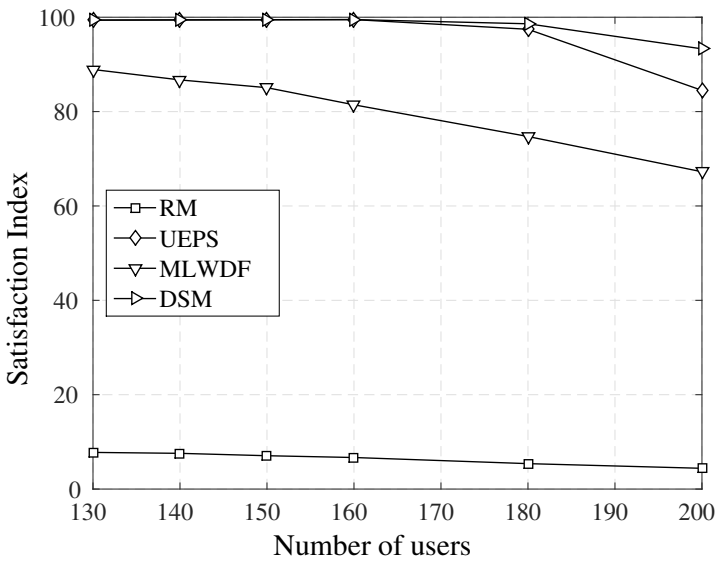

Figure A.9: Evaluation of different RRA techniques using FSB with 2 beams.

efficiently the multi-user diversity and spatial multiplexing. Notice that the relative capacity gains of DSM FSB2 in comparison with DSM ORB1 and DSM SISO, in terms of number of users for a satisfaction target of 95%, are 25% and 32%, respectively. DSM ORB1 also obtains a small capacity gain of 5% compared with DSM SISO, as a consequence of the array gain due to antenna directivity.

A.6 Conclusion

It is demonstrated by means of system level simulations that the TSM algorithm combined with FSB is effective towards the objective of user satisfaction maximization. It can also be concluded that the addition of more active beams in the transmitter does not necessarily help the scheduler to achieve higher cell throughput or improved user satisfaction. There is an optimal number of active beams that achieves the best trade-off between antenna array gain, spatial multiplexing gain and cross-interference among beams. TSM FSB2 with two active beams showed the best results.

When compared with other schedulers that also use FSB with two beams, TSM FSB2 presented the highest satisfaction and increasing system capacity with the number of users due to multiuser diversity. Moreover, TSM presents good computational complexity in the same order of PF and lower than SORA-NRT. Since we achieved the best results with a reduced number of beams, we have that the extra computational burden is largely compensated by the improved performance provided by the FSB beamforming scheme.

System level simulations indicate that the DSM scheduling algorithm combined with ORB or FSB beamforming is effective towards the objective of user satisfaction maximization. It can also be concluded that the addition of more active beams does not necessarily help DSM to achieve better user satisfaction. There is an optimal number of active beams that achieves the best trade-off between antenna array gain, spatial multiplexing gain and cross-interference among beams.

DSM ORB1 and DSM FSB2 were the combinations that showed the best results. When compared with other scheduling algorithms using the same beamforming schemes, they

presented the highest user satisfaction. When they are compared among each other, it is concluded that FSB is preferred because it provides the highest gains due to reduced interference.

The perspectives for future works include

i. evaluation of more realistic scenarios, considering imperfect CSI and inter-cell interference;

ii. analysis of computational complexity of the proposed algorithms.

Appendix B

Shifted Log-Logistic Function as a Generalization of the Logistic Function

The shifted log-logistic function is a generalization of the logistic utility function, converging to it when the shape parameter tends to zero. To simplify the analysis, we consider the auxiliary variable, used in Eq. (3.11), as $\eta = 1$.

The limit considered is given by

$$\lim_{\theta\to 0} w_j^{\text{S-Log}} = \lim_{\theta\to 0} \frac{\frac{1}{\lambda}\left(1+\frac{\theta(x_j[n]-x_j^{\text{req}})}{\lambda}\right)^{-1-1/\theta}}{\left(1+\left(1+\frac{\theta(x_j[n]-x_j^{\text{req}})}{\lambda}\right)^{-1/\theta}\right)^2} \tag{B.1}$$

Observe that Eq. (B.1) is equivalent to

$$\frac{\lim_{\theta\to 0}\frac{1}{\lambda}\left(1+\frac{\theta(x_j[n]-x_j^{\text{req}})}{\lambda}\right)^{-1-1/\theta}}{\lim_{\theta\to 0}\left(1+\left(1+\frac{\theta(x_j[n]-x_j^{\text{req}})}{\lambda}\right)^{-1/\theta}\right)^2} \tag{B.2}$$

The limit of the numerator can be written as

$$\lim_{\theta\to 0}\frac{1}{\lambda}\left(1+\frac{\theta(x_j[n]-x_j^{\text{req}})}{\lambda}\right)^{-1-1/\theta} \tag{B.3}$$

Considering $\frac{\theta(x_j[n]-x_j^{\text{req}})}{\lambda} = \frac{1}{y}$, the Eq. (B.3) becomes

$$\lim_{\theta\to 0}\frac{1}{\lambda}\left(1+\frac{\theta(x_j[n]-x_j^{\text{req}})}{\lambda}\right)^{-1-1/\theta} =$$

$$\lim_{y\to\infty}\frac{1}{\lambda}\left(1+\frac{1}{y}\right)^{-\frac{(x_j[n]-x_j^{\text{req}})y}{\lambda}} =$$

$$\left(\frac{1}{\lambda}\cdot\lim_{y\to\infty}\left(1+\frac{1}{y}\right)^{y}\right)^{(x_j[n]-x_j^{\text{req}})/\lambda} =$$

$$\frac{1}{\lambda}e^{-(x_j[n]-x_j^{\text{req}})/\lambda}. \tag{B.4}$$

Likewise, the limit of the denominator can be written as

$$\lim_{\theta\to 0}\left(1+\left(1+\frac{\theta(x_j[n]-x_j^{\text{req}})}{\lambda}\right)^{-1/\theta}\right)^2 \tag{B.5}$$

Regarding again that $\frac{\theta(x_j[n]-x_j^{\text{req}})}{\lambda}=\frac{1}{y}$, the Eq. (B.5) becomes

$$\lim_{y\to\infty}\left(1+\left(1+\frac{1}{y}\right)^{-y(x_j[n]-x_j^{\text{req}})/\lambda}\right)^2 =$$

$$\left(1+e^{-(x_j[n]-x_j^{\text{req}})/\lambda}\right)^2. \tag{B.6}$$

Combining Eq.(B.4) and Eq.(B.6), the limit initially considered can be written as

$$\frac{\frac{1}{\lambda}e^{-(x_j[n]-x_j^{\text{req}})/\lambda}}{\left(1+e^{-(x_j[n]-x_j^{\text{req}})/\lambda}\right)^2}. \tag{B.7}$$

Thus, when $\theta\to 0$, the shifted log-logistic converges to the logistic function.

Bibliography

[1] T. F. Maciel, "Avaliação de Desempenho de Técnicas de Controle e Atribuição de Potência para Aumento de Capacidade e Qualidade de Serviço na Rede GSM/EDGE," Master's thesis, Universidade Federal do Ceará, Abril 2004.

[2] 3GPP, "Spatial channel model for multiple input multiple output (MIMO) simulations," 3rd Generation Partnership Project, TR 25.996 V7.0.0, Jun. 2007.

[3] ——, "Physical layer aspects for evolved universal terrestrial radio access (UTRA)," 3rd Generation Partnership Project, TR 25.814 V7.1.0, Sep. 2006.

[4] G. Tychogiorgos and K. K. Leung, "Optimization-based Resource Allocation in Communication Networks," *Computer Networks*, vol. 66, pp. 32–45, Jun. 2014.

[5] Ericsson, "Ericsson Mobility Report: On the Pulse of the Networked Society," *Whitepaper*, Nov. 2015.

[6] Cisco, "Cisco Visual Networking Index: Global Mobile Data Traffic Forecast Update, 2014–2019," *Whitepaper*, Feb. 2015.

[7] A. Asadi and V. Mancuso, "A Survey on Opportunistic Scheduling in Wireless Communications," *IEEE Communications Surveys Tutorials*, vol. 15, no. 4, pp. 1671–1688, 2013.

[8] F. Capozzi, G. Piro, L. Grieco, G. Boggia, and P. Camarda, "Downlink Packet Scheduling in LTE Cellular Networks: Key Design Issues and a Survey," *IEEE Communications Surveys and Tutorials*, vol. 15, no. 2, pp. 678–700, Mar. 2013.

[9] R. Knopp and P. Humblet, "Information Capacity and Power Control in Single-Cell Multiuser Communications," vol. 01, Jun. 1995, pp. 331–335.

[10] J. Yang, Z. Yifan, W. Ying, and Z. Ping, "Average Rate Updating Mechanism in Proportional Fair Scheduler for HDR," in *IEEE Global Telecommunications Conference*, vol. 6, Nov 2004, pp. 3464–3466.

[11] R. Kwan, C. Leung, and J. Zhang, "Proportional Fair Multiuser Scheduling in LTE," *IEEE Signal Processing Letters*, vol. 16, no. 6, pp. 461–464, Jun. 2009.

[12] E. Liu and K. Leung, "Proportional Fair Scheduling: Anlytical Insight Under Rayleigh Fading Environment," in *IEEE Wireless Communications and Networking Conference*, 2008, pp. 1883–1888.

[13] M. Proebster, C. Mueller, and H. Bakker, "Adaptive Fairness Control for a Proportional Fair LTE Scheduler," in *International Symposium on Personal Indoor and Mobile Radio Communications*, Sep. 2010, pp. 1504–1509.

[14] B. Sadiq, S. J. Baek, and G. de Veciana, "Delay-Optimal Opportunistic Scheduling and Approximations: The Log Rule," in *IEEE International Conference on Computer Communications*, Apr. 2009, pp. 1692–1700.

[15] H. Ramli, R. Basukala, K. Sandrasegaran, and R. Patachaianand, "Performance of Well Known Packet Scheduling Algorithms in the Downlink 3GPP LTE System," in *IEEE Malaysia International Conference on Communications*, Dec. 2009, pp. 815–820.

[16] D. Skoutas and A. Rouskas, "Scheduling with QoS Provisioning in Mobile Broadband Wireless Systems," in *European Wireless Conference*, Apr. 2010, pp. 422–428.

[17] Y. Zaki, T. Weerawardane, C. Gorg, and A. Timm-Giel, "Multi-QoS-Aware Fair Scheduling for LTE," in *IEEE Vehicular Technology Conference*, May 2011, pp. 1–5.

[18] F. Kelly, "Charging and Rate Control for Elastic Traffic," *European Transactions on Telecommunications*, vol. 8, pp. 33–37, 1997.

[19] G. Song and Y. G. Li, "Cross-layer optimization for OFDM wireless networks - part I: Theoretical framework," *IEEE Transactions on Wireless Communications*, vol. 4, no. 2, pp. 614–624, Mar. 2005.

[20] ——, "Cross-layer optimization for OFDM wireless networks - part II: Algorithm development," *IEEE Transactions on Wireless Communications*, vol. 4, no. 2, pp. 625–634, Mar. 2005.

[21] M. Fathi and H. Taheri, "Utility-Based Resource Allocation in Orthogonal Frequency Division Multiple Access Networks," *IET Communications*, vol. 4, no. 12, pp. 1463–1470, Aug. 2010.

[22] R. B. Santos, F. R. M. Lima, and a. F. R. P. C. W. Freitas, "QoS Based Radio Resource Allocation and Scheduling with Different User Data Rate Requirements for OFDMA Systems," in *IEEE International Symposium on Personal, Indoor and Mobile Radio Communications*, 2007.

[23] F. R. M. Lima, S. Wänstedt, F. R. P. Cavalcanti, and W. C. Freitas, "Scheduling for Improving System Capacity in Multiservice 3GPP LTE," *Journal of Electrical and Computer Engineering*, no. 819729, 2010.

[24] E. B. Rodrigues and F. Casadevall, "Adaptive Radio Resource Allocation Framework for Multi-User OFDM," in *IEEE Vehicular Technology Conference*, Apr. 2009, pp. 1–6.

[25] F. R. M. Lima, W. C. Freitas, and F. R. P. Cavalcanti, "Scheduling Algorithm for Improved System Capacity of Real-Time Services in 3GPP LTE," in *XXVII Telecommunications Brazilian Symposium - SBrT*, Oct. 2009.

[26] E. B. Rodrigues, F. R. M. Lima, T. F. Maciel, and F. R. P. Cavalcanti, "Maximization of User Satisfaction in OFDMA Systems Using Utility-Based Resource Allocation," *Wireless Communications and Mobile Computing*, pp. 1–17, 2014.

[27] E. B. Rodrigues, F. H. C. Neto, T. F. Maciel, F. R. M. Lima, and F. R. P. Cavalcanti, "Utility-based scheduling and fixed switching beamforming for user satisfaction improvement in OFDMA systems," in *Procedings of the European Wireless Conference*, May 2014, pp. 1–6.

[28] E. B. Rodrigues, F. H. C. Neto, T. F. Maciel, and F. R. P. Cavalcanti, "Utility-Based Resource Allocation with Spatial Multiplexing for Real Time Services in Multi-User OFDM Systems," in *Vehicular Technology Conference (VTC Spring)*, May 2014, pp. 1–5.

[29] R. Bosisio and U. Spagnolini, "On the Sum-Rate of Opportunistic Beamforming Schemes with Multiple Antennas at the Receiver," in *IEEE International Conference on Communications*, 2007, pp. 1048–1053.

[30] R. Bosisio, J. L. Vicario, C. Anton-Haro, and U. Spagnolini, "The Effect of Imperfect Feedback on Broadcast Opportunistic Beamforming Schemes," in *European Wireless Conference*, April 2006, pp. 1–7.

[31] J. L. Vicario, "Antenna Selection Techniques in Single- and Multi-User Systems: a Cross-Layer Approach," Ph.D. dissertation, Universitat Politecnica de Catalunya, Jun. 2006.

[32] V. F. Monteiro, D. A. Sousa, F. H. C. Neto, E. B. Rodrigues, T. F. Maciel, and F. R. P. Cavalcanti, "Throughput-Based Satisfaction Maximization for a Multi-Cell Downlink OFDMA System Considering Imperfect CSI," in *Telecommunications Brazilian Symposium (SBrT)*, Sep. 2015.

[33] N. Bao, J. Li, W. Xia, and L. Shen, "QoS-Aware Resource Allocation Algorithm for OFDMA-WLAN Integrated System," in *IEEE Wireless Communications and Networking Conference*, Apr. 2013, pp. 807–812.

[34] I. Wong and B. Evans, "Optimal Resource Allocation in the OFDMA Downlink with Imperfect Channel Knowledge," *IEEE Transactions on Communications*, vol. 57, no. 1, pp. 232–241, January 2009.

[35] R. Aggarwal, M. Assaad, C. Koksal, and P. Schniter, "Joint Scheduling and Resource Allocation in the OFDMA Downlink: Utility Maximization Under Imperfect Channel-State Information," *IEEE Transactions on Signal Processing*, vol. 59, no. 11, pp. 5589–5604, Nov 2011.

[36] S. Stefanatos and N. Dimitriou, "Downlink OFDMA Resource Allocation Under Partial Channel State Information," in *IEEE International Conference on Communications*, June 2009, pp. 1–5.

[37] Z. Wang and L. Liu, "Adaptive Resource Management for Downlink OFDMA System with Imperfect CSI," *Electronics Letters*, vol. 50, no. 7, pp. 554–556, Mar. 2014.

[38] M. George and R. Koilpillai, "Fairness-Based Resource Allocation in OFDMA Downlink with Imperfect CSIT," in *International Conference on Wireless Communications Signal Processing*, Oct 2013, pp. 1–6.

[39] C. Mehlführer, M. Wrulich, J. C. Ikuno, D. Bosanska, and M. Rupp, "Simulating the Long Term Evolution Physical Layer," in *Procedings of the European Signal Processing Conference*, Glasgow, Scotland, August 2009. [Online]. Available: http://publik.tuwien.ac.at/files/PubDat_175708.pdf

[40] J. C. Ikuno, M. Wrulich, and M. Rupp, "System Level Simulation of LTE Networks," in *Proceedings of the IEEE Vehicular Technology Conference (VTC)*, May 2010, pp. 1–5.

[41] T. F. Maciel, "Suboptimal Resource Allocation for Multi-User MIMO-OFDMA Systems," Ph.D. dissertation, Technische Universität Darmstadt, Darmstädter Dissertationen D17, Sep. 2008.

[42] T. S. Rappaport, *Wireless Communications: Principles and Practice*, 2nd ed. Prentice Hall, 2002.

[43] 3GPP, "Deployment aspects," 3rd Generation Partnership Project, Tech. Rep. TR 25.943 V9.0.0, Dec. 2009.

[44] F. Gunnarsson, M. Johansson, A. Furuskar, M. Lundevall, A. Simonsson, C. Tidestav, and M. Blomgren, "Downtilted Base Station Antennas - A Simulation Model Proposal and Impact on HSPA and LTE Performance," in *IEEE Vehicular Technology Conference*, September 2008, pp. 1–5.

[45] R. Batista, T. Maciel, Y. Silva, and F. Cavalcanti, "Impact Evaluation of Imperfect CSI on the Performance of Downlink CoMP Systems," in *Brazilian Telecommunications Symposium*, Sep. 2011, pp. 1–5.

[46] 3GPP, "Evolved Universal Terrestrial Radio Access (E-UTRA); physical layer procedures," 3rd Generation Partnership Project, TS 36.213 V8.6.0, Mar. 2009.

[47] P. Ameigeiras, Y. Wang, J. Navarro-Ortiz, P. E. Mogensen, and J. M. Lopez-Soler, "Traffic Models Impact on OFDMA Scheduling Design," *EURASIP Journal on Wireless Communications and Networking*, pp. 1–13, Feb. 2012.

[48] 3GPP, "Evolved universal terrestrial radio access (E-UTRA); further advancements for E-UTRA physical layer aspects," 3rd Generation Partnership Project (3GPP), TR 36.814, Mar. 2010. [Online]. Available: http://www.3gpp.org/ftp/Specs/html-info/36814.htm

[49] J. Jang and K. B. Lee, "Transmit Power Adaptation for Multiuser OFDM Systems," *IEEE Journal on Selected Areas in Communications*, vol. 21, no. 2, pp. 171–178, Jan. 2003.

[50] M. Andrews, K. Kumaran, K. Ramanan, A. Stolyar, P. Whiting, and R. Vijayakumar, "Providing Quality of Service over a Shared Wireless Link," *IEEE Communications Magazine*, vol. 32, no. 2, pp. 150–154, Jun. 2001.

[51] S. Ryu, B. Ryu, H. Seo, and M. Shin, "Urgency and efficiency based wireless downlink packet scheduling algorithm in OFDMA system," in *IEEE Vehicular Technology Conference*, vol. 3, May 2005, pp. 1456–1462.

[52] Z. Jiang and Y. G. Li, "Max-Utility Wireless Resource Management for Best-Effort Traffic," *IEEE Transactions on Wireless Communications*, vol. 4, no. 1, pp. 100–111, jan 2005.

[53] H. Rinne, *Taschenbuch der Statistik*. Verlog Harri Deutsch, 2008.

[54] T. F. Maciel, W. C. Freitas, and F. R. P. Cavalcanti, "Joint Opportunistic Beamforming and Subcarrier Assignment for Maximization of User Satisfaction in OFDMA Systems," in *IEEE Vehicular Technology Conference*, Sep. 2010.